3D PHOTOGRAMMETRIC IMAGES TO EVALUATE FOOT MORPHOLOGY AND ANKLE KINEMATICS DURING GAIT OF MIDDLE EASTERN ADULTS

A Thesis submitted by

Ali Abdulmunim Ibrahim Al-Kharaz

BSc. and MSc. in Computer Sciences

For the award of

Doctor of Philosophy

2021

ABSTRACT

To prevent high fall rates, foot injury and ankle sprain during daily activities and sport, footwear should be designed based on foot shape and ankle kinematics. The purpose of this thesis is to develop an accurate 3D photogrammetric images captured by smartphone cameras technique that is non-invasive, low-cost and high-quality to analyse the morphology of the foot surface, investigate the foot shape characteristics of both genders, and evaluate the medial longitudinal arch (MLA) in static and dynamic conditions. Furthermore, the validation and investigation of ankle kinematics during gait according to gender is undertaken, as is an assessment of ankle kinematics in normal and unsteady gait.

The photogrammetry technique utilises images of objects captured by multiple cameras from differing viewpoints to produce a digital 3D model of objects. In photogrammetry, camera calibration is an important step to improve the accuracy of measured imaged coordinates (x, y). This system calibration process involves individual calibrations of 7-Galaxy smartphones and the internal accuracy is 0.36 pixels. In this study, 33 healthy voluntary participants (18 males and 15 females, aged between 25 and 47 years), all of whom were Middle Eastern postgraduate students at the University of Southern Queensland (USQ) were recruited.

In clinical settings, a number of landmarks were mounted on foot skin to measure the angles and the distances between anatomical bone locations. The results indicated that there were significant differences in some morphological characteristics of the feet of each gender. For example, the mean value of the foot length of males (26.01cm) was larger than females (22.39cm), and the mean values of arch length, ankle height and Chippaux-Smirak ratio for males was higher than for females. An accurate geometrical 3D close-range photogrammetry (CRP) method was used to evaluate the MLA in static (50% weight-bearing (WB), 10% WB, 90% WB standing and sitting non-WB) and dynamic motion during gait. MLA angle differences between males and females in static and dynamic conditions were also measured. In the static condition, the observation of the MLA angle was lower at about (137°) when sitting, indicating that the MLA was higher in non-WB. In the dynamic condition during walking, the higher mean value was found in the mid-stance phase (150.57°) when the foot tended to flatten.

The results of ankle kinematics during walking refer to significant differences between females and males for the transverse plane of range of motion of the ankle (F=12.21, Sig=0.013) however no significant differences of coronal and sagittal planes were found between genders. The CRP technique was also used to measure ankle kinematics during normal gait and three unsteady gait trials ((1) eyes closed, (2) on single beam, and (3) dragging ankle weights) in four phases of stance. We found that the eyes closed gait had higher ankle kinematic values than other gait conditions in the heel strike phase (3.38°, 11.72° and 8.48°) of the coronal, sagittal and transverse planes, respectively. Overall, the study was appropriate because it used a novel precise 3D images technique to evaluate foot morphology and ankle kinematics during gait.

CERTIFICATION OF THESIS

This Thesis is entirely the work of **Ali Abdulmunim Ibrahim Al-Kharaz** except where otherwise acknowledged. The work is original and has not previously been submitted for any other award, except where acknowledged.

Principal Supervisor: Senior Lecturer Dr Albert Chong

Associate supervisor: Prof. Dr Peter Milburn

Student and supervisors' signatures of endorsement are held at the University.

ACKNOWLEDGEMENTS

"In the name of Allah, the beneficent, the merciful"
I would like to begin this acknowledgment with Allah (God) who has provided me with the strength and wisdom to finish my thesis.

Next, I would like to express my gratitude to my PhD advisors, Dr Albert K. Chong, Dr Ben Hoffman and Dr Peter Milburn for their guidance, support and expertise in the photogrammetry technique and the development and completion of this research study. Without their direction and generous time commitment, this research study would not have been possible.

I am thankful to the Iraqi Ministry of Higher Education and Scientific Research for providing me with the scholarship to pursue this research. In addition, special thanks go to the Research Training Program (RTP) for its support of my thesis. Also, sincere thanks to USQ staff and my colleagues, especially the Middle Eastern students at USQ, who have helped me during this enjoyable experience.

I would like to express my thanks to Dr Barbara Harmes and Ms Sandra Cochrane for their trustworthy proofreading service. Thanks also go to Dr Enamel Kabir of USQ's Statistical Consulting Unit.

I also want to express my sincere gratitude to podiatrist, Dr Sam Johnston (of The Podiatrist clinic in Toowoomba, QLD), who shared his knowledge of marker positioning on the feet and guided my learning in this aspect of my research.

I would also like to express my deepest feelings to my dear brothers and sisters.

Last but not least, special thanks to my dear and sincere wife for her support and patience, supporting me in every possible way during my PhD journey, and to my newborn daughter 'Zahraa', who was given by god to us during the study period and always cheers me up with her incredible personality. I love you!

I am most greatly indebted to all of you.

TABLE OF CONTENTS

Abstract ……. i

Certification of thesis …… iii

Acknowledgements ……... iv

Table of Contents …… v

List of Figures ……..……. ix

List of Tables …….. xi

List of Author's Publications ……..... xii

List of Abbreviations ……..…… xiv

Chapter 1. Introduction ……. 1

1.1 General overview....……..... **1**
1.2 Research gaps …….... **2**
1.3 Research hypotheses ……..... **3**
1.4 Research aim ……. **3**
1.5 Research objectives ……... **4**
1.6 Research questions …… **4**
1.7 Research significance …… **5**
1.8 Research beneficiaries ……..... **5**
1.9 Research limitations ……..… **6**
1.10 Thesis layout ……..... **6**

Chapter 2. Literature review ……..... 9

2.1 Introduction …… **9**
2.2 Human foot morphology and ankle kinematics ……..... **9**
2.2.1 Foot morphology ……..... **9**
2.2.2 Ankle kinematics ……. **14**
2.2.3 Gait cycle analysis …….. **16**
2.3 Basic foot and ankle geometry measurement techniques …. …. **19**
2.3.1 Manual techniques ……. **20**
2.3.1.1 Measuring stick, Callipers and Brannock tools... **20**
2.3.1.2 Casting and foam impression tools ……. **21**
2.3.2 Optical techniques …….. **22**
2.3.2.1 X-ray, CT Scan, MRI and 3D scan…..…… **23**
2.3.2.2 Moiré method …….. **25**

2.3.2.3 Time-of-Flight (ToF) cameras ……. **26**
2.3.2.4 3D Images systems and photogrammetric techniques …… **28**
2.4 Discussion ……. **30**
2.5 Conclusion …… **34**

Chapter 3. Design of an accurate 3D images-based system for foot morphology and kinematics of ankle measurements……..……..35

3.1 Introduction …..... **35**
3.2 Theoretical background …… **35**
3.2.1 Mathematical fundamentals ……. **37**
3.2.2 Camera calibration ……..... **39**
3.2.3 Bundle triangulation ……. **42**
3.3 Practical requirements of the designed system …… **43**
3.4 Method ……... **46**
3.4.1 Software ……..... **46**
3.4.2 The designed system ……..... **47**
3.4.3 Reliability of designed system …….. **50**
3.4.3.1 High reliability foot morphology measurements ……. **50**
3.4.3.2 Two feet or one foot to measure ankle Kinematics ……. **51**
3.4.3.3 Statistical analysis …….. **52**
3.5 Results …… **53**
3.5.1 Smartphone lens stability analysis ..……..... **53**
3.5.2 Human foot morphology trials …….. **53**
3.5.3 Correlation between left and right feet of one subject ……54
3.6 Discussion …….. **54**
3.7 Conclusion ……..... **56**

Chapter 4. Close-range photogrammetry to measure foot morphology and investigate the differences between genders…… 57

4.1 Introduction …….. **57**
4.2 Methods ……..... **58**
4.2.1 Participants …….. **58**
4.2.2 Equipment and software …….. **59**
4.2.3 Foot anthropometrics and markers .....…... **60**
4.2.4 Statistical analysis ……... **63**
4.2.5 Experimental procedure …….. **63**
4.3 Results …….. **64**
4.4 Discussion ……..... **67**
4.5 Summary and conclusions …… **69**

Chapter 5. Evaluation of the medial longitudinal arch in static and dynamic behaviour during the stance phase of gait ……. 70

5.1 Introduction …… **70**

5.2 Methods …….. **72**
5.2.1 Participants ……. **72**
5.2.2 Equipment and software ……. **72**
5.2.3 Smartphone camera calibration …….. **72**
5.2.4 Experimental protocol …… **73**
5.2.5 Statistical analysis …….. **75**
5.3 Results ……. **76**
5.3.1 MLA angle in static and dynamic conditions ……. **76**
5.3.2 MLA angle gender differences ……..... **76**
5.3.3 Reliability …… **77**
5.4 Discussion …… **78**
5.5 Conclusion …… **81**

Chapter 6. Investigation of ankle kinematics according to gender during the stance phase of gait ……. 82

6.1 Introduction ……..... **82**
6.2 Methods …… **85**
6.2.1 Subjects ……..... **85**
6.2.2 Foot markers and software ……..... **85**
6.2.3 Experimental procedure ……... **86**
6.2.4 Statistical analysis …… **88**
6.3 Results ……... **88**
6.4 Discussion ……. **90**
6.5 Summary and conclusion ……. **93**

Chapter 7. Assessment of ankle kinematics during normal and unsteady walking ……. 94

7.1 Introduction ……... **94**
7.2 Methods …… **96**
7.2.1 Participants ……... **96**
7.2.2 Data collection procedure ……. **96**
7.3 Results ……... **98**
7.4 Discussion ……. **99**
7.5 Summary and conclusion ……..... **103**

Chapter 8. Conclusion and future directions …….……..... 104
8.1 Conclusion ……. **104**
8.2 Future directions ……..…..... **108**

References …… 109

Appendix A. Anthropometric data of participants ……. 139

Appendix B. Bundle adjustment principles …..…….. 140

Appendix C. Letter of confirm ……..…… 143

Appendix D. Participant information sheet and Consent form ……. 144

LIST OF FIGURES

1.1	Thesis organization …….....	**8**
2.1	The foot segments …….....	**10**
2.2	The longitudinal and transverse arches of the foot ……...	**12**
2.3	The three common planes of ankle kinematics……	**15**
2.4	Phases of the normal gait cycle …….…….	**18**
2. 5	Illustrating measurement, measuring stick, calliper and Brannock ……..……..	**21**
2.6	Casting process, Foam impression techniques, Dynamic impression during walking ……	**22**
2.7	Biplanar x-ray fluoroscopy system ……...	**24**
2.8	Images of foot at heel strike, mid stance, and heel off from CCD camera and Moiré method…….....	**26**
2.9	3D ToF camera operation ……..	**27**
2.10	Camera configuration around the foot ……...	**30**
3.1	The concept of image and object space …….	**37**
3.2	Exterior orientation and projective imaging ……..	**38**
3.3	Radial distortion versus radial position …….	**41**
3.4	Multi-image triangulation s1, s2 and s3 are three cameras, p_1 to p_5 are five target points, XYZ coordinates determined from intersecting rays …….……......	**43**
3.5	25-target array and invar scale bar for each smartphone Cameras' calibration in iWitness software …….…...	**46**
3.6	Convergent images of target array for each of the smartphone cameras …….……	**46**
3.7	Schematic of foot posture and gait direction …….....	**48**
3.8	Calibration process and results …….……..…..	**49**
3.9	Calibration parameters and internal accuracy ……...	**50**
3.10	The reference points to measure foot morphology in designed system …….....	**51**
3.11	Seven smartphone cameras to compute 3D coordinates of reference points on the foot ……	**51**
3.12	Ankle kinematic measurement of left and right feet during walking ……..……..	**52**
4.1	The fourteen right foot dimensions were measured ……	**60**
4.2	The reference points marked on the right foot ..……..…....	**64**
5.1	Array of target boards and an invar scale bar for smartphone camera calibration in iWitness Software ……	**73**
5.2	Five reference points to measure foot length and medial longitudinal arch angle …….…….	**74**

5.3	Subject 10% WB standing ……	**75**
5.4	The differences of MLA angle between gender in our study during MS stance phase gait and (Fukano and Fukubayashi) study in dynamic condition (landing) ……...	**79**
5.5	The change in MLA angle and standard deviation during the stance phase of gait for males and females ……...	**80**
6.1	Seven markers mounted on the right lower shank ……...	**85**
6.2	(a) Timing clock, (b) Flash of a LED, (c) Scale bar, (d) Ruler and (e) Four calibrated boards for synchronisation and accurate calibration procedure ……	**87**
6.3	Depicts the x-y-z coordinate to describe a screw axis Orientation of ankle ……..	**88**
6.4	Ankle kinematics during stance phase of gait for males and females ……	**92**
7.1	Three unsteady walking conditions ((a) Eyes closed, (b) On single beam, and (c) Dragging of ankle weights) with timing clock, flash of a LED, scale bar, ruler and four calibrated boards for the accuracy calibration procedure …….	**97**
7.2	Angles of three planes of ankle kinematics during stance phase of gait in normal, closed eyes, single beam, and dragging weight …….…….	**102**
B.1	Multi-image triangulation …….……..	**140**

LIST OF TABLES

2.1	Comparison of geometry techniques used for measuring foot morphology and kinematics of ankle……..	**33**
3.1	Smartphone Galaxy 6.0 specifications ……...……	**47**
3.2	Seven smartphone cameras calibrated intrinsic lens parameters ……..	**53**
3.3	Reliability of foot morphology measurement ……...	**54**
3.4	The correlation of the left and right feet (for one subject) of three planes for 4 phases of stance phase during gait…	**54**
4.1	Statistics (descriptive mean ± SD) of participating subjects ……..	**59**
4.2	Foot dimension definitions ……	**61**
4.3	Popular parameters for assessing the foot ……..	**62**
4.4	Mean and standard deviation of foot dimension and parameters for gender ……	**65**
4.5	Levene's test and t-test analysis of foot dimension and parameters …….	**66**
5.1	Subject characteristics, mean (SD) ……	**72**
5.2	Mean static and dynamic barefoot measurement of the MLA angle degrees with standard deviation (SD) …..…....	**76**
5.3	Mean static and dynamic barefoot measurement of the MLA angle degrees with standard deviation (SD), and Differences between genders ……	**77**
5.4	Mean reliability values between test-retest of MLA angle ……	**77**
6.1	Specifics of seven markers and locations …….	**85**
6.2	Mean ± SD of triplane angles during stance phase gait for males and females ……...	**89**
6.3	Mean reliability values between intra-sessions errors for ankle of gender groups during gait ……...	**89**
7.1	Specifics of seven markers and locations …….	**97**
7.2	Mean of triplane angles during stance phase of gait in normal, eyes closed, single beam and dragging ankle weights ……..	**99**
7.3	One-way ANOVA post Hoc Bonferroni to evaluate the ankle kinematic angles differences between normal and three unsteady of four stance phases of gait ……..…..	**99**
8.1	Overview of main points of objectives …….	**107**
A	Anthropometric data of participants ……..…	**139**

LIST OF PUBLICATIONS

Papers published

- **Al-Kharaz, A.** and Chong, A.K., 2018, June. High accuracy smartphone video calibration for human foot surface mapping. In *2018 IEEE 3rd International Conference on Image, Vision and Computing (ICIVC)* (pp. 542-545).

- **Al-Kharaz, A.** and Chong, A., 2019, March. 3D video images for comparing Indian and Iraqi women's foot width surface shape associated with stance phase of gait. In *Proceedings of the 2019 2nd International Conference on Information Science and Systems* (pp. 22-26).

- **Al-Kharaz, A.** and Chong, A., 2019, April. Analysis of gender related foot morphology in Iraqi adults using videogrammetry during gait. In *2019 IEEE 9th Symposium on Computer Applications & Industrial Electronics (ISCAIE)* (pp. 108-113).

- **Al-Kharaz, A.** and Chong, A.K., 2020. Impact of anthropometric characteristics on the medial longitudinal arch in static and dynamic loading using photogrammetry images. *Series on Biomechanics*, *34*(2), pp. 56-61.

- Abbas, N.S., Chong, A., **Al-Kharaz, A.** and Al-Hadeethi, H., 2020, April. Relationships between foot dimensions and plantar pressure distributed in older people. In *2020 IEEE 10th Symposium on Computer Applications & Industrial Electronics (ISCAIE)* (pp. 198-202).

- **Al-Kharaz, A.** and Chong, A., 2020, August. Investigation of tri-planar range of motion of ankle according to gender using photogrammetry technique. In *2020 IEEE International Conference on Signal Processing, Communications and Computing (ICSPCC)* (pp. 1-5).

- **Al-Kharaz, A.** and Chong, A., 2021. Reliability of a close-range photogrammetry technique to measure ankle kinematics during active range of motion in place. *The Foot*, vol. 46(1), pp. 1-5.

- **Al-Kharaz, A.** and Chong, A., 2021, Gender differences in foot morphology of Middle Eastern adults using close-range photogrammetry technique. 11th series of IEEE Symposium on Computer Applications & Industrial Electronics (ISCAIE 2021), Malaysia.

Papers under review

- **Al-Kharaz, A.** and Chong, A., 2021, Evaluation of ankle kinematics during the stance phase of gait according to the gender of adults using close-range photogrammetry. *The Foot, ELSEVIER.*

ABBREVIATIONS

AB	**Abduction**
AD	Adduction
AHI	Arch Height Index
ALI	Arch Length Index
AI	Arch Index
AHI_I	Arch Height Index to Truncated Foot Length
AHI_TFL	Arch Height Index to Total Foot Length
AHR	Arch Height Ratio
AJH	Ankle Height
AL	Arch Length
AS	Anterior Shank
BG	Ball Girth
BIB	Bimalleolar Breadth
BMI	Body Mass Index
CAD	Computer Aided Design
CAM	Computer Aided Manufacturing
CCD	Charge Coupled Device
cm	Centimetres
CMOS	Complementary Metal-Oxide-Semiconductor
CRP	close -Range Photogrammetry
CSI	Chippaux-Smirak Index
CSIR	Chippaux-Smirak Ratio
CT scan	Computed Tomography scan
DF	Dorsiflexion
DJS	Dynamic Joint Stiffness
EI	Eversion/Inversion
EI	External-Internal Rotation
EV	Eversion
FB	Foot Breadth
FI	Foot Index
FL	Focal Length
FL	Foot Length
GIS	Geographic Information Systems
GRF	Ground Reaction Force
HB	Heel Breadth
HBI	Heel-Ball Index
HD	High-Definition
HD	High Definition
HG	Heel Girth
HMF	Height at 50% of Foot Length

HO	Heel Off
HS	Heel Strike
IC	Initial Contact
ICC	Intraclass Correlation
IL	Instep Length
IM	Inter-malleolar Point
in	Inches
IP	Interphalangeal
ISB	International Society of Biomechanics
IV	Inversion
LAA	Longitudinal Arch Angle
LEDs	Light-Emitting Diodes
LF	Lateral of the Fibula
LM	Lateral Malleolus
LMPJ	Fifth Metatarsophalangeal Joints
LR	Loading Response
MB	Mid-Foot
MLA	Medial Longitudinal Arch
MM	Medial Malleolus
m	Metre
mm	Millimetre
MRI	Magnetic Resonance Imaging
MS	Mid-Stance
MTP	Metatarsophalangeal
ND	Navicular Drop
NDT	Navicular Drop Test
NH	Navicular Height
NNH_I	Normalised Navicular Height to Truncated Foot Length
NNH_TFL	Normalised Navicular Height to Total Foot Length
OBFL	Outside Ball-of-Foot Length
PF	Plantar Flexion
RMS	Root Mean Square
ROM	Range of Motion
SAI	Staheli Index
SEM	Standard Error of Measurement
SMPJ	Top of the Second MPJ
TFL	Truncated Foot Length
ToF	Time of Flight
WB	Weight Bearing

Chapter 1. Introduction

1.1 General overview

Because of the increasing interest in foot morphology and ankle kinematics, studies conducted in these areas have become more prevalent in the last two decades. These studies provide significant information about orthotics and treatment approaches for the human foot suffering abnormalities or ulceration. As a result, they also inform the design of appropriate therapeutic footwear that fits the shape of the individual foot. Therapeutic footwear helps to sustain many of the important functions of the body, including the maintenance of body balance, body weight distribution and shock absorbance (McPoil & Cornwall, 1996; Scott et al., 2007; Zhao et al., 2017; Buldt & Menz, 2018).

In clinical settings, static anthropometric measurements are used to determine foot morphology. These measurements are often inferred by studying the differences in the positions of bone landmarks using non-invasive techniques. They are easier to implement on surface markers that are commonly used in three-dimensional multi-segmented foot models (Li et al., 2017; Nicholson et al., 2018). Similarly, ankle kinematics are evaluated with dynamic anthropometric measurements which are calculated by assessing the angles from three-dimensional bone orientations (Liu et al., 2004b; Okita et al., 2009; Fukano et al., 2018).

Accurate 3D photogrammetric images of foot dimensions are important for allowing researchers to study foot morphology in static and dynamic loading, thus classifying the foot arch, and aiding in the development of a set of guidelines for footwear design. In medical applications, the measurement of the three-dimensional human foot and ankle (whether in static or dynamic condition), in normal and unsteady gait, requires a high level of accuracy. The need for accuracy is especially important in impeded gait which leads to an increased risk of falls and lower extremity injuries (Hill et al., 1999; Robinovitch et al., 2013). Accurate 3D photogrammetric images could provide orthopedic information in a more accurate and low-cost way.

Techniques commonly utilized to determine a 3D surface model of the human foot include close-range photogrammetric approaches (Kimura et al., 2008, Al-Kharaz & Chong, 2019b),

3D Scanner (Mauch et al., 2008; Menz et al., 2014), 3D computed tomography scan (CT scan), magnetic resonance imaging (MRI) (Budhabhatti et al., 2007; Antunes et al., 2008), and 3D Time-of-Flight **(**ToF) (Oggier et al., 2005; Liu et al., 2011).

Human foot morphology is diverse because of natural biological variance, climatic factors, lifestyle and population groups. In addition, age, sex and body mass index (BMI) lead to a significant impact on morphology (Hawes et al., 1994; Ashizawa et al., 1997; Otsuka et al., 2003; Voracek et al., 2007; Hong et al., 2011; Sacco et al., 2015; Al-Kharaz & Chong, 2019a). Adults with varying ethnicities may show differences in foot morphology and tend to have different foot shape characteristics (Hisham et al., 2012; Shariff et al., 2019; Shariff et al., 2020). Arch function depends on the shape of the foot, ligamentous stability and bony structure, while factors like race, age and gender are found to influence the formation of the MLA (Nielsen et al., 2009). Age and gender are both influential factors that may change ankle ROM. A number of studies have demonstrated that females have a higher ankle ROM compared to males (Fukano et al., 2018; Sung & Kim, 2018). Additionally, there is a decrease in ROM for subjects in the oldest age groups (Nigg et al., 1994; Brockett & Chapman, 2016). Unsteady gait, which occurs on narrow roads, descending walking and eyes closed walking may also be affected by gender (Nigg et al., 2010).

The participants in this study are from Middle Eastern countries. The Middle East refers to a number of states or territories such as Turkey, Syria, Lebanon, Iraq, Iran, Jordan, Egypt, Afghanistan, Libya, Saudi Arabia, Kuwait, Oman, Bahrain and Qatar. The history of the Middle East dates back to ancient times, and the geopolitical importance of the region has been recognized for millennia. The populations of the Middle East have body morphology differences compared with other ethnics group or other regions of the world (Al-Rawi et al., 1985; Abledu et al., 2015; Al-Kharaz & Chong, 2019a). Very few studies have analysed foot morphology or ankle kinematics of Middle Eastern populations. Therefore, this study could contribute to the biomechanics knowledge of Middle Eastern adults.

1.2 Research gaps

In spite of many existing research projects analysing human foot morphology and ankle kinematics during gait using several types of apparatus such as callipers and X-rays, according to the literature review in Chapter 2, four gaps required research. These gaps are:

1. Existing devices for measurements are not readily available and cannot offer precise measurements, thus there is a need to carry out research to determine the ease of proper use of the smartphone and stereophotogrammetric techniques for high accuracy dynamic 3D human foot/ankle imaging systems
2. Previous research has not analysed and evaluated foot characteristics and dynamic motion of the MLA of Middle Eastern adults
3. Published studies do not provide investigations of ankle kinematics (dorsiflexion/plantar flexion, inversion/eversion and adduction/abduction) during gait according to the gender of Middle Eastern adults
4. Ankle biomechanical characteristics during normal and unsteady gait have not been assessed and compared in previous studies.

1.3 Research hypotheses

The hypotheses to be tested in this study were:

1. Smartphone cameras and video imaging systems are low-cost, easy to use, precise and effective tools for capturing and addressing 3D spatial data in static and dynamic characteristics of the foot shape
2. Multi-stereophotogrammetric techniques can provide high quality, low cost and non-invasive ways to measure and evaluate human ankle kinematics during normal and unsteady stance phase of gait.

The hypothesis of this research can be formulated as:

"Smartphone video imaging and multi-stereophotogrammetric techniques can provide accurate techniques to study foot morphology and ankle kinematics during the stance phase of gait of Middle Eastern adults "

1.4 Research aim

The aim of this research is to study high accuracy 3D human foot characteristics and dynamic 3D ankle kinematics during gait using smartphone video imaging and multi-stereophotogrammetry.

1.5 Research objectives

The research aim and questions will be addressed through the following research objectives:

1. Determination of the quality of smartphone cameras and close-range photogrammetry systems for simultaneous accurate 3D imaging system of the human foot shape
2. Investigation of the 3D human foot shape characteristics of female and male Middle Eastern adults
3. Evaluation and determination of the MLA in static and dynamic conditions
4. Validation and investigation of 3D ankle kinematics during gait according to gender
5. Assessment and determination of ankle kinematics in normal and unsteady gait.

1.6 Research questions

This study needs to answer 15 significant research questions. These questions are:

1. What are the limitations of past and currently available techniques developed for capturing 3D imaging systems for the human foot and ankle during human gait?
2. Are commercial low cost and accurate smartphone video cameras suitable for capturing the geometrical change of ankle kinematics during gait?
3. Are the right foot measurements of a person similar to their left foot measurements?
4. Is close-range photogrammetry an appropriate technique to evaluate human foot morphology?
5. Are the 7-smartphone cameras suitable to measure foot dimensions?
6. Are the assessments of the dynamic measurement accurate, precise and reliable?
7. Are the cameras that were calibrated for developing 3D image-based measurement systems accurate?
8. Is there a difference in MLA geometry between static and dynamic conditions?
9. Are foot shape characteristics different between females and males for the Middle Eastern ethnic group?
10. What are the MLA differences between non-weight bearing (non-WB) and weight bearing (WB) in the static condition?
11. Are the MLA angles when sitting different from 50% weight-bearing standing?
12. Is close-range photogrammetry accurate for comparison of ankle kinematics between males and females during gait analysis?
13. What are the differences of ankle kinematics between normal and unsteady gait?
14. What is the ROM of ankle during normal gait?

15. What are the differences between eyes closed, walking on a single beam, and dragging ankle weights during unsteady gait?

1.7 Research significance

The significance of this research lies in the following:

1. Development of measure capture techniques for gait which allow for high-accuracy 3D anthropometric measurement of the foot
2. Determination of the relationship between static and dynamic MLA measures
3. Identification of differences between WB scores of the MLA in the static condition
4. Identification of any individual differences of foot length and weight variation with MLA scores
5. Understanding of the differences of ankle kinematics between normal gait and unsteady gait.

1.8 Research beneficiaries

Analysis of 3D photogrammetric images of the foot and ankle can be utilised in many applications such as medicine, forensic science, physiotherapy, anthropology, foot orthoses and prosthetics, footwear manufacturing, and sport and exercise. The following list addresses a number of significant practical applications that may benefit from the outcomes of this research:

1. The evaluation of 3D photogrammetric images can provide podiatrists and other clinicians with essential information about the dimensions and flexible dynamics of the feet of patients who suffer from a foot abnormality (whether from disease or injury) and help understand acute and chronic injuries in athletes and other physically dynamic individuals. This evaluation is essential in developing foot treatment strategies which may involve designing appropriate therapeutic footwear that matches the dynamic foot's characteristics. In addition, a 3D foot image offers precise information on foot movement to assist in the manufacture of foot prostheses
2. The 3D photogrammetric images can provide physiotherapists with a new understandings of ankle kinematics during normal gait and unstable gait
3. The knowledge of the ankle biomechanical variables could help to improve operative techniques and prosthetic design

4. Assessment of the MLA and recognition of altered foot alignment in pes planus and pes cavus and foot dimensions can assist in the design of footwear that minimises foot stress and strain
5. The evaluation of ankle motion during walking is essential to develop the production of foot orthoses in the management of foot and ankle disorders
6. Static and dynamic load distribution, as shown on 3D foot and ankle images, can help sports scientists and trainers in the analysis of foot and ankle motions of the athlete's feet, thus improving techniques and training programs.

1.9 Research limitations

The limitations of this research are:

1. Multi-stereophotogrammetry techniques can provide exterior information about foot/ankle characteristics in standing and during gait, but cannot detect the interior foot structures such as bone, tendons, ligaments and muscles.
2. The number of participants in this research was limited to 33 (18 males and 15 females), and other human activities like running or jogging were not considered.
3. The walking speed of subjects during test could not be determined accurately, i.e., the subject walked at a self-selected speed.

1.10 Thesis Layout

Figure 1.1 outlines the thesis structure. A brief of the remaining thesis chapters is reviewed below:

Chapter 2: Literature review

This chapter reviews basic foot morphology and ankle joint kinematics, and gait cycle analysis, and demonstrates the factors that have an effect on the foot and ankle. Furthermore, human foot/ankle measurement techniques include manual measurement techniques and optical scanning techniques for 3D models. The chapter also discusses and compares these techniques and the ability to use close-range photogrammetry and video imaging systems to capture the shape of the foot and measure ankle kinematics during gait. The chapter ends with a conclusion of the literature review.

Chapter 3: Design of an accurate 3D image-based system for foot morphology and kinematics of ankle measurements

This chapter describes the design of the accurate image-based measurement technique and contains a theoretical background, mathematical algorithms and the schematic of foot posture and gait direction. It also discusses the methods used to calibrate the smartphone cameras. In addition, this chapter investigates the reliability of the designed system. Discussion of the accuracy of the 3D image-based system is provided at the end of this chapter.

Chapter 4: Close-range photogrammetry to measure foot morphology and investigate the differences between genders

The introduction to this chapter focuses on the significance of foot shape helping to demonstrate the techniques which have been used to measure foot dimensions as well as the gender factors that affects foot characteristics. The chapter sets out the specific methodologies use to investigate the 3D shape of human foot characteristics. It also contains the results, giving correlates between foot dimensions and calculating the differences between genders. The results are discussed and the conclusions are presented based on the main findings of the chapter.

Chapter 5: Evaluation of the medial longitudinal arch in static and dynamic behaviour during the stance phase of gait

One of the most important structural characteristics of the foot is the MLA. The importance and role of the MLA are included in the introduction of this chapter. Specific methodology is used to compute the MLA angle and evaluate the MLA in static and dynamic behaviour during the stance phase of gait. In addition, this chapter computes and illustrates the differences in the MLA angle between females and males. A brief discussion and conclusion summarising the main findings ends the chapter.

Chapter 6: Investigation of ankle kinematics according to gender during the stance phase of gait

The introduction of this chapter reviews previous studies of ankle kinematics. It validates the dynamic ROM of the ankle (dorsiflexion/plantar flexion, inversion/eversion, and adduction/abduction) during the stance phase of gait using close-range photogrammetry, and

compares all the results between females and males. In addition, data collection and statistical analysis are discussed, and the outcomes are demonstrated through figures, graphs, and tables. A brief discussion and conclusion summarising the main findings complete the chapter.

Chapter 7: Assessment of ankle kinematics during normal and unsteady walking

The importance of studying unstable walking is included in the introduction to this chapter. The chapter evaluates ankle ROM during unsteady gait, including walking with eyes closed, walking on a single beam, and dragging ankle weights; all of which may increase the risk of falls during walking. The outcomes of this chapter contain the differences between normal and unsteady walking, and discussion compares the results with previous studies. The chapter ends with a brief summary and conclusion.

Chapter 8: Conclusion and future directions

This chapter summarises the main findings of the thesis and discusses future research directions.

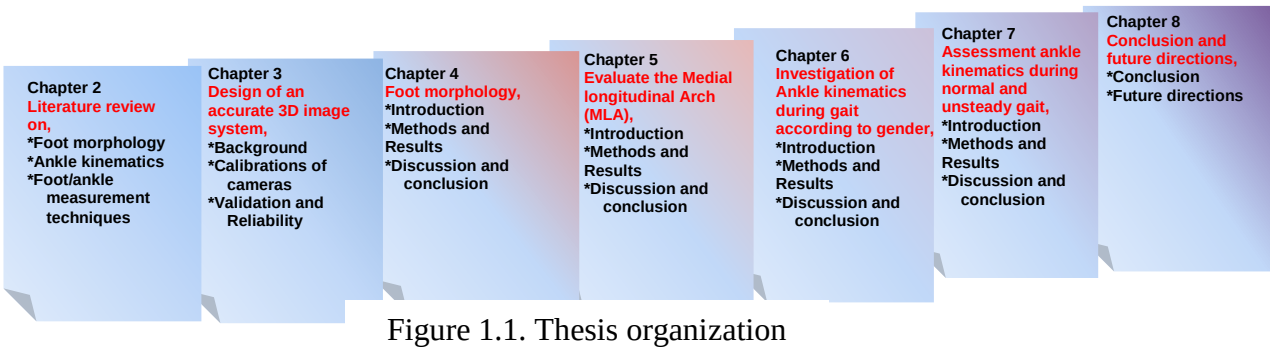

Figure 1.1. Thesis organization

Chapter 2. Literature review

2.1 Introduction

The chapter provides a detailed review of relevant literature to aid in the understanding of the research issues, direct the reader to the research gap, and provide an understanding of the research aim and objectives. The first part of the chapter explains human foot morphology and ankle kinematics. The second part demonstrates conventional foot measurement techniques and highlights their limitations. The chapter ends with conclusions showing that close-range photogrammetry is the least costly and most accurate technique to measure human foot morphology and gait analysis.

2.2 Human foot morphology and ankle kinematics

2.2.1 Foot morphology

Foot morphology is most important for orthotic design, forensics and manufacturing suitable footwear (Schwarzkopf et al., 2011; Davies et al., 2014; Lee & Wang, 2015; Zhao et al., 2017). The internal shape of the shoe must closely approximate the shape of a foot to be comfortable (Hawes & Sovak, 1994). The human foot is very complex. Each foot consists of 26 bones, more than 30 articulations, tendons and ligaments, and other surrounding soft tissues enabling three the fundamental functions of supporting, shock absorbing and weight bearing. (Abledu et al., 2015; BPT et al., 2015; Domjanić, 2015; Xu et al., 2018). The 26 bones (seven tarsals, five metatarsals, and 14 phalanges) and (six joints) ankle (talocrural), subtalar, midtarsal (Chopart), tarsometatarsal (Lisfranc), metatarsophalangeal (MTP) and interphalangeal (IP) joints) of the foot make up its three segments: the hindfoot, the midfoot and the forefoot as shown in Figure 2.1 (Riegger, 1988; Abboud, 2002; Sherman, 2010).

The hindfoot consists of the talus and calcaneus. The talus is orientated to transmit reactive forces from the foot through the ankle joint to the leg. Lying between the calcaneus and tibia, it communicates thrust from one bone to the other. The calcaneus is the largest and most posterior bone in the foot.

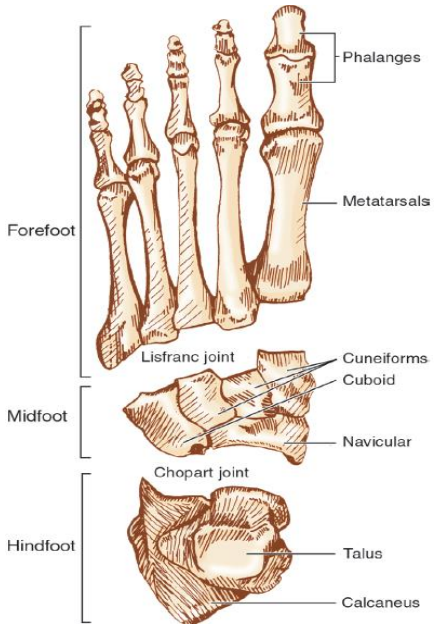

Figure 2.1. The foot segments (Sherman, 2010)

The navicular, cuboid and three cuneiforms make up the midfoot. The navicular medial to the cuboid articulates with the head of the talus anteriorly and is the keystone at the top of the medial longitudinal arch.

There are five metatarsals in the forefoot, all tapered distally and articulating with the proximal phalanges. The first metatarsal is the shortest and widest. The phalanges constitute digits. The big toe (hallux) consists of two phalanges, all other toes contain three. The heads of the proximal and middle phalanges tend to be trochlear shaped allowing for greater stability. Functionally, the toes contribute to weight bearing and load distribution and also effect propulsion during the push-off phase of gait (Abboud, 2002).

The characteristic of foot shape is varied as many factors are associated with foot morphology. Aside from natural biological variation, distinctive age classes and population groups show prevalent qualities in foot dimensions (Hawes et al., 1994; Ashizawa et al., 1997; Kouchi, 2003; Hisham et al., 2012; Sacco et al., 2015). Differences in foot shape are also influenced by factors such as BMI (Price & Nester, 2016; Zhao et al., 2017), age (Mauch et al., 2008), shoe wearing habits (Brathwaite et al., 2013; Barisch-Fritz et al., 2016), sex (Manna et al., 2001; Otsuka et al., 2003; Cho et al., 2004; O'Connor et al., 2006; Voracek et al., 2007; Krauss et al., 2010; Xu et al., 2018) and ethnicity (Picón-Reátegui et al., 1979; Chaiwanichsiri et al., 2008). Kouchi (1998) reported that Mongoloid populations have a wider foot compared to Caucasoid and Australian populations, and East Asian populations have a shorter foot length compared to

Southeast Asians and Africans. Hawes et al. (1994) found that the East Asian's forefoot is wider than that of their white counterparts. Sacco et al. (2015) revealed variation in anthropometric foot breadth between German and Brazilian children. Tobias et al. (2014) recruited 500 subjects of both genders. Their results demonstrated that men's foot length, height and breadth were significantly greater than that of their female counterparts. Mrozkowiak (2010) described the changes in mean length and width of the foot during fast and slow phases of growth between the ages of 4 and 18 years in the 9804 girls and 8699 boys. The results show that the rate of increase in the length and width of the foot in the female and male populations is steady between the ages of 4 and 18 years, but shows a drop at the age of 14 years.

A number of studies to determine sex through foot or foot pieces – as they are more accessible than any other part of the body in most cases – are very common in forensics. Atamturk (2010) compared 253 females and 253 males from Turkey and identified some of foot parameters to determine the sex. The findings of his study indicate that the calcaneus bone seems to have been the basic criterion to determine gender. A similar result was found in studies such as Bidmos & Asala (2003) and Moneim et al. (2008).

Foot shape dimensions including the length, breadth, height, and perimeter were the most commonly measured in previous studies (Hawes & Sovak, 1994; Witana et al., 2006; Krauss et al., 2010). Robinson et al. (1984) presented a photographic image technique and recruited a sample of 938 male and female subjects for measuring foot length and width, heel width, medial and lateral metatarsal - phalangeal joint length and height, and dorsum height. They found the impact of prolonged running on the shape of the foot. Witana et al. (2006) used a foot scanner to measure 18 foot dimensions of 20 Hong Kong students and evaluated them through comparisons with simulation, manual and commercial software. Hong et al. (2011) identified foot shape in 1,236 young Chinese men and 1,085 young Chinese women by measuring 19 foot shape variables including girth, length, width, height and angle. They found that foot width, medial ball length, ball angle and instep height showed significant differences between foot types in the same foot length for both genders. Zhao et al. (2017) investigated the characteristics of foot morphology for 108 Japanese adults. Their study showed that gender has the bigger impact on length, width, height and girth parameters of the foot. Xu et al. (2018) recruited 2543 Chinese children and 12 foot shape measurements were acquired. They concluded that foot morphology difference is associated with sex and age. Mauch et al. (2008) reported that deficient mass could be verified for the comprehensive foot morphology based on a foot type

classification. Yadav et al. (2015) recruited 110 medical students from Nepal to assess different foot measurements using foot caliper and digital photography methods and compared measurements.

The elastic properties of the arch of the human foot are important (Bibby et al., 1987). The arch of the foot affects the normal biomechanics of the lower limb and serves as an adaptable, supportive base for the entire body. The flexibility conferred to the foot by these arches facilitates functions such as walking and running by bearing the weight of the body and absorbing the shock produced during locomotion (Franco, 1987; Ward et al., 2011). The foot has three arches, two longitudinal (medial and lateral) arches across the length of the foot and one anterior transverse arch across the width of the foot. They are formed by the tarsal and metatarsal bones, and supported by ligaments and tendons in the foot (BPT et al., 2015). The lateral longitudinal arch is on the outer side of the foot, and the medial one on the inner side of the foot. The lateral arches act as pillars for the transverse arch (Ridola & Palma, 2001). See Figure 2.2. The medial longitudinal arch is more important as it provides necessary shock absorption during activity (Xiong et al., 2010).

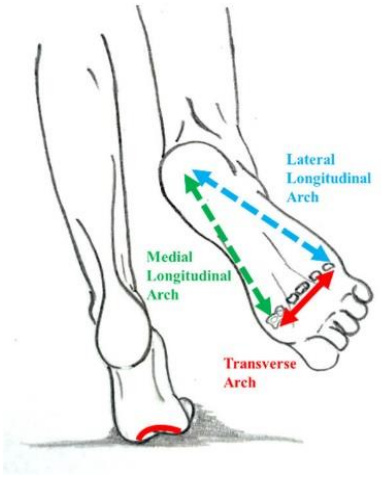

Figure 2.2. The longitudinal and transverse arches of the foot (Zeidan et al., 2019)

The relationship between foot length and longitudinal arch height have been studied. Nielsen et al. (2009) demonstrated that the dynamic navicular drop (ND) is influenced by foot length and gender. For a positive correlation between foot length and dynamic ND. The correlation r measures the strength of the linear relationship between two quantitative variables and in their study, the r value was found to be approximately 0.25. In contrast, Hill et al. (2017) reported

no significant relationships between arch height and foot length. However, the MLA has been shown to play an important role in shock absorbance and provides the most significant support to the foot during weight-bearing activities (Ker et al., 1987; Ogon et al., 1999). Its significance lies in its ability to dissipate plantar pressure forces (Balsdon et al., 2016). Clinical assessments regard the MLA as the main source of foot variability (Razeghi & Batt, 2002), and it is the largest arch of the foot and is regarded as the most important foot arch in clinical assessments due to its influence on lower limb function (Nigg et al., 1994; Murley et al., 2009), postural stability (Cote et al., 2005) and foot pain (Burns et al., 2006). The MLA is made up of the calcaneus, talus, navicular, cuneiform, and the medial metatarsal bones (Abboud, 2002). Stolwijk et al. (2014) used markers to measure foot length and mounted the markers on the heel, first metatarsal and navicular to measure the MLA at different speeds. This study indicated a flattening of the MLA during gait.

Mickle et al.'s (2008) study agreed with previous research that preschool boys had a significantly thicker midfoot fat pad than girls, displayed significantly flatter feet than the girls, and had a significantly thicker midfoot fat pad than girls. They measured the degree of flat-footedness of each child's arch height using the AI. Balsdon et al. (2021) measured the MLAs of 13 participants of different foot types: five pes planus, four pes cavus, and four normally arched. The MLA angle was measured to quantify kinematic differences between foam and plaster impression methods for custom foot orthoses by three-dimensional bone models using biplane fluoroscopy images during midstance.

A number of methods are currently used to quantify the MLA in a static state (Xiong et al., 2010):

1. Visual observation which depends on the clinician's experience
2. Foot print parameters such as the AI, the ALI, Staheli's Index and the Chippaux-Smirak Index. The fundamental premise of these indices is that the height of the arch is related to the footprint
3. Posture-related indices such as Valgus Index and the Foot Posture Index
4. Dimension-related indices such as arch height or navicular height, dorsum height/foot length, navicular drop and navicular drift
5. Foot function-related indices such as the rear-foot-forefoot angle and the Centre-of-Pressure Excursion Index

6. Angle-related indices such as Longitudinal Arch Angle (LAA), the rear foot angle, and calcaneal-first metatarsal angle.

The most popular techniques use the navicular bone measurements as a point of reference for assessing the MLA. These static measurements are then used to predict the behaviour of the foot arch in a dynamic state. The Navicular Drop Test (NDT) was originally developed by Brody (1982) to quantify sagittal plane mobility of the mid-foot. The NDT measures the change in height of the navicular bone when the foot position is changed from subtalar neutral (loaded) to a relaxed WB state (minimally loaded). Brody (1982) reported that a navicular drop value of approximately 10 mm is regarded as normal, and anything greater than 15 mm is classified as abnormal. The MLA is mainly responsible for related structural problems throughout the lower limb.

Deviations in the normal structure of the MLA produce unbalanced, functionally unstable conditions of the foot such as pes cavus or pes planus (Franco, 1987). Giladi et al. (1985) demonstrated that subjects with pes planus were less likely than subjects with normal or pas cavus to show the development of stress fractures in the lower extremity. Dahle et al. (1991) study was an assessment of MLA posture. In their study, subjects having a LAA equal to 90° were classified as having low arches, whereas individuals with a LAA equal to 180° were considered to have high arches. Subjects with a LAA between 120° and 150° were classified as having normal arches. Balsdon et al. (2019) reported the MLA angle in different foot types was between 120.8° and 141.1°. Traditionally, feet are classified as being high, normal or low arched. A larger MLA angle indicates a decrease or lowering of the MLA (flat arch), whereas a smaller, more acute angle indicates an increase in height of the MLA (high arch).

Arch function depends on the shape of the foot, bony structure ligamentous stability and muscular fatigue, while factors like race (Stewart, 1970), footwear (Sachithanandam & Joseph, 1995) and gender (Volpon, 1994) are found to influence the formation of the MLA (Ogon et al., 1999).

2.2.2 Ankle kinematics

The human ankle joint plays a principal role in mechanics and energetics during gait and other activities of daily living (Brockett & Chapman, 2016; Panero et al., 2017; Hedrick et al., 2019). The ankle joint is considered one of the most important joints for balancing strategy execution to decrease fall risk (Studenski et al., 1991). Kinematics is the study of bodies in motion without

considering the forces that cause body movement. It describes and analyses positions, velocities and angles in a specific plane. The three common planes used in the description of gait kinematics are the sagittal plane for the flexion-extension movements, the frontal (coronal) for inversion and eversion movements, and the transversal (Axial) plane for the internal-external rotations, as shown in Figure 2.3.

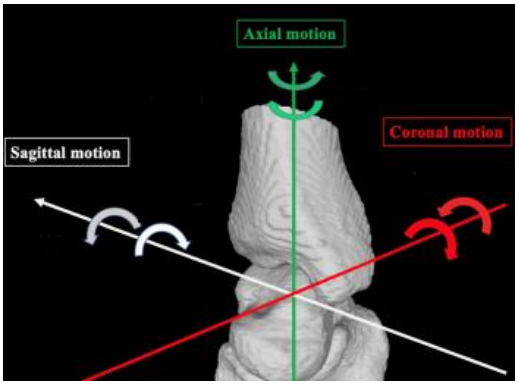

Figure 2.3. The three common planes of ankle kinematics (Kaneda et al. 2019)

Most studies have been interested in knee, hip, and ankle kinematics (Bonnefoy-Mazure & Armand, 2015). Because the ankle joint complex is crucial to human locomotion, accurate knowledge of the kinematics of these joints is essential for proper diagnosis and treatment of injuries and diseases in this region (Wong et al., 2005). Ankle sprain is a common sports-related injury, with an estimated 302,000 new ankle sprains each year in the UK (Ferran & Maffulli, 2006). The most common mechanism of lateral ankle sprain is excessive inversion and internal rotation of the hindfoot while the leg is in external rotation (Ferran et al., 2009). Evaluation of ankle motion is required in footwear design, forensics, medical reasons and the diagnosis acute or chronic injuries in athletes (Fawzy & Kamal, 2010; Blenkinsopp et al., 2012; Davies et al., 2014).

The ankle joint consists of a bony fit between the talus and the tibia proximally and medially (internally), and the talus and the fibula laterally (externally). The width between the malleolus is greater anteriorly than posteriorly. The anterior width of the ankle is wider (mean 28.5 mm) than the posterior width (mean 21.5 mm), and the articular component of the lateral malleolus is longer than that of the medial malleolus (Kerkhoffs et al., 2020).

Because the axes of motion for the ankle, subtalar, and midtarsal joints are oblique in three planes, motions within the sagittal plane are dorsiflexion (DF/upward) and plantar flexion (PF/downward), the coronal plane are inversion (IV) and eversion (EV), and the transverse

plane are adduction (AD), or internal rotation, of the foot and abduction (AB), or external rotation. Combinations of these motions across both the subtalar and tibiotalar joints create three-dimensional motions called supination and pronation (Riegger, 1988; Chan & Rudins, 1994). Motion about these axes cannot occur simultaneously, and the transition between axes during motion is estimated to occur close to the neutral position of the joint (Brockett & Chapman, 2016).

Numerous studies have been carried out to analyse the kinematic characteristics of the ankle joint complex (Roaas & Andersson, 1982; Leardini et al., 1999). For clinical applications, joint mobility is often quantified by active (Youdas et al., 1993; Thoms & Rome, 1997; Grossman, 2003; Krause et al., 2011) or passive (Grossman, 2003; Krause et al., 2011) ROM in prone (Kim et al., 2015) and during gait (Kidder et al., 1996; Rao et al., 2006). Age and gender are both influential factors that may change ankle ROM. Lee and Hertel (2008) compared gender differences between 18 and 50 years of age. This demonstrated that younger females (20-39 years old) have a higher ankle ROM compared to males. However, with increasing age, older females demonstrated less dorsiflexion and greater plantar flexion compared to male patients in the oldest age group (70-79 years old). Additionally, there was a decrease in ROM for both genders in the oldest age groups. Murray et al. (1985) described minimal differences of ROM between females and males. The ROM during stance was greatest for dorsiflexion/plantar flexion (DP) in both genders and least for eversion/ inversion (EI) in males group (Sung & Kim, 2018). Gabriel et al. (2008) compared dynamic joint stiffness (DJS) of the ankle in the sagittal plane during natural cadence along a 12m pathway walking in both genders. They mounted five skin markers on the lateral aspect of the leg and the foot. Their results demonstrated DJS was not significantly different between females and males during the second sub-phase, but that DJS was significantly higher in males than females during the fourth sub-phase.

2.2.3 Gait cycle analysis

The gait cycle can be defined as a period of time between any two nominally identical events in the gait process. It was identified as the most common movement during daily routines such as jogging, walking and running (Bonnefoy-Mazure & Armand, 2015; Panero et al., 2017). Gait analysis is an important instrument in various fields of clinical research and its protocols are intended to make kinematics interpretable for clinicians (Krauss et al., 2008b).

Human gait depends on a complex interplay of the major parts of the nervous, musculoskeletal and cardiorespiratory systems. Individual gait pattern is influenced by age, personality, mood and sociocultural factors. Generally, gait cycle is considered to begin when one foot strikes the ground and end when the same foot strikes the ground again (called initial contact or IC). During the gait cycle, lower limb considered an alternate stance phase (foot in contact with the ground) and swing phase (foot without ground contact). Thus, a gait cycle is divided into a period of stance phase (about 60% of the cycle) and a period of swing phase of the lower limbs (about 40% of the cycle) (Bonnefoy-Mazure & Armand, 2015). Each phase is associated with one limb and is composed of different sub phases. As shown in Figure 2.3, the stance phase consists of the following sub-phases: heel strike (A), loading response (B), midstance (C), terminal stance (D). The swing phase consists of the following sub-phases: preswing (E), toe-off, mid-swing (F) and terminal swing (G).

Root (1977) divides the gait cycle into two separate phases: the stance and swing phase. The description provided by Root (1977) focused almost entirely on the movement of the foot during the stance phase. The stance phase is divided by Root (1977) into three separate phases: the contact phase, midstance phase and propulsion. More specifically, the main phases of stance phase that will be detected are shown as follows (Mohammed et al., 2016):

- Initial contact: During the initial contact, the leg starts contacting the ground and the Ground Reaction Force (GRF) appears only at the heel level
- Loading response: Time period immediately following initial contact to the lift of the contralateral extremity from the ground, during which weight shift occurs
- Midstance: When both the forefoot and heel start contacting the ground
- Terminal stance: As the centre of body mass moves forward in the terminal stance phase, the heel starts taking off, as shown in Figure 2.4. In this phase, only the forefoot touches the ground.

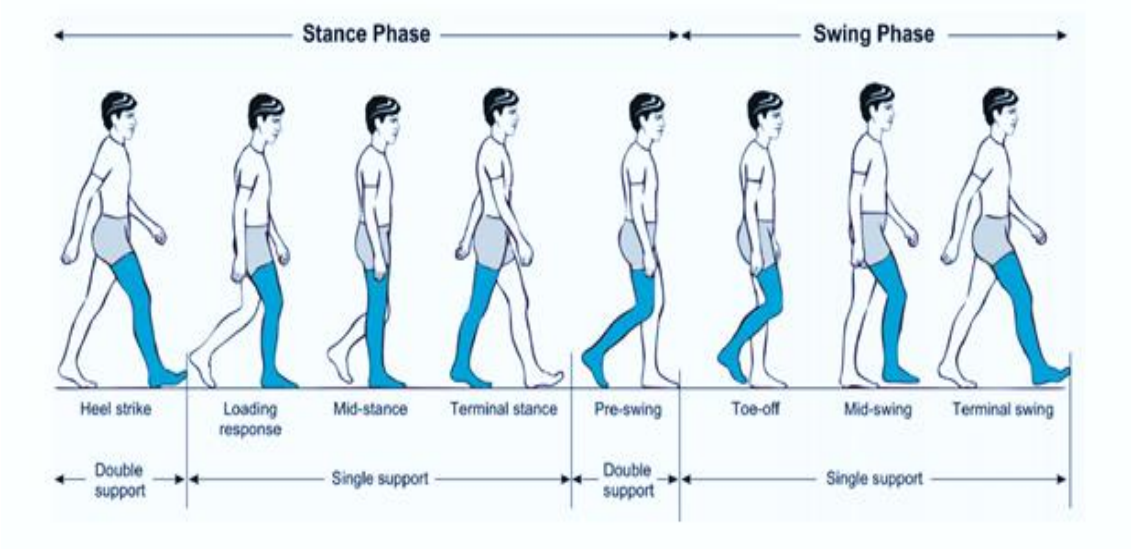

Figure 2.4. Phases of the normal gait cycle (Pirker & Katzenschlager, 2017)

Gait analysis is commonly used to evaluate lower extremity kinematics and kinetics of both normal and pathological motion patterns (Cross et al., 2017). It is an important assessment tool that uses physical measurements and models, including the movement of the person's centre of mass, joint kinematics, ground-reaction forces, the resultant loads, body segment energy variation and muscular work. Motion capture acquires the data of a moving human via sensors and processes the acquired data using a mathematical model. In motion capture, either conventional photography or optoelectronic systems are used for the acquisition of quantitative information (Surer & Kose, 2011).

Marker-based motion capture uses video-based optoelectronic systems, and retro-reflective markers are attached on the human body. Marker-based analysis is generally performed by mounting retro-reflective markers on subjects' bodies and reconstructing their 3-D position via video-based optoelectronic systems. Retro-reflective markers are used together with infrared stroboscopic illumination produced by an array of light-emitting diodes (LEDs) mounted around the lens of each camera. The thresholds of the cameras can be adjusted so that only bright reflective markers are sampled and the markers are recognized via image-based methods. If the marker is visible from at least two calibrated cameras at the same time, the 3-D position of a marker in a reference frame fixed to the laboratory (global frame) can be reconstructed. The estimation of 3-D points of objects from two or more images is called 'stereophotogrammetry' (Surer & Kose, 2011).

2.3 Basic foot and ankle geometry measurement techniques

Measurement techniques of the human foot have become widely used for many clinical applications including orthopaedics, orthotics, sports medicine (Davies et al., 2014; Moorthy & Mond, 2018) and the design and manufacture of footwear (McHenry et al., 2015; Grau & Barisch-Fritz, 2017; Hill et al., 2017; Mishra et al., 2017; Zhao et al., 2017; Dobson et al., 2018). The medical field makes extensive use of different scanning techniques such as X-rays, CT, MRI and ultrasound. These techniques are quite useful for providing information about the internal organs like bones of foot (Haleem & Javaid, 2019). However, many of these scanning techniques are not suitable for capturing external organs like the foot surface and a minor to measure dynamic foot during gait. Therefore, in this section, the review is limited to techniques related to the study of static condition foot and ankle images. To date, a number of techniques have been utilised to capture the foot and ankle (Witana et al., 2006; Cornwall & McPoil, 2011; Liu et al., 2011; Štajer et al., 2011; McHenry et al., 2015; Dobson et al., 2018). According to the literature, the most common techniques are:

1. Measurement sticks, callipers and Brannock devices (Nixon et al., 2006; Witana et al., 2006; Schaiwanichsiri et al., 2008; Cornwall & McPoil, 2011; McHenry et al., 2015; López-López et al., 2016)
2. Casting and foam impression (Guldemond et al., 2006; Štajer et al., 2011, Bushey, 2012)
3. 3D scanner (Mauch et al., 2008; Zhao et al., 2008; Luximon & Luximon, 2011; Menz et al., 2014; McHenry et al., 2015; Grau & Barisch-Fritz, 2017; Dobson et al., 2018)
4. ToF cameras (Lindner et al., 2010; Castaneda et al., 2011; Liu et al., 2011)
5. X-ray and CT scan (Razavi et al., 2003; Cheung & Zhang, 2005; Antunes et al., 2008; Spyrou & Aravas, 2012)
6. MRI (Dai et al., 2006; Cheung & Nigg, 2008).
7. Image-based close-range photogrammetry (Coudert et al., 2006; Luhmann & Robson, 2006; Luhmann, 2010; Al-Baghdadi et al., 2011; Alshadli et al., 2011; Kimura et al., 2011)
8. Camera projector system (Kimura et al., 2008; Schmeltzpfenning et al., 2011)
9. Moiré technique (Takasaki, 1970; Madden & Karlan, 1979; Gomes et al., 2010; Vecchio et al., 2012).

Some of these techniques are measurement by contact and others are non-contact. Based on their features, we can divide the techniques in two groups: manual and optical techniques. The

features and the limitations of each technique are highlighted in following sections.

2.3.1 Manual techniques

2.3.1.1 Measuring sticks, callipers and Brannock tools

The simple, manual tools are used to measure foot dimensions and shoe length (Schwarzkopf et al., 2011; McHenry et al., 2015). Most measure in inches (in) and centimetres (cm). Digital calliper measurement tends to be influenced by human error (Lee et al., 2014). Details of these measurements can be found in Cornwall and McPoil (2011) and Pohl and Farr (2010).

The Brannock device is the most common foot measurement technique for developing shoes and measurement of foot length, arch length, and foot width. The device name was given to the inventor name Charles Brannock (Figure 2.5). Rossi (1983) reported a large survey of foot dimensions of a total of 4000 women and 2800 men. The measurements were conducted by many shop assistants across the USA. A flat ruler and a Brannock device were used to collect two length and two breadth measurements. The measuring position was not standardized and varied from non-weight-bearing to full-weight-bearing. Xiong et al. (2010) determined foot deformations with nine foot dimensions using the Brannock device.

Nixon et al. (2006) assessed the prevalence of poorly fitting footwear in individuals with and without diabetic foot ulceration by measurement stick. McHenry et al. (2015) focused on establishing the correct sizing and tolerances for safe and effective footwear in order to prevent the discomfort and injury described while maintaining performance characteristics. They found a mean size reduction of almost four UK shoe sizes between the climbers' street shoe size and that of their climbing footwear using a calibrated foot/shoe ruler.

Tomassoni et al. (2014) assessed age-related changes of foot morphology for developing appropriate footwear with particular reference to the elderly using a tape measure and calliper. They found that foot circumference was the parameter showing the most relevant age-related differences both in males and in females.

Although the measuring stick, callipers and Brannock devices are inexpensive, lightweight, easy to carry, non-invasive, accurate enough for most of foot length and width measurements,

and suitable for linear foot/shoe measurements such as shoe size, foot length and ball width, these devices cannot be assumed to be appropriate for heel girth or ball girth, as the relationship between ball width and girth is not standardised. Moreover, these techniques more widely used to create an axis going from the pternion to the second toe or hallux. This will ensure that the axis position is dependent on the foot size. The disadvantage of these devices are that some feet may have deformed second toes or hallux valgus (Witana et al., 2006), thereby creating an inappropriate central axis. Therefore, they are used to measure normal subjects' feet. Furthermore, the shoe orders may need a more accurate measurement of foot dimensions to select optimum shoe size. Therefore, these devices are not sufficiently accurate to measure foot/shoe (Menz et al., 2014).

In addition, these devices are not suitable to measure internal foot segments' locomotion and cannot be used to examine the foot during gait analysis.

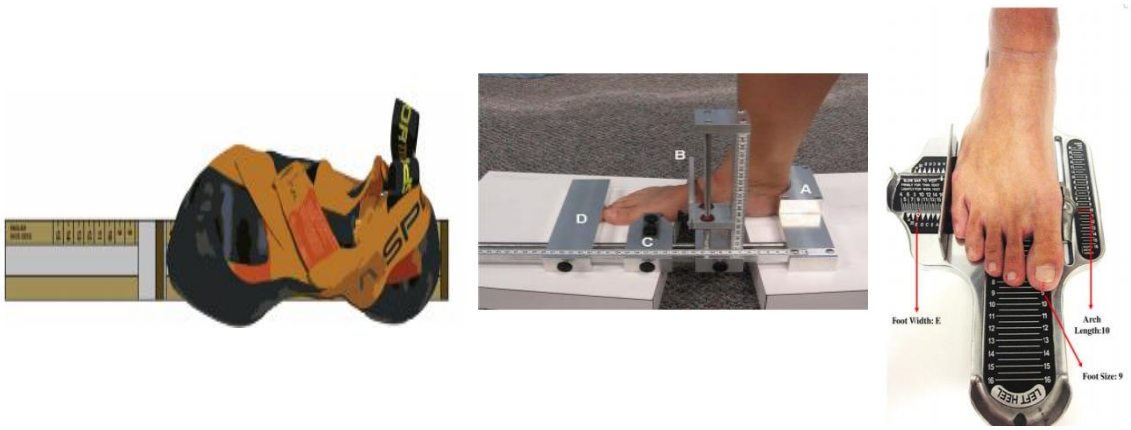

Figure 2.5. Illustrating measurement (from left): measuring stick (McHenry et al., 2015), calliper (Pohl & Farr, 2010), and Brannock (Kong et al., 2015)

2.3.1.2 Casting and foam impression tools

In podiatry, foot impression foams are still the preferred method for designing semi weight-bearing custom insoles (Rogati et al., 2019). Preferred custom-made foot orthotic fabrication processes are casting and the use of foam impression tools (Chuter et al., 2003, Ross, 2018). Although, both techniques are considered relatively traditional, they are still commonly utilised in clinical examinations due to the low cost of required equipment and materials (Štajer et al., 2011). However, new technology has emerged permitting the use of 3D scanning, computer aided design (CAD) and computer aided manufacturing (CAM) in the fabrication of foot molds and custom foot orthotic components (Dombroski et al., 2014). The existing casting and foam

impression tools have been designed to obtain negative casts or impressions of static human feet and 3D foot models of the foot during walking (Štajer et al., 2011), see Figure 2.6.

Patients are often cast for custom foot orthoses in subtalar joint neutral, and the most common impression (or casting) methods used by practitioners include plaster bandage, foam box, fiberglass (Balsdon et al., 2021). However, a number of drawbacks are associated with the use of casting and foam impressions methods which reduce. These major drawbacks are: inefficiency, unclean process, low accuracy and the requirement of a static foot position (Al-Baghdadi et al., 2012).

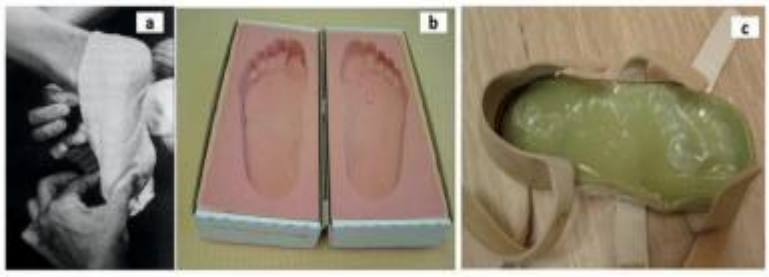

Figure 2.6. (a) Casting process; (b) Foam impression techniques; (c) Dynamic impression during walking (Al-Baghdadi et al., 2012)

2.3.2 Optical techniques

Optical technology, as a non-contact measurement technique, has gained more attention in the last few decades because of its non-destructive imaging characteristics combined with high accuracy and sensitivity (Goda et al., 2019). Generally, optical measurement techniques can be classified into two main approaches. The first approach uses laser beams which move across the scanned surface and reflect back to a light sensor (Urbanova et al., 2015). They consist of 3D scanning systems (Telfer & Woodburn, 2010; Menz et al., 2014), CT and MRI systems (Cheung & Nigg, 2008; Luximon & Luximon, 2011; Spyrou & Aravas, 2012). The second approach uses white light and is called image-based systems like video camera systems (Coudert et al., 2006; Luhmann, 2010; Al-Baghdadi et al., 2011; Alshadli et al., 2011) and ToF cameras systems (Lindner et al., 2010; Castaneda et al., 2011; Liu et al., 2011).

Optical measurement methods, such as photographic, 3D scanners or video camera systems, might offer several advantages over manual clinical measurement methods. Recently, optical techniques have been adopted for the fast topographic mapping of foot surface (Ross, 2018;

Balsdon et al., 2019). Since light is the means of measurement, the total absence of mechanical contact can be achieved along with high measurement speed. Consequently, foot measurements are feasible with such non-invasive techniques. A brief overview of optical techniques is provided in this section.

2.3.2.1 X-ray, CT scan, MRI and 3D scan

X-ray, CT, MRI, and laser scanning provide a platform to study anatomy and physiology and aid in diagnosis and disease monitoring (Haleem & Javaid, 2019). It is the type of electromagnetic radiation probably most well-known for their ability to see through a person's skin soft tissue such as organs, skin that cannot absorb high-energy rays, and pass beams through them and reveal images of the bones beneath it and use small amounts of radiation to create images of your body (Furlanetto et al., 2012).

Lundberg et al. (1989) investigated ankle and subtalar joint kinematics for eight healthy subjects using x-ray tubes and a reference grid. Biplanar x-ray fluoroscopic system have recently become wide-spread in dynamic kinematic measurement of humans. Ito et al. (2015) confirmed that biplanar x-ray fluoroscopy for direct assessment of 3D bone kinematics was sufficiently accurate for actual analysis of foot kinematics (Figure 2.7). Stagni et al. (2005) used x-ray projections to measure ankle joint morphology, including length, height and width, for 36 patients with ankle sprain or trauma. The level of radiation exposure is considered safe for most adults, but not for a developing baby. However, dense materials like bones absorb radiation when the status of bone is captured through the X-ray (Haleem & Javaid, 2019).

CT combines multiple X-ray images into a 3D model of a region of interest. It provides detailed information about the body such as brain and its vessels, heart, lungs, neck, spine, shoulder, reproductive system and in some studies to demonstrate that diabetic subjects (Ledoux et al., 2006; Telfer et al., 2017) with a high-resolution image (Haleem & Javaid, 2019). It works on the principle that a high number of 2D scans is produced using an X-ray source and these slices are merged together into one 3D model (Herman, 2009). CT reaches up to 0.2 mm spatial resolution in an output 3D model (McCollough & Zink, 1999). Although it reaches the desired resolution, it cannot be used because of the high expositions of ionizing radiation. For this reason, use of this modality is recommended as rarely as possible and repeated scanning is completely out of the question. CT devices are also very expensive to purchase and operate (Chromy & Zalud, 2014).

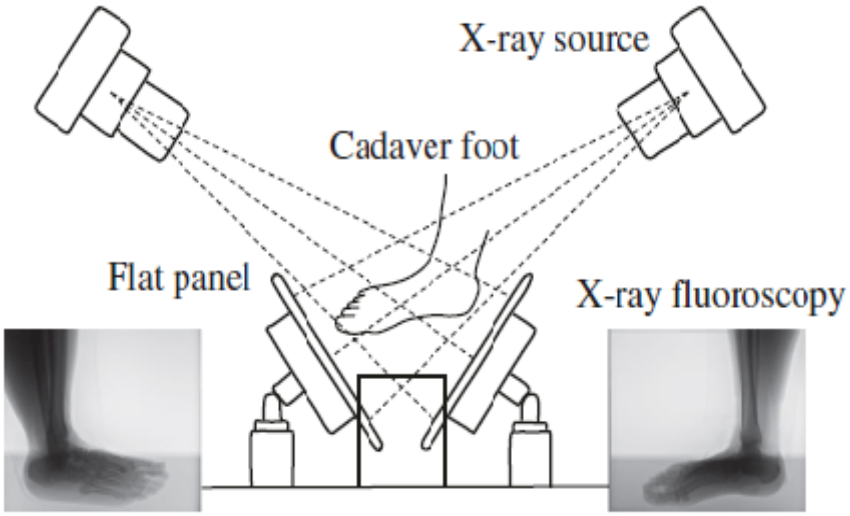

Figure 2.7. Biplanar X-ray fluoroscopy system (Ito et al., 2015)

Compared to the technologies mentioned above, MRI is the best modality for capturing 3D models of bone, soft tissue, organs and other internal structures of the body (Haleem & Javaid, 2019). It doesn't use X-rays, and with sufficient resolution (approximately 1 mm), does not produce harmful radiation, so it can be used repeatedly (Novelline & Squire, 2004). So, there is no limitation on number of models scanned. But, MRI is complex, and machines are expensive to purchase and operate (Chromy & Zalud, 2014).

The 3D scanner has become a complementary scanning tool for other scanning technologies, and is having a significant impact on a variety of medical applications (Treleaven & Wells, 2007) and footwear manufacturing (Menz et al., 2014). It is applied to measure the dimensions of a foot template (Barisch-Fritz et al., 2014; Mchenry et al., 2015; Grau & Barisch-Fritz, 2017; Dobson et al., 2018). Most of the existing 3D foot measurement systems use laser scanning technologies which take several seconds to scan the foot which is not feasible for dynamic foot applications. Krauss et al. (2008a) investigated sex-related differences in foot morphology. In total, 847 subjects were scanned using a 3D foot scanner. Their study supplements the field of knowledge for the manufacturing of shoes. Mauch et al. (2008) used 12 relevant 3D foot measures for 1437 girls and 1450 boys using a three-dimensional (3D) foot scanner. The benefits of using 3D foot scanning are that it allows a high number of participants to be scanned speedily and the measurement is sturdy, and it is efficient and provides repeatable digital

representations of foot/ankle shape. The 3D scanner is also used to obtain digital footprints to assemble reliable foot dimensions (Telfer & Woodburn, 2010; Lee et al., 2014). Lee et al. (2015) compared foot shape and foot dimensions of Taiwanese and Japanese females and 3D foot scanning were used for their comparison.

The difference between 3D scanning with X-rays, CT scan, MRI scan and ultrasound is that scanning through 3D scanning provides information about the outer surface of the body whereas scanning by X-rays, ultrasound, CT, MRI ultrasound technologies provide internal geometry of body parts like bone, tissue and organs. However, 3D scanning techniques are not appropriate for capturing the dynamic alterations of the foot shape during gait.

There are two main drawbacks associated with 3D scanners: high initial set-up cost (Lee et al., 2014) and the requirement of proper static foot positions during scanning. Therefore, scanner systems are not suitable for capturing accurate digital 3D surfaces of the dorsal of the foot during gait (Al-Baghdadi et al., 2012).

2.3.2.2 Moiré method

Moiré topography is one of the optical measurement techniques based on the effect, Moiré, which is produced by the overlapping of two optic grids or periodic structures with slight differences (Yeras et al., 2003). Brooks and Heflinger (1969) introduced projection Moiré techniques for gauging the surface deformations of an object or differences in the surface configuration of two similar objects.

Takasaki (1970) was the first researcher to conduct human body measurement and evaluation using the Moiré technique. Takasaki (1982) found that Moiré techniques were very suitable for the measurement of unstable, soft objects such as the human body, hence the technique began to be widely used in medical research, for the detection and assessment of conditions such as scoliosis or curvature of the spine. Del Vecchio et al. (2012) measured the plaster mold of a human foot through an optical system based on projection Moiré and phase-shifting and compared the results with the measurement obtained from a coordinate measuring machine. The Moiré method can be divided into a projection of light and the shadow-based method of measurement. Moiré technology relies on fringe counting for measurements which introduced measurement uncertainties and sign ambiguities. To deal with this issue, a great deal of

information regarding the shape of the measured object is required. The technique uses two gratings, namely a master grating and a reference grating, from which contour fringes can be generated and resolved by a charge coupled device (CCD) camera.

Although the current technology has the advantage of easy application, fast processing, and low cost experimental setup (Cortizo et al., 2003), the complexity in construction and the measurement accuracy are the drawbacks in industrial and commercial applications (see Figure 2.8). When it comes to the foot, measurement errors of 2.0 mm have been reported around the MLA and high levels of uncertainties were found in the Z coordinate. Applications and related references can be found in Bieman and Harding (1997) and Chen et al., (2000).

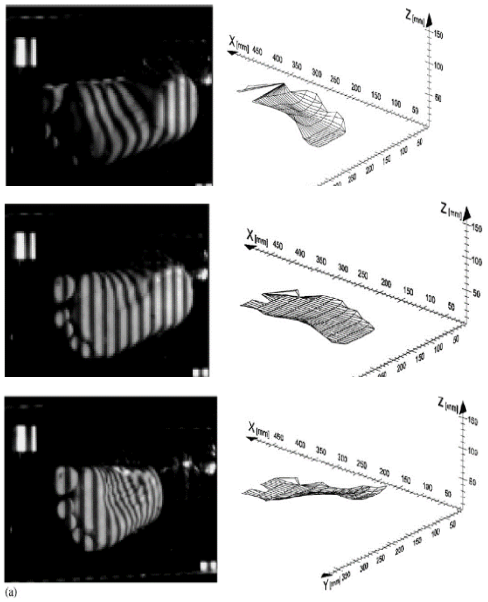

Figure 2.8. Images of foot at heel strike, mid stance, and heel off from CCD camera and Moiré method, (Cortizo et al., 2003)

2.3.2.3 Time-of-Flight (ToF) cameras

3D ToF technology is revolutionizing machine vision and is being applied in various areas such as automotive, healthcare, smart advertising, gaming and entertainment by providing 3D imaging using a low-cost complementary metal-oxide-semiconductor (CMOS) pixel arrays together with an active modulated light source from a source point to the receiver point (Moring et al., 1989; Li, 2014). Figure 2.9 illustrates the ToF concept.

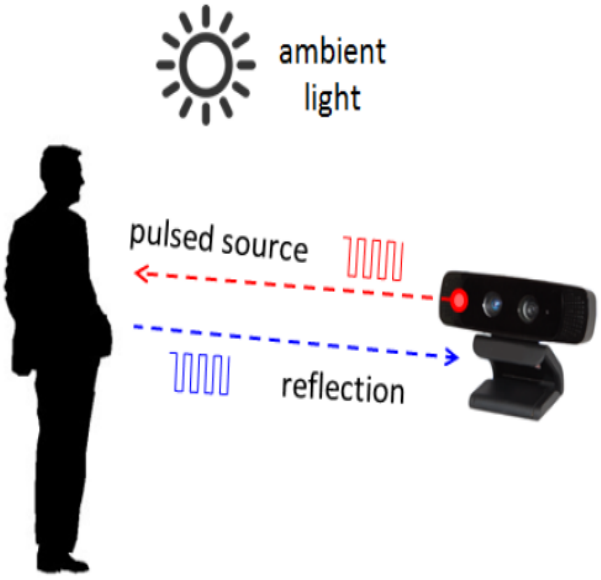

Figure 2.9. 3D ToF camera operation (Li, 2014)

Basically, ToF cameras systems can provide 3D image information of captured objects for up to 50 frames in a second (Oggier et al., 2005; Sturmer et al., 2008; Liu et al., 2011). The ToF camera has been utilised to investigate the dynamic behaviour of the human foot and to visualise the 3D foot surface during gait (Sturmer et al., 2008; Liu et al., 2011). Sturmer et al. (2008) utilised the camera to develop a dynamic foot morphology scanning system for measuring and visualising dynamic deformation of 3D foot models during walking. The system consisted of three synchronised SR4000 ToF cameras (one in the left camera, one in the right camera and one in the bottom camera) fixed onto a walk-away platform.

Liu et al. (2011) used three ToF cameras to determine foot deformation from dynamic 3D models. The deformation was determined using the point set registration technique for consecutive image frames provided by Myronenko and Song (2010). Samson et al. (2014) also used the ToF technology with three cameras to investigate the behaviour of the foot during dynamic foot rollover. The intra-class correlation (ICC) between trial reliability was greater than 0.88.

A ToF camera has a variety of advantages. It can measure 3D depth maps at video rate and thus lends itself to integration into a fast object scanner. It is an active sensor that measures the travel time of infrared light, and as a result does not interfere with the scene in the visual spectrum. Its core components are a CMOS chip and an infrared light source which gives the potential for low cost production in high volume. Finally, its practical operation is no different from a video

camera and can be easily used by everyday users (Cui et al., 2010). Therefore, TOF cameras are an attractive solution for a wide range of applications due their compact construction, ease-of-use, high accuracy and frame-rate makes.

During gait, using the ToF camera for the acquisition of 3D foot data during gait can provide moderate-cost, highly accurate and non-invasive 3D surface models of the human foot (Sturmer et al., 2008; Liu et al., 2011). Jensen et al. (2009) used a version of the ToF camera (the SwissRangerTMSR4000 compared to the SR3000) to improve reflection and precision. However, the technique has some limitations: 1) low quality and low resolution images, 2) the generated 3D foot models may contain a lot of noise and 3) the technique is suitable only for monitoring and visualising slow movement of the human body, such as slow gait, due to the limited number of image frames captured per second (i.e. 40 or 50). More detail of the technique can be found in Oggier et al. (2005), Sturmer et al. (2008) and Liu et al. (2011).

However, CT, MRI and scanner systems are not popular for measuring the foot because these sensors require the foot to be in a static position for a short duration. The advanced ToF camera systems can produce low-resolution dynamic 3D models only. In comparison, the reliability of high-definition (HD) video cameras and photogrammetric image processing techniques for obtaining a dynamic 3D surface of the foot is confirmed in Kimura et al. (2005), Coudert et al. (2006) and Al-Baghdadi et al. (2011). Kimura et al. (2005) developed a 12 video camera system for the 3D measurement of the whole foot during gait. Their results show that a 3D measurement accuracy of ±0.5 mm could be achieved. A video camera can offer low cost, high quality and non-invasive 3D dorsal surface images of the foot during normal gait (Kimura et al., 2005; Amstutz et al., 2008; Al-Baghdadi et al., 2011; Chong, 2011).

2.3.2.4 3D Images systems and photogrammetric techniques

The photogrammetry technique falls into the second group of optical techniques. It is used to extract the geometry, displacement and deformation of a structure using photographs or digital images (Goda et al., 2019). Photogrammetry has been extensively used in the aerospace, civil engineering, wind power blade, and structural monitoring fields (Sansoni et al., 2009; Liu et al., 2012; Valença et al., 2012; Nishiyama et al., 2015). Recently, researchers have used photogrammetry to investigate the dynamic characteristics of structures (Lee & Rhee, 2013; Gwashavanhu et al., 2016). In the last few years, video cameras have been used for capturing

and modelling the three dimensional surface of the whole human body and for more specific dynamic segments of the human body such as the foot (AL-Baghdadi et al., 2011; Ferber & Benson, 2011; Hong et al., 2011; Chong et al., 2015; Al-Kharaz & Chong, 2019a), the leg (Alshadli et al., 2011), and the arm (D'Apuzzo, 2003). Sinclair et al. (2014), using an eight camera motion analysis system, found gender differences in multi-segment foot kinematics and plantar fascia strain during running. Azevedo et al. (2020) compared the multisegmented foot kinematics between professional dancers and non-dancers, during forward and lateral single-leg jump-landings using 10-camera three-dimensional motion capture system. Mousavi et al. (2020) used a three camera, 3D motion capture system to investigate the validity and reliability of a smartphone application for selected lower-limb kinematics during treadmill running.

Photogrammetry is a fast, accurate 3D measurement method in static and dynamic conditions based on photography. Kinematic data captured by video camera system is one of the most powerful tools to analyse the human motion (Kim et al., 2009).

Ferber and Benson (2011) recruited 20 subjects and placed retroreflective markers on the right limb to measure AHI and MLA using an eight camera motion capture system while participants walked on a treadmill. Chong et al. (2015) applied video clips and photogrammetric 3D image processing techniques to investigate the plantar deformation as a result of having a strip of kinesiology tape on the plantar surface through the loading phase of walking. Three camera pairs were arranged around the force plate into a running lane for dynamic surface and deformation measurements of the dorsal foot during running (Blenkinsopp et al., 2012), see Figure 2.10.

Figure 2.10. Cameras configuration around the foot (Coudert et al., 2006)

The 3D photogrammetry reconstruction technique employs the bundle adjustment principle, where the geometric model and the orientation of the bundles of light rays in a photogrammetric shape is implemented by the least squares procedure (Wester-Ebbinghaus, 1988). It typically uses one of the stereo techniques (defocus, shading or scaling) to measure the 3D shape. Close-range photogrammetry applies to objects ranging from 1m to 200m in distance, with accuracies under 0.1mm at the smaller end (manufacturing industry) and 1cm accuracy at the larger end (architecture and construction industry) (Luhmann & Robson, 2006). It is utilised because it is accessible to a majority of professionals, it is a low-cost tool, and presents reproducible results with easy registration and archiving. Interest in this evaluation technique has increased as one advantage of photogrammetry is that it is a non-invasive tool for posture evaluation (Antoniolli et al., 2018).

2.4 Discussion

The foot is the base of support for the chain of motion and body posture (Mauch et al., 2008). Foot morphology and function has received increasing attention from both biomechanics researchers and footwear manufacturers (Shu et al., 2015). In addition, the scientific study of human movement and kinematics of the ankle have considered performance and function by applying the sciences of biomechanics, anatomy, physiology, and neuroscience (Musumeci, 2016). Therefore, this chapter has focused on previous research which measures foot shape and ankle kinematics during gait.

Although there are many studies measuring foot dimensions and analysing foot characteristics in different ethnicities (Kouchi, 1998; Manna et al., 2001; Witana et al., 2006; Zhao et al., 2017; Xu et al., 2018), there is an apparent lack of research in the foot morphology of the Middle East population. Furthermore, the measurements in this study including an analysis and comparison between females and males for many dimensions of foot bones.

The MLA provides an elastic connection between the forefoot and the hindfoot and energy transfer during gait (Balsdon et al., 2016), and shock absorbance during landing and walking. Many techniques have been used to measure MLA but most of these are either inaccurate or expensive (Cavanagh & Rodgers, 1987; Villarroya et al., 2009). Furthermore, the most popular methods use the navicular drop test to evaluate the MLA in static state. In contrast, the close-range photogrammetry technique has high accuracy and low cost compared with other techniques. In addition, it is suitable technique in static and dynamic states.

One of factors found to impact the formation of MLA is sex (Volpon, 1994; Scott et al., 2007; Krauss et al., 2008a). Therefore, it is essential to study the differences between genders practically with various states such as non-WB, partial-WB, and WB (Bandholm et al., 2008; Fukano & Fukubayashi, 2012).

Ankle kinematics assessment is essential for medical problems and footwear design (Fawzy & Kamal, 2010; Sinclair et al., 2012; Kim et al., 2015). Gender differences affect ankle kinematics and females are thought to have better ankle joint flexibility than males, causing females to have larger ankle ROM than males. (Fukano et al., 2018; Sung & Kim, 2018). Therefore, this study focuses on ankle kinematics during walking and finds the differences between males and females of Middle Eastern adults using the close-range photogrammetry technique.

Ankle kinematics during unsteady walking conditions such as uneven land, narrow paths and sloping surfaces (Gates et al., 2013; Koehler-McNicholas et al., 2017; Hamacher et al., 2019) increase the risk of fall and lower extremity injuries (Damavandi et al., 2010; Robinovitch et al., 2013), and may require further analysis. Dixon and Pearsall (2010) reported a decreased inversion of the up-slope ankle and increased inversion of the down-slope ankle on the cross-slope walking surface. Tulchin et al. (2010b) studied the effects of surface slope on foot kinematics in healthy adults and found differences in sagittal plane ROM. Comparing the ankle kinematics of the normal and unsteady gait of the same subjects shows how much ROM is

necessary to avoid acute ankle sprain while walking.

Based on previous studies, various techniques are available to measure foot shape and ankle kinematics. Consequently, shoe manufacturers and foot specialists such as podiatrists and physiotherapists can find it difficult to choose the best foot modelling procedure. The outcomes of this review confirm the findings of other researchers and these results are summarized according to their manual and optical type techniques in Tables 2.1.

Table 2.1 provides a comparison of the geometry techniques used for measuring foot morphology and ankle kinematics. Despite being simple, non-invasive and inexpensive, manual techniques are unsuitable for human gait and inaccurate due to the impact human error (Lee et al., 2014; Menz et al., 2014). Accuracy is essential if the technique is to be used for high accuracy measurement applications (Samson et al., 2012).

Most optical technologies continue to have limitations. For example, ToF cameras and radiography techniques are expensive technologies and not suitable for motion artefacts (Vecchio et al., 2012; Samson et al., 2014; Thabet et al., 2014). To understand foot function, it is necessary to measure the foot in a dynamic condition, hence the above mentioned technologies are unsuitable. Most of the current optical and laser-based foot scanning devices are either too expensive for small clinics, are non-commercial applications, or do not allow foot scanning in WB conditions (Rogati et al., 2019).

AL-Baghdadi et al. (2011) evaluated the accuracy of a photogrammetric technique for capturing 3D foot models during gait using a newly developed imaging system that can capture precise, dynamic 3D dorsal and plantar surfaces of the human foot during gait with an accuracy ±0.3 mm. Video imaging techniques can also offer a lower cost system for capturing dynamic foot surfaces during slow movement with the best 3D foot model quality. On the other hand, the video camera system using low speed video camera is unreliable for capturing 3D foot parameters during fast foot movement (running, jogging or jumping). Blenkinsopp et al. (2012) used three stereo-pairs of high speed cameras (250 fps) to rebuild a 3D model of the dorsum of the foot during running. Their method enabled foot morphology to be assessed but no accuracy information was provided in the study. However, high-speed cameras capable of recording at 200 or more frames per second, can provide an accurate and reliable imaging system for capturing the human foot during fast movement. But, high speed cameras would be costly in a clinical environment.

Table 2.1. Comparison of geometry techniques used for measuring foot morphology and kinematics of ankle

Tec. type	*Technique*	*Authors*	*Accuracy*	*Advantages*	*Disadvantages*
Manual	Stick, callipers and Brannock tools	(Menz et al., 2014; Moorthy & Mond, 2018)	Low	- Simple - Light weight - Low cost - Non-invasive	- Inaccurate - Not fitting for girth measurement - Difficult to use in gait
	Casting and foam impression	(Štajer et al., 2011; Al-Baghdadi et al., 2012)	Low (> 3mm)	- Low cost - Non-invasive	- Inaccurate - Difficult to use in gait
Optical	3D scanner	(Zhao et al., 2008; Schmeltzpfenning et al., 2011; Lee et al., 2014; Novak et al.,2014)	High (<0.5mm)	-High accuracy for static foot scanning -Non-invasive	- High cost - Takes time even to position suitable foot
	MRI and CT	(Dai et al., 2006; Budhabhatti et al., 2007; Wu, 2007; Cheung & Nigg, 2008; Chromy & Zalud, 2014)	Moderate (< 1mm)	-High accuracy	-High cost -Invasive, especially CT scanner - Difficult to use in gait - Only internal geometric like bone
	ToF cameras	(Oggier et al., 2005; Sturmer et al., 2008; Myroneko & Song, 2010; Liu et al., 2011; Samson et al., 2012; Samson et al., 2014)	- High <0.8° angular error and Between trial reliability ICC better than 0.88	-Compact size - Relatively lower cost compared to other scanning technologies - Fast data acquisition rates - High accuracy - Non-invasive	- Time consuming data processing - High cost -Low resolution -Numerous sources of measurement errors -No validity and accuracy information for foot applications.
	Moiré technique	(Cortizo et al., 2003; Vecchio et al., 2012)	Errors greater than 2 mm	-Low cost experimental setup -Automation - Fast processing	-Low measurement accuracy -High levels of uncertainty in the z coordinate
	Image-based close-range photogrammetry	(Kimura et al., 2005; Wang et al., 2008; Coudert et al., 2006; Amstutz et al., 2008; Al-Baghdadi et al., 2011; Blenkinsopp et al., 2012; Yoshida et al., 2012; Antoniolli et al., 2018)	High <0.8 mm Error range = 0.23 mm – 0.37 mm	-High precision and accuracy - Low cost - Non-invasive -Instantaneous data capture ability - Post processing capability -Rapid data acquisition	-Requires camera synchronisation for dynamic applications

2.5 Conclusion

A number of techniques that can be used to obtain accurate 3D measurements of the human foot have been investigated in this chapter. The assessment of these techniques was based on measurement accuracy, advantages and disadvantages. In the case of foot morphology, the manual techniques have been found to be the most appropriate techniques for measuring foot during standing. For the capture of the 3D foot model during gait, the investigation revealed the weakness in the current clinically applied methods. These weaknesses have come from the use of static modelling approaches to observe the dynamic changes during foot movement. Based on the achievable high quantity of the 3D model obtained by video imaging technique and ToF camera systems, it is recommended that they be used to capture dynamic models.

This overview demonstrates that no previous research studies have investigated the capture of accurate foot morphology and ankle kinematics during gait using a precise photogrammetric technique and optical video imaging system. Thus, in the current investigation, the video imaging technique is adopted for capturing human foot shape including medial arch and measuring the kinematics of the human ankle during four stance gait phases (heel-strike, loading response, mid-stance and terminal stance) while walking.

As a result of the advantages of the close-range photogrammetric technique (outlined in this chapter) which outweigh the disadvantages, this technique is developed for the application of the dynamic assessment of the ankle during gait. Details of the design and development of the close-range photogrammetric technique for capturing foot morphology and ankle kinematics during gait are provided in the next chapter.

Chapter 3. Design of an accurate 3D images-based system for foot morphology and kinematics of ankle measurements

3.1 Introduction

This chapter details the design of the accurate image-based measurement technique used for foot morphology and ankle kinematics during gait based on the concepts of close-range photogrammetry. Accuracy, precision and reliability assessments of the designed system will be investigated in this chapter, thus achieving the research aim and objectives outlined in Chapter 1. The chapter begins with a theoretical background of the concepts used to construct 3D models from 2D images. The concepts include the mathematical fundamentals, camera calibration and bundle triangulation. The next section explains the requirements of the designed system. After that, the methodology of the designed dynamic photogrammetric system and an initial testing of the capability of the developed system is investigated. The final section includes a discussion of the capability of the developed system and the expected research contribution that can be achieved from its use.

3.2 Theoretical background

Photogrammetry is a three-dimensional measurement technique which uses central projection imaging as its fundamental mathematical model. As the imaging geometry within the camera and the location of the imaging system in object space are known, every image ray can be defined in 3D object space. Close-range photogrammetry offers the potential of measurement precision to 1:500,000 with respect to the largest object dimension (Luhmann, 2010). Photogrammetry is comprised of two fields – terrestrial and aerial photogrammetry. Terrestrial implies that the images are taken from the ground while aerial photogrammetry is usually taken from an aerial platform such as a drone or satellite. Terrestrial photogrammetry is classified as being close-range photogrammetry if the distance between the camera(s) position and the object is less than 300 metres. Close-range photogrammetry has a variety of applications (Luhmann et al., 2014; Evin et al., 2016; Fawzy, 2019). The following are applications (with examples) that are among the most important in close-range photogrammetry (Luhmann et al., 2014):

- Automotive, machine and shipbuilding industries
  - – Inspection of tooling jigs
  - – Reverse engineering of design models
  - – Manufacturing control
  - – Optical shape measurement
  - – Recording and analysing car safety tests
  - – Robot calibration

- Aerospace industry
  - Measurement of parabolic antennae
  - Control of assembly
  - Space simulations
- Architecture, heritage conservation, archaeology
  - Reconstruction of damaged buildings
  - Mapping of excavation sites
  - 3D city models and texturing
- Engineering
  - As-built measurement of process plants
  - Measurement of large civil engineering sites
  - Deformation measurements
  - Pipework and tunnel measurement
  - Mining
  - Road and railway track measurement
- Police work and forensic analysis
  - Accident recording
  - Scene-of-crime measurement
  - Legal records
  - Measurement of individuals
- Animation and movie/film industries
  - Body shape record
  - Motion analysis
  - 3D movies
  - Virtual reality
- Medicine and physiology
  - Dental measurement
  - Spinal deformation
  - Plastic surgery
  - Neuro surgery
  - Motion analysis and ergonomics
  - Microscopic analysis
  - Computer-assisted surgery

Close-range photogrammetry has significant links with aspects of graphics and photographic science. For example, computer graphics and computer vision, digital image processing, geographic information systems (GIS), cartography and, recently, links with biomedical analysis used by 3D reconstruction techniques from 2D images sourced from film, digital sensors or video sensors employing the bundle adjustment principle where the geometric model and the orientation of the bundles of light rays in a photogrammetric relationship is developed analytically and implemented by the least squares procedure (Wester-Ebbinghaus, 1988; Luhmann, 2010; Fraser, 2015). It is carried out with bright markers on the surface of the object being measured, and multiple video sensors used to record a dynamic scene. This makes it essential to synchronise the sensors to record the exact position on the object. Extensive

research has been carried out by Fraser (1992) to improve accuracy to one part in 1,000,000 and minimise errors associated with motion artefacts (Johnson et al., 2009; Leifer et al., 2011). Photogrammetric measurements extract metric data in the 3D object space from 2D images. The photograph is a perspective (central) projection. During the image formation process, the physical projection centre object side is the centre of the entrance pupil while the centre of the exit pupil is the projection centre image side. The two projection centres are separated by the nodal separation. The two projection centres also separate the space into image space and object space as indicated in Figure 3.1. The collinearity equations in 3.1 provide the perspective projection relationship between the 3D coordinates in the object space and corresponding 2D coordinates in the image plane (Liu et al., 2012).

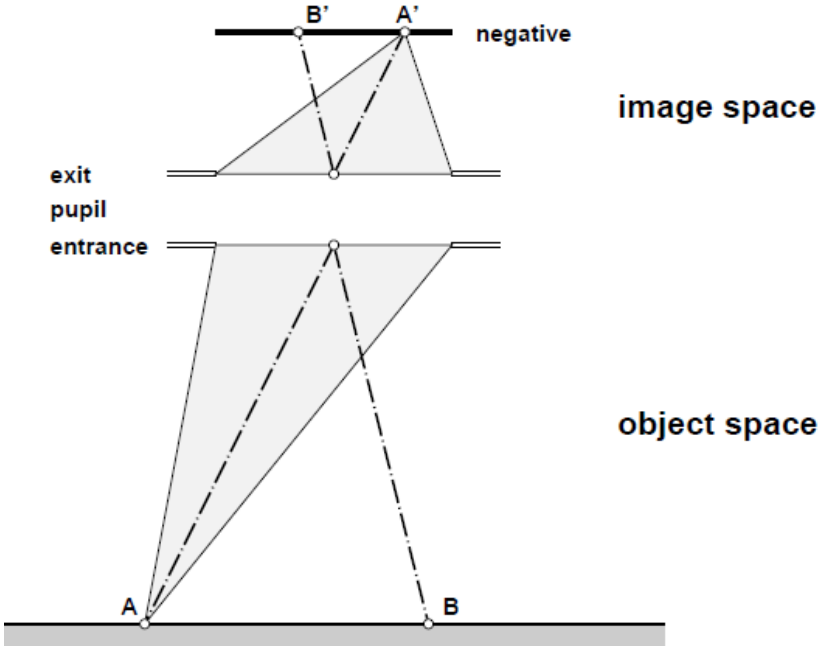

Figure 3.1. The concept of image and object space (Schenk, 2005)

3.2.1 Mathematical fundamentals

The basic problem in analytical photogrammetry is to mathematically relate the positions in space of imaged objects (X, Y, Z) to the positions of their image points in the plane of the image (x, y, z) and vice versa (Mikhail et al., 2001; Zhang & Yao, 2008). The collinearity condition is used to develop solutions to this problem which is that the camera station, the image point, and the imaged object all lie on a straight line. Usually, the form of the image coordinates of an object are expressed as functions of the interior orientation as defines the form of the bundle of

rays emerging from the perspective center to the points in the object space. Interior orientation parameters that consist of: a) the perspective center position (The point at which the three lines connecting the polygon vertices of perspective triangles (from a point) concur), b) the principal distance (the distance of the perpendicular line from the perspective center (center of lens opening) to the image plane of the camera), c) the principal point (point on the image plane which is at the base of the perpendicular from the 'centre of the lens', or more correctly, from the rear nodal point) position (x_i', y_i') relative to the image plane's reference system and d) the lens distortion (lens produces curved lines where straight lines should be) parameters (Δx and Δy). To solve the transformation of the object coordinates (X, Y, Z) into corresponding image coordinates (x, y, z), it is essential to determine the exterior orientation parameters as defines position and orientation in the object space for object transformations. This consists of six parameters which describe the spatial position and orientation of the camera's coordinate system with respect to the global object coordinate system (Luhmann & Robson, 2006), see Figure 3.2. These parameters are comprised of three projection center coordinates (X_0, Y_0, Z_0) and three parameters around the three axes (ω, φ, κ) around the X, Y, Z axes respectively (Chong et al., 2013). The set of equations is known as the collinearity equations (Equations 3.1). These equations are used to link the interior orientation and the exterior orientation parameters (Liu et al., 2012; Kortaberria et al., 2017) as shown below, and are derived in Appendix B.

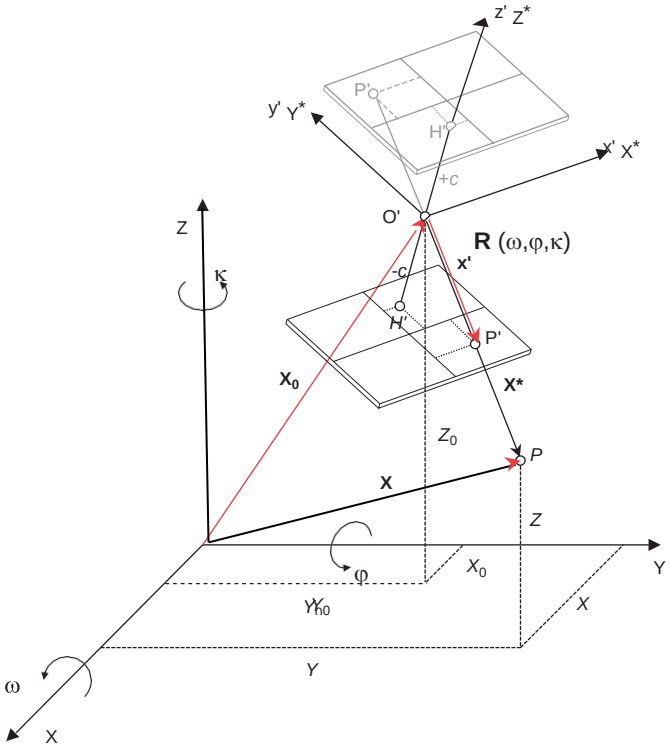

Figure 3.2. Exterior orientation and projective imaging (Luhmann & Robson, 2006)

$$x' = x'_0 + z'\frac{r11(X - X_0) + r21(Y - Y_0) + r31(Z - Z_0)}{r13(X - X_0) + r23(Y - Y_0) + r33(Z - Z_0)} + \Delta x'$$

$$y' = y'_0 + z'\frac{r12(X - X_0) + r22(Y - Y_0) + r32(Z - Z_0)}{r13(X - X_0) + r23(Y - Y_0) + r33(Z - Z_0)} + \Delta y' \quad \ldots (3.1)$$

Where, x′, y′ are the image coordinates and x'_0 , y'_0 represent the position of the offset principal point, z' is the principal distance, is equal to (-f) the focal length of the measured image and Δ x′, Δ y′ represent the lens distortion parameters. These equations describe the transformation of object coordinates (X, Y, Z) into corresponding image coordinates (x′, y′) as functions of the interior orientation parameters (x'_0, y'_0, z', Δ x′, Δ y′) and exterior orientation parameters (X_0, Y_0, Z_0, ω, ϕ, κ) of one image. In the local coordinate system which results, object coordinates are denoted by X*, Y*, Z* (Hui et al., 2012).

Where rij (i,j=1,2,3) are the elements of the rotation matrix M=M(κ)M(ϕ)M(ω)=[rij] that are functions of the Euler orientation angles(ω ,ϕ, κ), equations 3.2 (Liu et al., 2012; Borlin, 2014).

$$\begin{aligned}
&r11 = \cos\phi \cos\kappa,\\
&r12 = \sin\omega \sin\phi \cos\kappa + \cos\omega \sin\kappa,\\
&r13 = -\cos\omega \sin\phi \cos\kappa + \sin\omega \sin\kappa,\\
&r21 = -\cos\phi \sin\kappa,\\
&r22 = -\sin\omega \sin\phi \sin\kappa + \cos\omega \cos\kappa, \qquad \ldots (3.2)\\
&r23 = \cos\omega \sin\phi \sin\kappa + \sin\omega \cos\kappa,\\
&r31 = \sin\phi,\\
&r32 = -\sin\omega \cos\phi,\\
&r33 = \cos\omega \cos\phi.
\end{aligned}$$

3.2.2 Camera calibration

Camera calibration is an important part of the photogrammetric process for obtaining the lens

parameters such as the principle distance or calibrated focal length, the lens distortion parameters and the lens decentring parameters which are required for subsequent image processing to eliminate systematic errors from the processed 3D data (Fryer, 2001). This type of calibration involves the determination of the principal distance or calibrated focal length, the principal point offset (Xp, Yp), radial lens distortion parameters (K_1, K_2, and K_3), the decentring parameters (P_1 and P_2) and, in some instances, the dynamic fluctuation (affinity and shear) (Jiang & Jauregui, 2010). Generally, equations (3.3) are used in the photogrammetry self-calibration bundle adjustment (Wolf & DeWitt, 2000; Chong et al., 2009; Al-Kharaz & Chong, 2018):

$$\Delta x' = \Delta x'_0 - \frac{x'}{PD}\Delta PD + K_1 x' r'^2 + K_2 x' r'^4 + K_3 x' r'^6 + P_1 (r'^2 + 2x'^2) + 2P_2 x' y' - C_1 x^1 + C_2 y'$$

$$\Delta y' = \Delta y'_0 - \frac{y'}{PD}\Delta PD + K_1 y' r'^2 + K_2 y' r'^4 + K_3 y' r'^6 + 2P_1 x' y' + P_2 (r'^2 + 2y'^2) + C_2 x'$$

...(3.3)

Where

$\Delta x'$, $\Delta y'$: Axis-related correction values for imaging errors,
$\Delta x'_0$, $\Delta y'_0$: Small corrections for perspective centre (Xp, and Yp),
ΔPD : Small corrections for principle distance,
K_1 , K_2 , K_3 : Lens distortion parameters,
p_1 , p_2 : Decentring distortion parameters,
c_1 , c_2 : Affinity and shear parameters, and
r' : Radial distance.

The camera parameters used to reconstruct the bundle of rays relative to the object space from the image points are known as the interior orientation parameters. Any distortion in the lens alters the ideal central projection and needs to be determined and accounted. Lens distortion is one of the main factors affecting camera calibration (Fryer & Brown, 1986; Wang et al., 2008). There are two types of lens distortion: radial lens distortion (δr) and tangential lens distortion (Δx and Δy) (Fryer, 2001).

Radial lens distortion is a significant problem in the analysis of digital images (Hartley & Kang, 2007). Radial distortion is caused by the flawed radial curvature of a lens (Wang et al., 2008). It is the result of the radial displacement of an imaged object from the principal point (Vass & Perlaki, 2003). The magnitude of radial distortion varies with the radial position and is dependent on changes in the focus of the camera lens. A Gaussian radial distortion graph is

used to depict the relationship between the radial distortion and the radial position, see Figure 3.3.

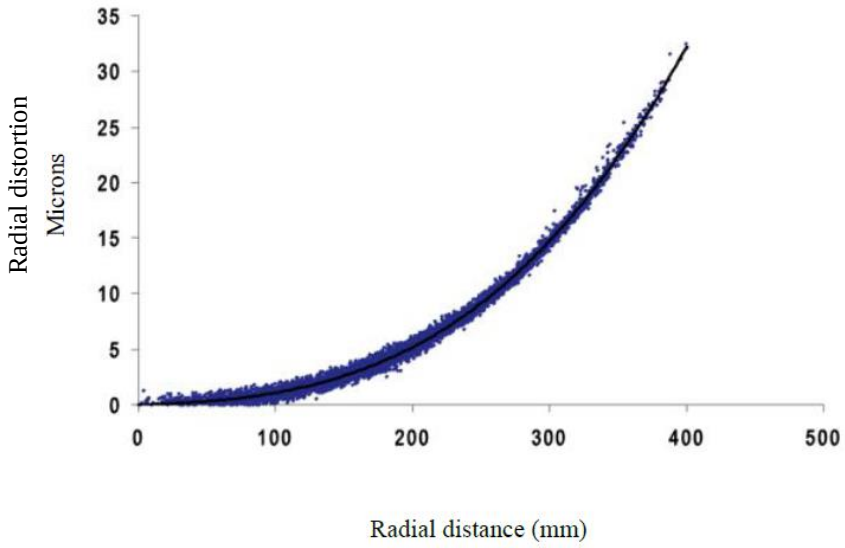

Figure 3.3. Radial distortion versus radial position (Hartley & Kang, 2007)

The radial distortion (δr) which is measured in microns (μm) is modelled using the following polynomial relationship (Wang et al., 2008):

$$\delta r = K_1 r^2 + K_2 r^4 + K_3 r^6 + \ldots + K_n r^{n*2} \quad \ldots (3.4)$$

Where, K_1, K_2, K_3 are the radial distortion coefficients corresponding to infinity focus, *n is a degree of polynomial*, and r is the radial distance in millimeters which is calculated in Equation 3.5 as:

$$r = [(xo - xi)^2 + (yo - yi)^2]^{0.5} \quad \ldots (3.5)$$

The tangential lens distortion is a result of any vertical or rotational displacement of the lens elements within the objective. Brown (1971) developed a function to compensate for the tangential lens distortion (Δx, Δy) on an image point that is represented by x, y (Fryer, 2001):

$$\Delta x = P_1 (r^2 + 2(xo - xi)^2) + 2P_2 (xo - xi)(yo - yi) \quad \ldots (3.6)$$

$$\Delta y = P_2 (r^2 + 2(yo - yi)^2) + 2P_1 (xo - xi)(yo - yi) \quad \ldots (3.7)$$

Where, P_1 and P_2 are the coefficients of the decentring distortion at infinity focus, *x0* and *y0*

are the undistorted coordinates in the image plane, (x_i, y_i) is principle point, and r is the radial distance.

3.2.3 Bundle triangulation

The bundle method of photogrammetric triangulation, more usually known as bundle adjustment, is vital to close range photogrammetry (Luhmann & Robson, 2006). Bundle triangulation (bundle block adjustment, multi-image triangulation, multi-image orientation) is a method for the simultaneous numerical fit of an unlimited number of spatially distributed images (bundles of rays) (Luhmann et al., 2014). When multiple cameras are used to image an object from different convergent views, a multi-image triangulation is achieved, see Figure 3.4. This produces line convergences in the image space which can be used to solve for the point in the object space. A bundle adjustment is a method used to simultaneously determine the 3D object coordinates, the camera calibration parameters, orientation of the images, and accuracy and reliability information through the process of triangulation in a single 'bundle' (Triggs et al., 1999; Luhmann & Robson, 2006).

The bundle adjustment computations are determined through a least squares estimate (Brown, 1976; Granshaw, 1980) which is used to determine the best possible agreements between the measurements and their residuals with the definite model (Cooper and Robson, 2001). The bundle adjustment technique is the most accurate, powerful and flexible technique used in photogrammetry due to the large number of degrees of freedom resulting from the large number of elements that are combined in the same calculation (Luhmann & Robson, 2006). The bundle adjustment theory and mathematical model are highlighted in Appendix B.

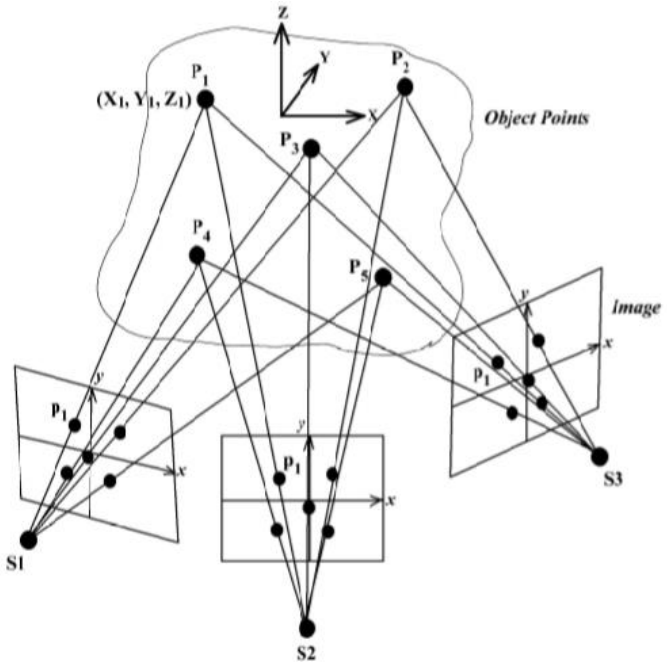

Figure 3.4. Multi-image triangulation s1, s2 and s3 are three cameras, p_1 to p_5 are five target points, XYZ coordinates determined from intersecting rays (iWitnessPRO User Manual)

3.3 Practical requirements of the designed system

The main requirements for the practical work in this thesis include the design of an accurate image-based measurement tool to study the 3D foot morphology and dynamic ankle changes in the stance phase during gait. The practical requirements for the designed measurement system for this project are as follows:

1. Easy to setup
2. Low cost solution
3. Able to measure dynamic 3D anthropometric measurements of the foot and ankle
4. Able to achieve a high level of static and dynamic object measurement accuracy
5. Able to capture the dorsal foot and ankle from the medial, lateral, anterior and posterior positions using multiple stereo and convergent images
6. Able to incorporate and synchronise video camera data during imaging.

As the main design requirement is to develop a photogrammetric system that can be used to measure a dynamic scene to a high level of accuracy, instantaneous records from multiple video-based sensors are required. For this purpose, smartphones have become an important and

common electronic device in everyday life (Ebrahim, 2004; Derawi et al., 2010). Recent research has indicated that the number of smartphone users is expected to reach 2.87 billion in 2020 (www.statista.com). Many applications have used the smartphone camera (Raghavendra et al., 2013; Wang et al., 2014; Al-Kharaz & Chong, 2019a).

A number of factors that determined the distance between camera and object include the image resolution, scale of image, number of control points, field of view and number of image points (Saadatseresht et al., 2005). Equation 3.8, identifies the maximum allowable camera to object distance (Dmax):

$$Dmax = \frac{\bar{\sigma} f \sqrt{k}}{q\sigma} \quad \ldots (3.8)$$

Where, $\bar{\sigma}$ is the object point's coordinate standard errors,
σ is the image point coordinate standard errors,
f is the camera principal distance,
k is the average number of exposures at each camera station, and
q is the factor of the camera station configuration strength, a larger value for the q indicates the higher geometric strength for the network.

To carry out the automatic smartphone cameras' calibration via iWitness software which is designed for determining 3D object point coordinates from 2D images recorded with a digital camera or cameras. In order to apply iWitness to digital images created by take or scan images, some instructions were required (iWitnessPRO User Manual, 2018):

- The smartphone cameras to be calibrated in order to ensure photogrammetric measurement is both accurate and reliable
- An array of coded calibration targets were placed on white carton box area, approximately 2.5 x 1.5m, on which to position the coded targets. This formed the target range, which was photographed from a camera-to-object distance of about 3-4m, depending on the lens focal length and field of view. The red codes, which were printed from a pdf file were saleable. It is very desirable that some of the target point array do not lie in a perfect plane; more than one of the coded targets were placed out of the plane by 15-20cm or more. In spite of the planar array is still working but a target array with some 3D distribution is much better than a planar array

- Both target array stability and fixed focus are very important, therefore all targets did not move at all. It is very useful to set this and then leave it set for the subsequent 3D measurement projects. All smartphone cameras have a set manual focus then focus lock. It is very important to calibrate the camera at the same zoom/focus that will be employed for follow-up measurements. Typically, the focus will be set to infinity and the zoom at one of its 'hard stops', usually zoomed fully out (widest field of view). Once these settings are made, the operator can balance the requirements of imaging distance versus target field dimensions. The 'focal length' actually refers to the Principal Distance, which changes with focusing. The nominal lens focal length usually relates to infinity focus. Also, with zoom cameras this focal length value can vary dramatically, but we seek only one value for the camera used in the survey. Radial distortion can reach significant levels in digital camera lenses and it needs to be corrected when computing the 3D feature point positions to even modest accuracy levels. Radial distortion also varies with focusing which is a further reason not to alter focus or zoom within a measurement network. Furthermore, attention needs to be given to lighting, with well-exposed images displaying minimum saturation or underexposure. Therefore, LED projectors were used during the video recording calibration. A high-precision invar scale bar (length 864 mm) with an accuracy (±0.025mm) was placed on the middle of the calibration box. The scale bar had two high signalized targets attached to both ends to recognize and measure the scale length precisely from the captured images. To evaluate the accuracy of each calibration procedure, the measured calibrated length of the scale bar was compared to the true length. Example layouts are shown in Figure 3.5
- Images were recorded in mixed 'landscape', 45 degree and portrait orientation. It is absolutely critical that this 90˚ variation of roll angle is present. It is not really important which images are rolled 90˚, but at least two must be. About 25 images were captured in different view and orientation for each smartphone camera. The camera roll arrangements in Figure 3.6 are example configurations.

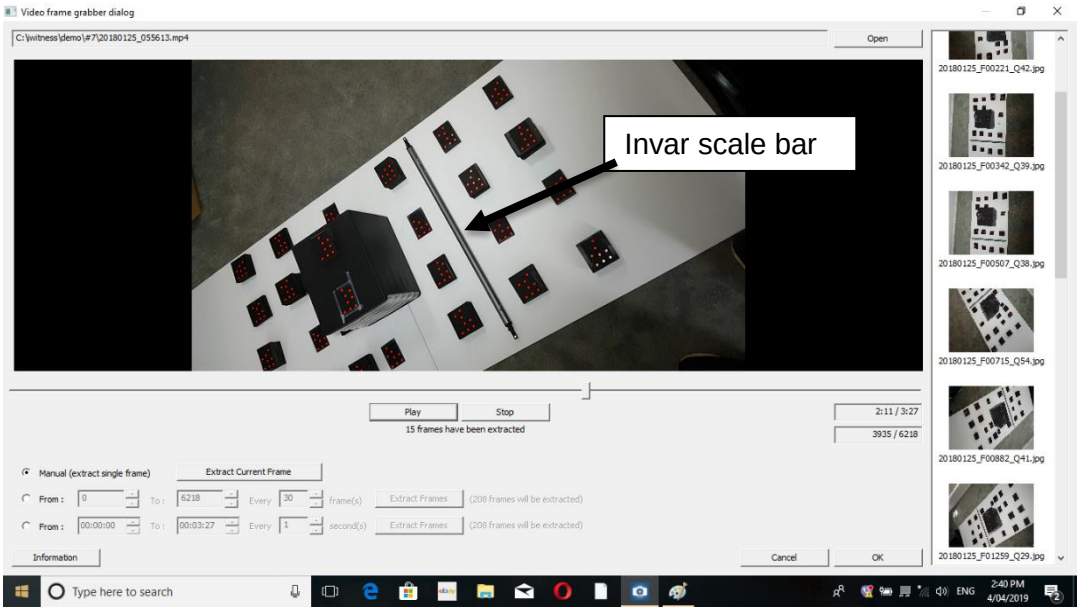

Figure 3.5. 25-target array and invar scale bar for smartphone cameras' calibration in iWitness software

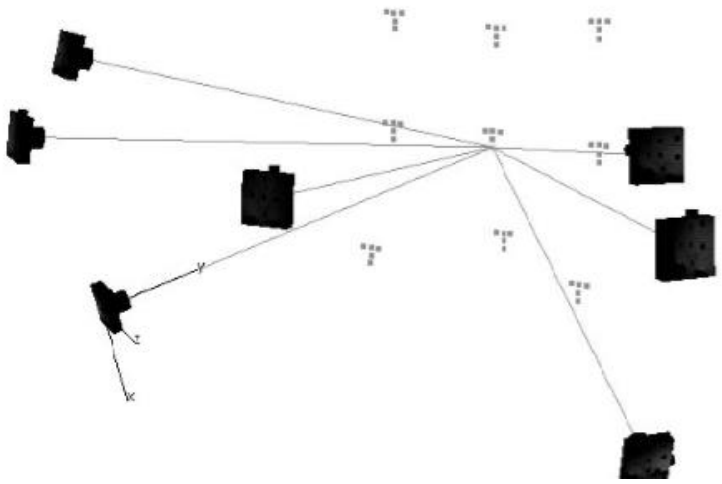

Figure 3.6. Convergent images of target array for each of the smartphone cameras

3.4 Method

3.4.1 Software

For calibration of the designed system, two software were used. To extract the image frames from the video clips, Virtual Dub (V.1.6.15) freeware was selected. With Virtual Dub

(V.1.6.15), 60 images can be extracted from every second of video recording. For determining 3D object point coordinates from 2D images recorded with a digital camera or cameras in both accurate and reliable measurement, off-the-shelf multi-image bundle adjustment software, iWitness*PRO*-V4 Photometrix software (2018), was utilised for the smartphones' calibration.

3.4.2 The designed system

High definition (HD) Samsung Galaxy S6 cameras were selected. These cameras provided the most cost-effective solution for high quality video recording and large internal memory storage capability (Wang et al., 2014; Al-Kharaz & Chong, 2018). The smartphone camera specifications are listed in Table 3.1.

Table 3.1. Smartphone Galaxy 6.0 specifications

Imaging sensor	*1/ 2.6 inch (5.5 mm x 4.1 mm)*
Pixel size	0.001µm
Focal length	4.3mm
Format size	1920 ×1080 (5.17x2091 mm)
Video frames	60fps

Participants stand on the ground in a normal upright posture and walk at a natural pace with the smartphone cameras set up on a tripod to record the video clips for the foot from the medial, lateral, dorsal, anterior and posterior sides simultaneously. Basically, the number of imaging sensors used in any photogrammetric project is dependent on the object coverage which requires sufficient overlapping correspondences between the images (Barazzetti et al., 2010). Usually 55% - 60% overlap strength between images provides a first approximation of an optimal sensor configuration (Fraser, 1996).

From Equation 3.8 the maximum allowable distance determined for this project was 1.3 metres. The values for q and k were representative of a strong network geometry and were selected as q = 0.8 and k = 1 (Fraser, 1996). A minimum camera to object distance of 0.9 metres was selected to provide sufficient coverage of the foot location, the anthropometric (retro-reflective) targets and the control target boards were placed on the right side of the foot location, Figure 3.6. The convergence angle between cameras was selected as 45° with distances between

camera pairs specified at 0.5 metres to achieve the appropriate overlap percentage between images.

The custom-built mounts consist of scale bar with predefined base distances where the distance between the centres of the camera lenses can be adjusted according to the project requirements. The smartphones devices were labelled S1 to S7 and were setup in the same position each time the foot posture and gait trials were conducted. A schematic diagram of the convergent camera pair setups achieved through the smartphone configurations used to image the foot is shown in Figure 3.8.

For smartphone synchronisation during recording, a timing clock and 3-flash LED were used at 30 second intervals; each flash lasted 0.05 seconds for the subject's foot posture and during gait, see Figure 3.7.

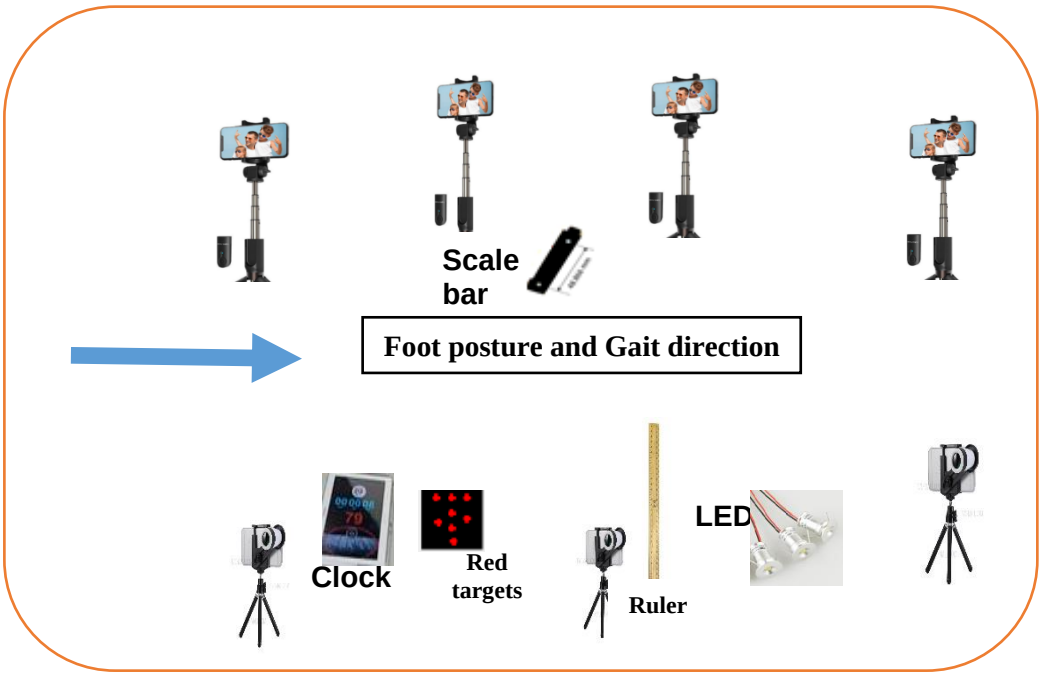

Figure 3.7. Schematic of foot posture and gait direction

Before utilizing the designed system for data collection, camera calibration is an important step in photogrammetric work to improve the accuracy of measured imaged coordinates (x, y). The system calibration process involved individual calibrations of the seven Galaxy smartphones. The calibration methods are discussed in the following sections.

In this study, all tests of foot morphology and ankle kinematics during gait depended on 2 mm diameter reference points which were mounted on the dorsal foot and ankle regions. A number of podiatrists provided knowledge and guidance for positioning of the markers on these region. See the letter of confirmation for one podiatrist in Appendix C.

All seven smartphone cameras were calibrated by finding the focal length (c), principal point (X_p, Y_p), radial distortions (k_1,k_2,k_3), decentring distortions (p_1,p_2), and linear distortion (B_1, B_2). The selected cameras were calibrated individually using a self-calibration technique (Fraser & Al-Ajlouni, 2006; Remondino & Fraser, 2006; Udin & Ahmad, 2011; Al-Kharaz, & Chong, 2018).

Each image is sequentially processed, and once the calibration is complete, the calibration results are displayed as indicated in Figure 3.8.

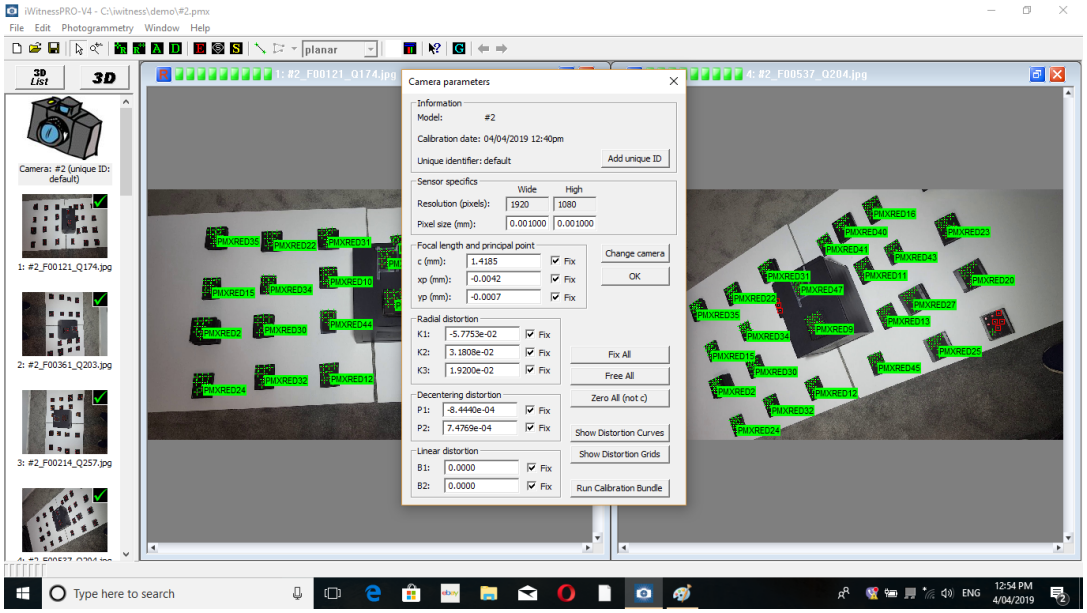

Figure 3.8. Calibration process and results

An acceptable calibration is generally indicated by an internal accuracy of referencing value about 0.3 pixels. Seven smartphones were calibrated and the internal accuracy was 0.36 pixels, see Figure 3.9.

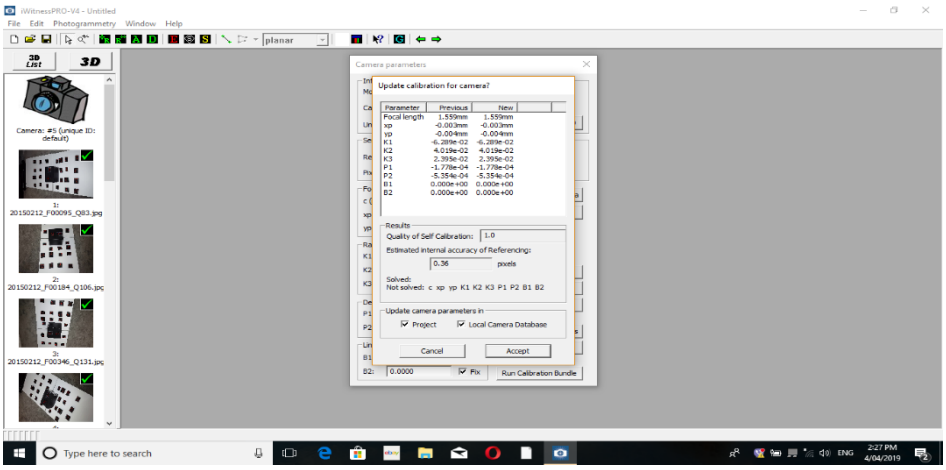

Figure 3.9. Calibration parameters and internal accuracy

3.4.3 Reliability of designed system

To measure the reliability of the designed system, one subject's foot was used to test the static (foot morphology) condition and consistency ankle of kinematics during gait.

3.4.3.1 High reliability foot morphology measurements

Because they reflect the foot's anatomical structure, surface reference points are essential for motion and foot shape analysis (Liu et al., 2004a). In this test, 11 reference points of 2mm in diameter were used on the dorsal foot region. Figure 3.10 shows the captured images that computed some basic 3D foot shape measurements including foot length, foot breadth, heel breadth, bimalleolar breadth, height at 50% of foot length, and navicular height of right foot for an adult. For more details about reference point locations see next chapters. After mounting the reference points, participants stood in an upright bipedal position with their weight equally distributed on both bare feet, while seven smartphone videos were used to record for about 5 seconds. The timing clock and three flashes of an LED were adjusted to synchronise with the video clips. To evaluate the accuracy of each calibration procedure, the measured calibrated length of the scale bar length of 48.866 mm and precision of ±0.05 mm (AL-Baghdadi et al., 2011; Alshadli et al., 2011) and ruler were utilized to evaluate the accuracy of the derived 3D foot coordinates.

Figure 3.10. The reference points to measure foot morphology in designed system

Seven images were used, the 3D shapes coordinate for the foot was collected, and the distance of each parameter of foot dimension was calculated using the self-calibration bundle adjustment, see Figure 3.11. For reliability of testing, the procedure was repeated three testing sessions, and the ICC of measurements were found.

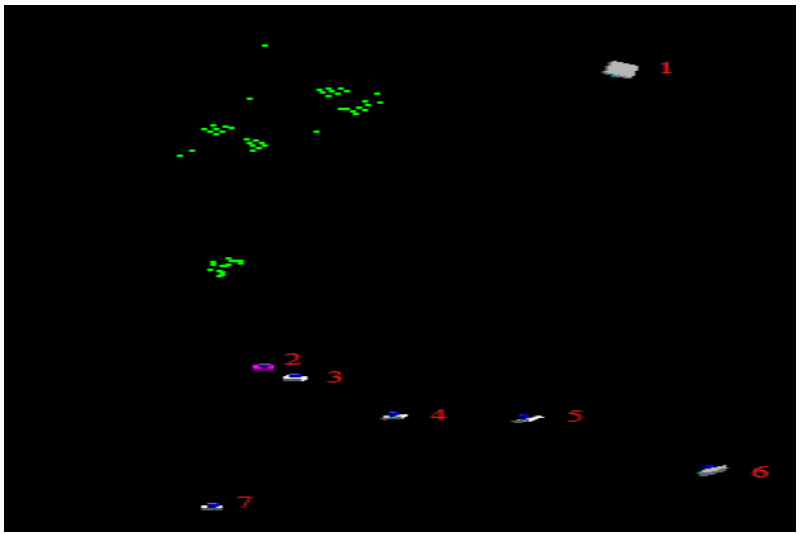

Figure 3.11. Seven smartphone cameras to compute 3D coordinates of reference points on the foot

3.4.3.2 Two feet or one foot to measure ankle kinematics

One of the major lower extremity joints used during normal daily walking is the ankle joint. Evaluation of ankle kinematics is dependent on one foot or two feet. The degree of association between right and left feet in the same subject could be greater than the association between different subjects. This means that you cannot use two feet from the same person in the sample as they are related (not independent of each other; i.e. they are paired). The use of the two feet

of one subject is no longer acceptable in research due to this lack of independence. (Menz, 2004; Bus & de Lange, 2005; Menz, 2005).

The right leg is the dominant leg in medical and sport research (de la Vega et al., 2015; Holowka et al., 2018; Behling & Nigg, 2020; Behling et al., 2020). Therefore, the right leg of all participants was used for each measure of all operations discussed in the next chapters. However, right and left ankle kinematics during gait for one subject was measured to establish the level of consistency between two feet. Seven reference points were mounted on the left and right feet, and the subject was asked to walk at a self-selected speed while the seven cameras captured the motion, see Figure 3.12. Subsequently, data was collected and analysed using iWitness software. For more details of reference point position and analysis, see Chapter 6.

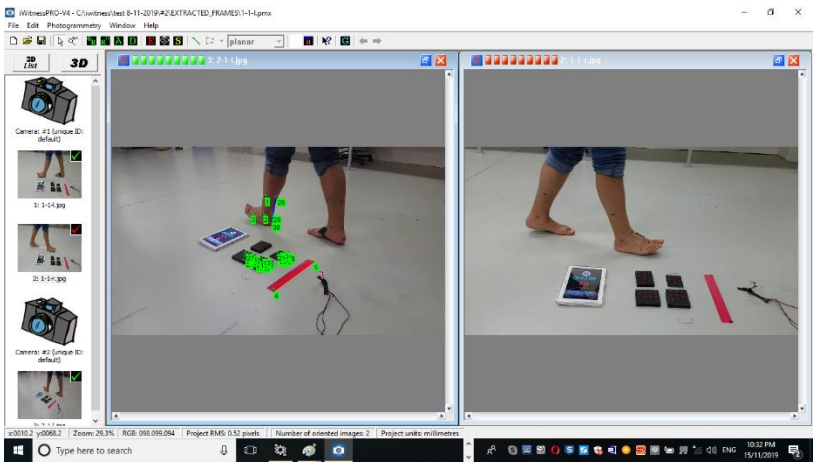

Figure 3.12. Ankle kinematic measurement of left and right feet during walking

3.4.3.3 Statistical analysis

Data analysis was implemented using the Statistical Software for Social Sciences (SPSS) version 25 for Windows (IBM Company). Intrarater reliability was determined through data analysis from the three testing sessions to measure foot shape. The intraclass correlation coefficient (ICC) and standard error of measurement (SEM) data for the distance measures were computed. Descriptive statistics and Pearson correlation were computed to find the relationship between left and right feet.

3.5 Results

3.5.1 Smartphone lens stability analysis

The parameter values of calibrated lens of the seven smartphones used in this research are provided in Table 3.2. These parameters include the camera focal length (FL), the coordinates of the principle point of auto-collimation (Xp and Yp), the radial lens distortion parameters (K_1, K_2 and K_3), and the decentring distortion parameters (P_1 and P_2). Linear distortion parameters, B_1 and B_2, effectively model any relative error in the specified pixel size. They can generally be set 'fixed' to zero and ignored. Generally, Xpand Ypare close to zero (e.g. 0.5mm or less). Overall, root mean square (RMS) error values can be expected to range from about 0.1 to 2.0 pixels, the smaller value indicating greater accuracy. Most commonly, an RMS value of around 0.2-1.5 pixels is good when using a calibrated camera. The results in Table 3.2 indicate the stability of the lenses for all seven smartphone cameras.

Table 3.2. Seven smartphone cameras calibrated intrinsic lens parameters

N	*FL* *(mm)*	*Xp* *(mm)*	*Yp* *(mm)*	*K_1* *(coefficient)*	*K_2* *(coefficient)*	*K_3* *(coefficient)*	*P_1* *(coefficient)*	*P_2* *(coefficient)*	*RMS* *(pixels)*
#1	1.7	-0.0407	-0.0237	-6.6751e-02	2.8551e-02	1.5354e-02	-5.4262e-04	-5.3674e-05	0.56
#2	1.4	-0.0042	-0.0007	-5.7753e-02	3.1808e-02	1.9200e-02	-8.4440e-04	7.4769e-04	0.46
#3	1.5	0.0017	0.0101	-4.4230e-02	2.7185e-02	1.9490e-02	-1.1553e-03	-5.8129e-04	0.63
#4	1.4	-0.0285	0.0017	-5.1763e-02	2.6423e-02	1.6538e-02	8.0998e-04	1.3029e-03	0.71
#5	1.5	-0.003	-0.004	-6.289e-02	4.019e-02	2.395e-02	-1.778e-04	-5.354e-04	0.36
#6	1.5	0.0142	-0.0083	-6.4124e-02	3.7086e-02	2.2092e-02	3.5010e-04	2.0969e-04	0.36
#7	1.7	-0.005	-0.006	-3.276e-02	1.413e-02	6.228e-03	9.688e--5	4.300e-05	0.28

3.5.2 Human foot morphology trials

3D foot shape measurements for an adult were captured and repeated in three testing sessions. The reliability of measurements was found using intraclass correlation coefficient (ICC) and standard error of measurement (SEM), see Table 3.3. The values of ICC indicated a high level of agreement between the repeatable measures. The average value of ICC was high (0.88) for all foot parameters which means test-retest measurement is a very accuracy of image sensor.

Table 3.3. Reliability of foot morphology measurement

Foot morphology parameters	*ICC*	*SEM*
Foot length	0.91	2.9
Foot breadth	0.94	3.3
Heel breadth	0.89	3.5
Bimalleolar breadth	0.81	4.1
Height at 50% of foot length	0.90	2.8
Navicular height	0.88	3.2
Average	0.88	3.3

3.5.3 Correlation between left and right feet of one subject

The outcomes of left and right subject ankle kinematics during gait indicate that there are high correlation in three planes of ankle (0.968), Table 3.4 show this correlation. Mean difference between the subject's left and right feet on three planes for 4 phases of stance during gait ranged between 0.05 and 0.4 mm.

Table 3.4. The correlation of the left and right feet (for one subject) of three planes for 4 phases of stance phase during gait

	Correlations	*Right foot*	*Left foot*
Right foot	Pearson Correlation Sig. (2-tailed)	1	0.968**
	N	12	12
Left foot	Pearson Correlation Sig. (2-tailed)	0.968**	1
	N	12	12

**. *Correlation is significant at the 0.01 level (2-tailed)*

3.6 Discussion

This chapter demonstrates the design of an accurate 3D images-based system for foot morphology and ankle kinematics measures using smartphone cameras to capturing the video images and applies the close-range photogrammetry technique to compute the 3D coordinate points. The design requirements such as the number and type of imaging sensors, geometry of the sensors and distribution of project control were optimised. The photogrammetry technique

utilises images of objects captured by multi-cameras from differing viewpoints to determine the digital 3D model of objects. Mathematical models are used to transform the 2D image to 3D digital models. It is necessary to apply calibration procedures for calibrating smartphone cameras to remove various image distortions such as lens distortions and sensor geometrical distortion. 25 convergent images were used in the calibration to determine the effect of increasing the number of convergent images on the 3D RMS of the control targets. Therefore, close-range photogrammetry provides high precision 3D measurement of the objects. The many advantages provided by this technology include its high level of measurement accuracy and precision (De Menezes et al., 2010; Chong, 2012; Al-Kharaz & Chong, 2018), low cost (Chong, 2011), non-invasiveness (Ladeira et al., 2001, Ahmadi and Layegh, 2014), rapid rate of data acquisition (Kau et al., 2011) and post-processing ability (Luhmann et al., 2014). Furthermore, the system can be developed to allow the capture of images from different imaging sensors, making it ideal for measuring moving objects (Wong et al., 2008).

The RMS of smartphone camera calibration ranging between 0.28 and 0.71 pixels demonstrates stability of all smartphone cameras. In the foot morphology, six foot shape parameters were computed and repeated for the same adult for three sessions. The average reliability using ICC and SEM indicated high level of agreement of the repeatable measures. ICC and SEM were used to determine the measurement accuracy of the image sensors, and indicated a high level of agreement between the repeatable measures. The correlation value (0.968) and the mean differences not exceeding (0.4) indicate that the results of the foot measurements were strongly convergent and the differences between left and right feet could be ignored.

The significant key points of this chapter can be summarised as follows:

1. Accurate 3D photogrammetric images to achieve high level of static and dynamic measurement accuracy

2. Incorporating and synchronising high resolution of seven smartphone cameras can generate high accuracy of 3D shape images

3. 3D images-based systems to measure foot morphology and ankle kinematics have high reliability

4. The discrepancies between the left and right feet for measures in conducting the same measurements were not statistically significant.

3.7 Conclusion

A low cost 3D close-range photogrammetric system for measuring foot morphology and ankle kinematics during gait was presented in this chapter. The system was developed as a cost effective solution for obtaining high accuracy 3D static and dynamic foot measurements. Detailed comparative accuracy, precision and reliability analysis tests of foot morphology measurements using the developed image-based system is assessed in Chapter 4.

Chapter 4. Close-range photogrammetry to measure foot morphology and investigate the differences between genders

4.1 Introduction

The foot plays an important role in supporting body weight, preserving balance and absorbing ground reaction forces generated during general daily activities and sports (Zhao et al., 2017). Therefore, clarifying which factors affect foot morphology may be helpful in understanding the basis of foot deformities and foot dysfunction. Furthermore, inappropriate footwear can cause foot pain and deformity (Nixon et al., 2006; Krauss et al., 2010; Schwarzkopf et al., 2011; Hill et al., 2017; Zhao et al., 2017; Buldt & Menz, 2018). Therefore, to design suitable footwear, fit foot shape characteristics should be considered (Janisse, 1992; Lee et al., 2012; Lee & Wang, 2015; Mishra et al., 2017). Foot morphology is also essential for forensics, orthotics design and medical purposes (forensic scientists, anatomists, physicians, anthropologists, podiatrists, and many other groups) and to understand acute and chronic injuries in athletes and other physically dynamic individuals (Krauss et al., 2008a; Davies et al., 2014; Moorthy & Mond, 2018; Al-Kharaz & Chong, 2019b). Human foot morphology is diverse because a number of factors may have a significant impact on morphology (e.g. ethnicity (Hawes et al., 1994; Ashizawa et al., 1997; Kouchi, 1998; Mauch et al., 2008; Hisham et al., 2012), living habits (Branthwaite et al., 2013), age (Scott et al., 2007; Mauch et al., 2008; Ciccarelli et al., 2011), gender (Krauss et al., 2008a; Krauss et al., 2011; Echeita et al., 2016) and BMI (Mauch et al., 2008; Price & Nester, 2016; Zhao et al., 2017).

Various techniques that have been used to measure foot morphology including visual assessment (Dahle et al., 1991), foot printing (Shiang et al., 1998; Ciccarelli et al., 2011; Moorthy & Mond, 2018), calliper-based measurements (McPoil et al., 2009; Tomassoni et al., 2014; Hajaghazadeh et al., 2018), digital photography (Wang et al., 2008; Pohl & Farr, 2010; Yadav et al., 2015), radiographic imaging (Williams & McClay, 2000; Murley et al., 2009), and 3D scanning (Xiong et al., 2010; Lee et al., 2012; Lee & Wang, 2015; Mishra et al., 2017). In addition, the close-range photogrammetry technique has been used for a large number of medical applications (Majid et al., 2005) and has distinct advantages over other 3D model building methods. Being non-contact, cheap, portable, non-invasive and instantaneous, it

achieves the greatest accuracy with high contrast and real-world colour, and texture and it provides a permanent record. A permanent record allows re-measurement if it is needed (Black & Pappa, 2003; Majid et al., 2005; Al-Kharaz & Chong, 2019b). The close-range photogrammetry technique requires only minimal accompanying equipment with setup and conventional cameras (Schenk, 2005; Evin et al., 2016) such as smartphone cameras that have properties like being secure, easy to use, portable, having video download, and an ability to edit that can be used for particular effects (Al-Kharaz & Chong, 2019a).

Many studies have reported that foot morphology differs between genders in different ethnic populations (Picón-Reátegui et al., 1979; Hawes et al., 1994; Kouchi, 1998; Cho et al., 2004; Gonda & Katayama, 2006; Chaiwanichsiri et al., 2008; Moorthy & Mond, 2018). Kouchi (1998) reported that Mongoloid populations have a wider foot compared to Caucasoid and Australian populations, and East Asian populations have a shorter foot length compared to Southeast Asians and Africans. Hawes et al. (1994) found that the East Asian's forefoot is wider than that of their white counterparts. Sacco et al. (2015) revealed variances in anthropometric foot breadth between German and Brazilian children. However, there have been only a few studies investigating the foot shape of Middle Eastern populations. One of these studies measured 21 foot dimensions in northwest Iran (Hajaghazadeh et al., 2018) but a sample measuring technique was used and only in northwest Iran. Therefore, there are scant studies offering knowledge on the morphology of Middle Eastern adults' feet, and so it is necessary to measure foot morphology of Middle Eastern adults. Furthermore, this chapter investigates the differences between the two participating genders.

4.2 Methods

4.2.1 Participants

Thirty-three participants with healthy feet (18 males 28-47 years and 15 females 25-46 years, male BMI ranging from 21.54 to 35.85 kg/m^2 and female BMI ranging from 18.93 to 30.48 kg/m^2) were recruited for this research. The participants were chosen from postgraduate students from Middle Eastern countries studying at the University of Southern Queensland. No participant had a history of foot surgery or problems affecting foot function. The anthropometric data of participants were observed to be normally distributed using the Shapiro-Wilks test. Table 4.1 shows the anthropometric data of the participants. The anthropometric data of every

participant is provided in Appendix A. Every participant read and signed an informed consent form before their assessment. The study was approved by the Research Human Ethics Committee of the University Southern Queensland where it was performed (approval number H18REA168). The Participant Information Sheet and Consent Form are provided in Appendix D. The same participants apply to all chapters of the thesis.

Table 4.1. Statistics (descriptive mean ± SD) of participating subjects

GENDER (N=33)	AGE (years)	WET (kg)	HEIGHT (cm)	BMI (kg/m^2)
MALES (N=18)	37 ± 6	89.90 ±13.26	175.72 ±6.55	29.12 ±3.96
SHAPIRO-WILK VALUE	0.235	0.644	0.542	0.915
FEMALES (N=15)	37 ± 6	64.89 ±8.71	160.67 ±4.20	25.26 ±4.16
SHAPIRO-WILK VALUE	0.742	0.592	0.347	0.151

4.2.2 Equipment and software

Body height was determined with a measuring tape and weight was measured by a digital scale. Seven smartphone Galaxy 6.0 devices were used (pixel count =1920*1080, focal length=4.3 mm, pixel size=0.0012, video frames=60 fps). All seven smartphones were placed on tripods around the participants and facing towards them. The smartphones captured video recordings of the participants standing upright. Virtual Dub software (v 1.6.15) was used to convert the video frames to images for measurement (Al-Kharaz & Chong, 2019a).

Camera calibration is essential for all smartphone cameras involved in accurate measurements. Camera calibration software is more user friendly for nonmetric film-based cameras and digital cameras (Fryer, 1989; Fraser & Edmundson, 1996). The process includes the determination of the CCD format size, principal point of auto collimation, principal distance, and radial lens distortion parameters (Majid et al., 2005). Software iWitnessPRO-V4 Photometrix (2018) was used to calibrate the smartphone cameras to avoid errors from lens distortions and to determine foot coordinates using a bundle adjustment technique. Calibration was undertaken to reduce measurement error. Calibration for testing the accuracy of smartphones was carried out before

using the devices for research. The range of measurement error using RMSE was less than 0.07 pixels for all images' adjustment.

4.2.3 Foot anthropometrics and markers

Fourteen dimensions of the right foot, including the length, breadth, height, and perimeter were measured (Figure 4.1), and 2mm diameter self-adhesive stickers were placed at anatomical locations.

The dimensions were those most commonly measured in previous studies (Hawes & Sovak, 1994; Witana et al., 2006; Krauss et al., 2010), see Table 4.2. In addition, some of the comprehensive parameters for assessing the arch and foot were computed after extracting the coordinate points of foot dimension and determining the distance between points, see Table 4.3.

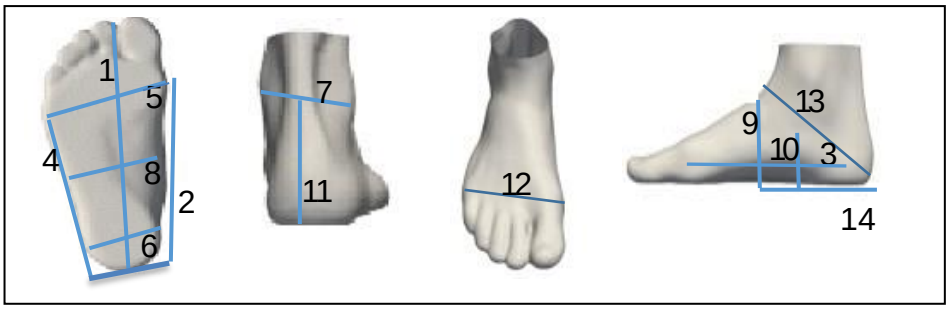

Length: 1, 2, 3, 4, 14; Breadth: 5, 6, 7, 8; Height: 9, 10, 11; Perimeters: 12, 13

Figure 4.1. The fourteen right foot dimensions were measured

Table 4.2. Foot dimension definitions

No.	*Foot dimension*	*Definitions*
1	foot length (FL)	The distance between the most posterior aspect of the heel and the tip of the longest toe measured along the foot axis (Hill et al., 2017).
2	truncated foot length (TFL)	The perpendicular distance from the posterior aspect of the heel to the joint line of the first metatarsophalangeal joint (Hill et al., 2017).
3	arch length (AL)	The distance along the Brannock axis from the pternion to the most medially prominent point on the first metatarsal head (Witana et al., 2006).
4	outside ball-of-foot length (OBFL)	The distance from the most posterior aspect of the heel to the fifth MTP (Mauch et al., 2008).
5	instep length (IL)	The distance between the most posterior aspect of the heel and the instep (Xu et al., 2018).
6	foot breadth (FB)	The maximum horizontal breadth (Y-direction), across the foot perpendicular to the Brannock axis in the region in front of the most laterally prominent point on the fifth metatarsal head (Witana et al., 2006).
7	heel breadth (HB)	The breadth of the heel 40mm forward of the pternion (Witana et al., 2006).
8	bimalleolar breadth (BIB)	The distance between the most medially protruding point on the medial malleolus and the most laterally protruding point on the lateral malleolus measured along a line perpendicular to the Brannock axis (Witana et al., 2006).
9	mid-foot breadth (MB)	The maximum horizontal breadth, across the foot perpendicular to the Brannock axis at 50% of foot length from the pternion (Witana et al., 2006).
10	height at 50% of foot length (HMF)	The maximum height of the vertical cross-section at 50% of the foot length from the pternion (Witana et al., 2006).
11	navicular height (NH)	The maximum length of the vertical line from body surface to the navicular tuberosity (Kanai et al., 2019).
12	ankle joint height(AJH)	The maximum length of the vertical line from the body surface to the ankle joint (Tomassoni et al., 2014).
13	ball girth (BG)	The circumference of the foot, measured with a tape touching the medial margin of the head of the first metatarsal bone, the top of the first metatarsal bone and the lateral margin of the head of the fifth metatarsal bone (Witana et al., 2006).
14	heel girth (HG)	The minimum girth around the back heel point and dorsal foot surface (Witana et al., 2006).

Table 4.3. Popular parameters for assessing the foot

No.	*Parameters*	*Definitions*
1	foot index (FI)	(foot breadth/foot length)*100 (Moudgil et al., 2008; Sen et al., 2011).
2	arch height ratio (AHR)	AHR (%) =navicular height×100/foot length (Xu et al., 2018; Kanai et al., 2019).
3	arch height index (AHI)	AHI= instep height/medial ball of foot length (Butler et al., 2006; Zhao et al., 2017).
4	normalised navicular height to total foot length (NNH-TFL)	NNH_TFL=navicular height/total foot length (Hill et al., 2017).
5	normalised navicular height to truncated foot length (NNH-I)	NNH_ I = navicular height/truncated foot length (Hill et al., 2017).
6	arch height index to total foot length (AHI-TFL)	AHI _TFL=instep height/total foot length (Hill et al., 2017).
7	arch height index to truncated foot length (AHI-I)	AHI_I= instep height/truncated foot length (Hill et al., 2017).
8	Chippaux-Smirak index (CSI)	CSI= the ratio between minimum width of midpoint and the widest width of toes (Papuga & Burke, 2011; Tománková et al., 2015; Costea et al., 2017).
9	Chippaux-Smirak index ratio (CSIR)	CSIR=CSI*100 (Costea et al., 2017).
10	heel-ball index (HBI)	HBI=BHEL*100/BBAL(Krishan et al., 2012). Where BHEL=foot breadth at heel BBAL=foot breadth at ball
11	Staheli index (SAI)	SAI= the ratio between minimum width of midfoot and the widest width of the heel (Papuga & Burke, 2011; Costea et al., 2017).

Where: FI was used to determine the foot types such as, slender, standard, and broad (Jung et al., 2001; Sen et al., 2011). Both AHR and AHI are comprehensive parameters for assessing the arch and foot. A value for AHI close to 0 represents a lower arch, and a value for ASI close to 1 represents a stiffer arch (Zhao et al., 2017). NNH_TFL, NNH_ I, AHI _TFL, and AHI_I to evaluate MLA and measure a relationship between arch height and foot length (Hill et al., 2017). The Chippaux-Smirak index (CSI) and Staheli index (SAI) classify arch foot types, the results of (CSIR) were High Arched [0-20); Normal [20-30); Intermediary [30-40); Low arch [40-45); Flat >45 (Onodera et al., 2008; Costea et al., 2017). HBI may be applied in sex

determination when a part of the foot is used for medico-legal investigation (Krishan et al., 2012).

4.2.4 Statistical analysis

The mean, standard deviation, minimum, and maximum values were computed as descriptive statistics. Levene's test of equality of variance and independent samples of the t-test were used to determine the gender differences using Statistical Software for Social Sciences (SPSS) version 25 for Windows (IBM Company), and each statistical analysis was considered significant if $p<0.01$ and $p<0.05$. Intraclass correlation coefficients (ICCs) were calculated on the test-retest for each of the 33 feet.

4.2.5 Experimental procedure

Height and weight were measured using a fixed tape on the wall and a digital weight scale. The ball and heel girth were measured by tape before mounting the markers. All of the reference points were marked manually. After mounting the reference points, participants stood in an upright bipedal position, with their weight equally distributed on both bare feet (Krauss et al., 2011), while seven smartphone videos were used to record for about 5 seconds Timing clock and three flashes of an LED were used at 30 second intervals; each flash lasted 0.050 seconds, adjusted to synchronise with the video clips. When the seven videos photographed by seven cameras are cut into images, the images will be cut at the same synchronization in each video, depending on the time that appears at each image in the timing clock and the color shown in LED flash. To evaluate the accuracy of each calibration procedure, the measured calibrated length of the scale bar and ruler were compared to the true length, see Figure 4.2. Seven images were used, the 3D shapes coordinate for each foot was collected, and the distance of each parameter of foot dimension was calculated using the self-calibration bundle adjustment.

Figure 4.2. The reference points marked on the right foot

4.3 Results

Mean values and standard deviations were calculated for the 18 males and 15 females to characterize the 14 foot dimensions and 11 parameters of the foot. As in Table 4.4, according to difference in means, we noted that most of the mean parameters were higher in males except FI 0.870 and AHI_TFL 0.002.

Levene's and t-tests for the right foot, in the case of the female group, were compared to the male group with reference to all foot dimensions in this study. The results indicated that there were significant differences ($p<0.05$ and $p<0.01$) in most morphologic characteristics of the feet of each gender. In addition, the mean differences of HG, FL, AHR, and CSIR (4.544, 3.617, 3.011, and 3.766 respectively) were much higher between males and females, indicating that the heel girth, foot length, arch height ratio and Chippaux-Smirak index were longer and wider for males., see Table 4.5.

Analysis to determine test-retest reliability and intraclass correlation coefficients (ICCs) was determined for each participant. The measurements were between 0.78 and 0.91 for all parameters.

Table 4.4. Mean and SD of foot dimension and parameters for gender

Foot dimension and parameters	*Total n=33*				*Males*				*Females*	
	Mean cm	SD	Min. cm	Max. cm	Mean cm	SD	Min. cm	Max. cm	Mean cm	SD
FL	24.200	1.080	24.000	28.000	26.011	1.181	20.900	24.000	22.393	0.978
FB	9.480	0.660	9.000	12.000	10.083	0.845	8.000	10.000	8.867	0.476
MB	5.930	0.440	5.600	7.300	6.483	0.472	4.300	6.100	5.375	0.416
HB	6.080	0.490	5.700	7.800	6.544	0.549	5.000	6.500	5.613	0.422
BIB	9.310	0.570	8.480	11.410	9.777	0.742	8.200	9.930	8.836	0.405
BG	22.440	1.340	21.000	28.000	23.683	1.641	19.000	23.000	21.200	1.032
HG	31.570	1.210	31.000	37.000	33.844	1.641	28.000	31.000	29.300	0.775
TFL	18.610	1.670	14.070	23.530	19.261	2.013	15.880	21.220	17.959	1.324
AL	15.590	1.160	15.010	19.520	16.372	1.075	13.040	17.870	14.802	1.243
HMF	6.630	0.960	5.340	9.120	7.111	0.879	4.270	7.810	6.148	1.038
NH	4.530	0.690	3.900	7.200	5.240	0.757	3.010	4.600	3.825	0.615
OBFL	16.620	1.420	11.010	20.300	17.048	2.030	14.760	17.830	16.197	0.805
IL	12.460	1.110	10.770	14.200	12.503	0.892	9.800	15.280	12.418	1.332
AJH	7.780	0.680	7.260	10.120	8.663	0.774	5.790	7.900	6.886	0.576
AHR	18.670	3.090	15.820	28.240	20.178	3.035	13.090	21.260	17.167	3.146
FI	39.200	2.380	33.330	43.140	38.761	2.590	36.960	45.450	39.631	2.164
AHI	0.300	0.040	0.230	0.410	0.301	0.043	0.210	0.370	0.290	0.045
NNH_TFL	0.190	0.030	0.160	0.280	0.203	0.030	0.130	0.210	0.171	0.032
NNH_I	0.240	0.030	0.230	0.320	0.273	0.031	0.170	0.260	0.213	0.033
AHI_TFL	0.280	0.040	0.220	0.360	0.274	0.033	0.190	0.340	0.277	0.051
AHI_I	0.360	0.040	0.320	0.420	0.369	0.032	0.250	0.430	0.342	0.056
CSI	0.630	0.050	0.570	0.760	0.646	0.045	0.510	0.730	0.607	0.051
CSIR	62.610	4.810	56.670	75.790	64.490	4.453	50.590	72.500	60.723	5.163
HBI	64.220	4.590	59.090	73.680	65.017	3.978	55.000	75.000	63.422	5.193
SAI	0.980	0.030	0.940	1.030	0.992	0.028	0.860	0.980	0.957	0.034

Table 4.5. Levene's test and t-test analysis of foot dimension and parameters

Foot dimension	*Levene's Test*	*P*	*T-Test*	*P*	*Mean Difference*	*Std. Error Difference*	*95% Confidence Interval of the Difference*	
							Lower	Upper
FL	0.137	0.714	9.461	0.000**	3.617	0.382	2.837	4.397
TFL	0.685	0.414	2.146	0.040*	1.302	0.606	0.064	2.540
AL	0.378	0.543	3.891	0.000**	1.570	0.403	0.747	2.393
OBFL	3.926	0.056	1.524	0.138	0.851	0.558	-0.287	1.990
IL	1.483	0.233	0.219	0.828	0.085	0.388	-0.707	0.878
FB	2.820	0.103	4.954	0.000**	1.216	0.245	0.715	1.717
HB	0.991	0.327	5.371	0.000**	0.931	0.173	0.577	1.284
BIB	5.016	0.032*	4.390	0.000**	0.940	0.214	0.503	1.377
MB	1.097	0.303	7.087	0.000**	1.108	0.156	0.789	1.427
HMF	2.574	0.119	2.887	0.007**	0.963	0.333	0.282	1.643
NH	0.041	0.840	5.811	0.000**	1.414	0.243	0.918	1.911
AJH	0.908	0.348	7.349	0.000**	1.777	0.241	1.284	2.270
BG	2.405	0.131	5.076	0.000**	2.483	0.489	1.485	3.481
HG	3.875	0.058	9.830	0.000**	4.544	0.462	3.601	5.487
AHR	1.067	0.310	2.791	0.009**	3.011	1.078	0.810	5.211
FI	0.771	0.387	-1.035	0.309	-0.870	0.841	-2.587	0.845
AHI	0.651	0.426	0.720	0.477	0.011	0.015	-0.020	0.042
NNH_TFL	0.938	0.340	2.960	0.006**	0.032	0.010	0.009	0.054
NNH_I	0.634	0.432	5.314	0.000**	0.060	0.011	0.037	0.083
AHI_TFL	9.758	0.004**	-0.152	0.880	-0.002	0.014	-0.032	0.027
AHI_I	9.769	0.004**	1.731	0.093	0.026	0.015	-0.004	0.058
CSI	0.049	0.827	2.276	0.030*	0.038	0.016	0.003	0.072
CSI ratio	0.095	0.760	2.251	0.032*	3.766	1.673	0.353	7.179
HBI	1.456	0.237	0.999	0.326	1.594	1.596	-1.661	4.851
SAI	0.042	0.839	3.229	0.003**	0.034	0.010	0.012	0.056

*Mean significant if p<0.05

** Mean significant if p<0.01

4.4. Discussion

This chapter discusses the gender differences of foot morphology of Middle Eastern adults using close-range photogrammetry. Fourteen dimensions of the right foot were measured for 33 Middle Eastern adults and 11 popular parameters were used to assess the foot shape. According to Tables 4.4 and 4.5, FL, AL, AJH, BG, HG, AHR, CSI ratio, and HBI of males had a higher mean than females. The results indicated that there were significant differences in some morphologic characteristics of the feet of each gender. The gender variety in foot morphology reported was consistent with the variety found in previous studies (Krauss et al., 2008a; Hong et al., 2011; Krauss et al., 2011; Tomassoni et al., 2014), indicating that men had longer, higher and wider feet than women.

According to Hong et al. (2011) the range of the common FL values in women was smaller than in men. In our study, the FL of males 26.011cm was larger than females 22.393cm. This result was consistent with Tomassoni et al. (2014) who focused on Caucasian participants, particularly people born in Italy, and showed that the measurement of foot length of men was 26.17cm and of women was 23.37cm. In addition, Tobias et al. (2014) recruited 250 males and 250 females from Western Nigeria. The results demonstrated that the length, height and breath of men's feet were significantly greater than those of women. These results can be compared with those of Lee et al. (2015) whose study showed the differences between Taiwanese and Japanese females. It was reported that mean FL in Japanese women was 23.02cm and in Taiwanese women it was 23.53cm. These results accord with our results for FL of Middle Eastern women. Luo et al. (2009) reported that the feet of females and males differ with respect to FL, TFL and AL, which is similar to our results for these dimensions.

In the current study, the BIB and HB was significantly different between genders; the mean value of BIB was 9.777cm for men and 8.836cm for women, and HB value was 6.54cm for men and 5.61cm for women. These results were compatible with those of Bindurani et al. (2017) and Agnihotri et al. (2007). Bindurani et al. (2017) determined that there was a correlation of various measurements of the feet with sex. The mean values of FL, FB, and BIB were significantly higher in males than females. Agnihotri et al. (2007) were able to determine sex (male/female) by foot measurements. They found the average foot length was about 3cm greater in males compared to females and the average foot breadth of males was about 1cm wider than

that females. The difference in ankle width, Achilles tendon width, and heel width between males and females was also distinct in the 3D foot shape (Stanković et al., 2018). Chaiwanichsiri et al. (2008) compared foot characteristics between genders and showed that the foot breadth, ball girth, toe depth, and ankle height in the men were larger than women while arch length and foot length were the same in both genders. Our results for these dimensions agree with this study, where the AL was 16.372cm for men and 14.802cm for women, while BG was 23.683cm for men and 21.20cm for women. According to Moudgil et al. (2008), concerning sex detection based on foot measurements among the North-Indian population, there were no significant differences between the male and female foot index. This outcome is consistent with our study and the mean differences of females was slightly higher than males 0.87.

The Heel-ball index (HBI) is a new index from foot dimensions to determine sexual dimorphism. Krishan et al. (2012) reported that the mean HBI is 64.3 for men and 65.5 for women, indicating that women have higher HBI than men. In contrast, our study showed that the mean HBI of men was higher than that of women (65.017 and 63.422, respectively).

The evaluations of foot arches, including the MLA are very important in the clinical arena (Cashmere et al., 1999). Many parameters are used to assess this arch: arch height index (AHI), normalised navicular height to total foot length (NNH_ TFL), normalised navicular height to truncated foot length (NNH_ I), arch height index to total foot length (AHI_ TFL), arch height index to truncated foot length (AHI_I), Chippaux-Smirak index (CSI), Chippaux-Smirak index ratio (CSIR), and Staheli index (SAI). Our study measured these parameters and may give an indication of the range from pes planus (flat foot/ low-arched) to pes cavus (high-arched) of the foot arch type. Costea et al. (2017) computed CSIR of the feet of elderly women to classify foot typology. They found the mean of the index between 28.71 to 27.24 for left and right foot, respectively, and the average type of feet in the normal foot where the index value is between 20 and 30. In comparison with the current study, the CSIR was 64.490 for men and 60.723 for women which implies the average of male and female with a flat foot has the index value >45. The close-range photogrammetry technique is one of techniques used to measure the object in high precision (De Menezes et al., 2010; Luhmann, 2010), low cost (Chong, 2011) and non-invasiveness (Ladeira et al., 2001). A limited number of researchers have used a close-range photogrammetry technique to evaluate the human body, particularly the foot shape (Van Loon et al., 2010; Catherwood et al., 2011). However, no previous study has examined the foot

characteristics of Middle Eastern adults according to gender. The results show the accuracy of close-range photogrammetry as a means of measuring foot dimensions and identifying differences between genders.

4.5 Summary and conclusions

In this chapter, geometric morphometric methods using a close-range photogrammetry technique were applied to study the shape of feet of Middle Eastern adults of both genders. The close-range photogrammetry technique has enabled us to measure the foot in high precision and at low cost. The findings confirm the men have longer feet than women. The results indicate that the mean of FL, AL, AJH, BG, HG, AHR, and CSI ratio for males was higher than females. Furthermore, the BIB and HB differed significantly between genders. In contrast, there were no significant differences between the male and female foot index. In addition, the mean HBI of men was higher than that of women. The high value of CSIR for both genders indicates that the participants in our results have flat feet. These outcomes for many shapes and dimensions show significant differences between genders that may be useful in the diverse fields of designing well-fitting and comfortable footwear for both men and women, for medicine and, as an extension, for criminal investigations. Arch shape is very important in the clinical researches that is medial longitudinal arch which evaluated in the next chapter.

Chapter 5. Evaluation of the medial longitudinal arch in static and dynamic behaviour during the stance phase of gait

5.1 Introduction

One of the most important structural characteristics of the foot is the MLA (Shiang et al., 1998). The mechanical behaviour of the MLA is important in both research and the clinical arena (Cashmere et al., 1999; Zuil-Escobar et al., 2018) because the MLA shows a high degree of flexibility and provides an elastic connection between the forefoot and the hindfoot (Balsdon et al., 2016). Furthermore, shock absorbance is provided via lengthening in initial loading and recoiling to form a relatively rigid lever facilitating energy transfer during gait. This area of the foot is particularly important for foot function. For example, some foot pain due to altered foot alignment in pes planus and pes cavus is related to MLA, and approximately 25% of sports-related knee injuries are related to MLA stability (Bandholm et al., 2008; Nielsen et al., 2009; Yalçin et al., 2010; Nilsson et al., 2012; Balsdon et al., 2019).

Depending on the structure of the MLA, foot type is classified as either pes cavus (high-arched), pes planus (flat foot/ low-arched) or normally arched (Morrison et al., 2007; Chang et al., 2010; Woźniacka et al., 2013; Balsdon et al., 2016). Currently, a number of techniques and apparatus are used to evaluate and classify the foot in static or dynamic conditions based on measurements of the MLA. Giladi et al. (1985) demonstrated that subjects with pes planus were less likely than subjects with normal or pas cavus to show the development of stress fractures in the lower extremity by a visual assessment alone. Dahle et al. (1991) used the longitudinal arch angle to classify foot type by visual observation and assessment of medial longitudinal arch posture. However, visual categorization of the arch is highly inconsistent (Giladi et al., 1985; Cowan et al., 1994). Other techniques to evaluate the MLA, for example footprint parameters, can be obtained by ink (Cavanagh & Rodgers, 1987; Volpon, 1994; Villarroya et al., 2009). Hawes et al. (1992) measured the highest point of the soft tissue along the MLA in full weight bearing by footprint measurements. Although these techniques can be easily obtained and are non-invasive and inexpensive, the measurements do not necessarily represent the state of the bony architecture of the foot (Williams & McClay, 2000). Furthermore, the major associated disadvantages are difficulties in interpretation and the imprecision of measurements (Shiang et al., 1998; Yalçin et al., 2010; Zuil-Escobar et al., 2018). Some researchers have incorporated

the use of radiographs or photographs like X-ray and ultrasound to classify the medial longitudinal arches of their subjects (Villarroya et al., 2009; Fukano & Fukubayashi, 2012). Radiographs have several limitations, including ionizing radiation exposure and, therefore, potential health risks. Moreover, they are relatively expensive and require special facilities (Shiang et al., 1998). Other researchers have used a 3D scanner (Chang et al., 2012) and biplane fluoroscopy (Balsdon et al., 2016; Balsdon et al., 2019) to measure the MLA, both of which use real time rays and have greater accuracy for bone images. Furthermore, they have only been used to a limited extent in developing countries because of the high cost and because they are invasive techniques (Hajaghazadeh et al., 2018). In addition, they are most useful for static conditions or just the first step when walking. The literature states that after the first four strides, there is an increase in walking speed. Thus, a person's walking cannot be considered their average speed until the fifth stride (Balsdon et al., 2019). According to Muir et al. (2014), the steps of normal walk begin after the first four strides. Therefore, the first strides may not be representative of the normal gait speed of the participants (Balsdon et al., 2016).

However, the close-range photogrammetry technique is concerned with obtaining reliable information from images about the properties of surfaces (Whitehead & Hugenholtz, 2014). It is extensively used in the civil engineering, aerospace, structural monitoring (Liu et al., 2012; Valença et al., 2012; Nishiyama et al., 2015), and physiotherapeutic applications (Antoniolli et al., 2017), and is suitable for dynamic applications (Gwashavanhu et al., 2016; Al-Kharaz & Chong, 2019a). It also has been used in the medical field (Chong et al., 2008; Chong, 2011) because it is a non-invasive technique, low cost compared with radiography techniques and achieves the greatest accuracy with high contrast, solid-coloured circular targets. The high contrast is most often achieved using retro-reflective targets with smartphone cameras (Black & Pappa, 2003; Al-Kharaz & Chong, 2019b). In addition, 60 frames per second (fps) smartphones can record videos and the resolution is adequate for foot movement stereo-image capture. Furthermore, smartphones are secure, easy to use, portable, have video download and an ability to edit that can be used for particular effects (Al-Kharaz & Chong, 2019b). Therefore, images captured with smartphones and photogrammetric techniques are precise, three dimensional techniques to measure foot in static and during gait (Al-Kharaz & Chong, 2019a). This chapter used an accurate geometric 3D method (CRP) to evaluate the MLA in static (non-WB sitting and 50% WB, 10% WB, 90% WB standing) and dynamic motion during gait, based on the MLA angle. In addition, MLA angle differences between males and females in static and dynamic conditions were measured.

5.2 Methods

5.2.1 Participants

The MLA of the right foot of thirty-three healthy adult participants were tested while sitting, equal, partial bodyweight standing, and during the stance phase of walking were measured. Subject characteristics are presented in Table 5.1.

Table 5.1. Subject characteristics, mean (SD)

Gender	*Age (y)*	*BMI (kg/m^2)*	*Foot length (cm)*	*Foot breadth (cm)*	*Heel breadth (cm)*
Female	37 (6)	25.26 (4.16)	22.39 (0.98)	8.87 (0.48)	5.61 (0.42)
Male	37 (6)	29.12 (3.96)	26.01 (1.18)	10.08 (0.84)	6.54 (0.55)
Average	37 (6)	27.19 (4.06)	24.20 (1.08)	9.48 (0.66)	6.08 (0.48)

5.2.2 Equipment and Software

Height and weight for each participant were measured using a fixed tape on the wall and a digital weight scale. Three Smartphone Galaxy 6.0 devices (pixel count =1920*1080; focal length=4.3 mm; pixel size=0.0012; video frames=60 fps) were used to capture videos from the medial aspect of the foot being recorded. To convert the video frames to images for measurement, Virtual Dub software (v 1.6.15) was used and iWitnessPRO-V4 Photometrix software (2018) was used to calibrate the smartphone cameras to avoid errors from lens distortions and to determine foot coordinates using a bundle adjustment technique. MATLAB software calculated the angle created by these three markers in the coordinate system using the dot product of two vectors, from the most medial aspects of the medial calcaneus, navicular tuberosity and head of the first metatarsal joined by straight lines (Tome et al., 2006), the function code as shown:

```
>> acos(dot(u,v)/(norm(u)*norm(v)))
```

Where the u and v are vectors. Microsoft Excel software and SPSS version 25 for Windows (IBM Company) were used to analyse data and conduct each statistical analysis.

5.2.3 Smartphone camera calibration

Digital camera calibration is essential to achieve the precision of the measurement task (Hamid

& Ahmad, 2014). To carry out the automatic smartphone camera calibration using iWitnessPRO-V4 Photometrix software, an array of target boards were put with an invar scale bar on a white carton box area. The invar scale bar had two high signalized targets attached to both ends to identify and measure the scale length precisely from the captured images. To evaluate the accuracy of each calibration procedure, the measured calibrated length of the scale bar was compared to the true length; example layouts are shown in Figure 5.1. Orthogonal roll angles were used for the camera; images were recorded in mixed 'landscape', 45° and portrait orientation. 25 images were captured in different view and orientation for each smartphone camera. Three smartphone cameras were calibrated by finding the focal length (c), principal point (x_p, y_p), radial distortions (k_1, k_2, k_3) and decentring distortions (p_1, p_2), and linear distortion (B_1, B_2) as mentioned in Chapter 3. The selected cameras were calibrated individually using a self-calibration technique (Udin & Ahmed, 2011; Fraser, 2015; Al-Kharaz & Chong, 2018). An acceptable calibration is generally indicated by an internal accuracy of referencing value about 0.3 pixels. Three smartphones were calibrated and an internal accuracy was 0.32 pixels.

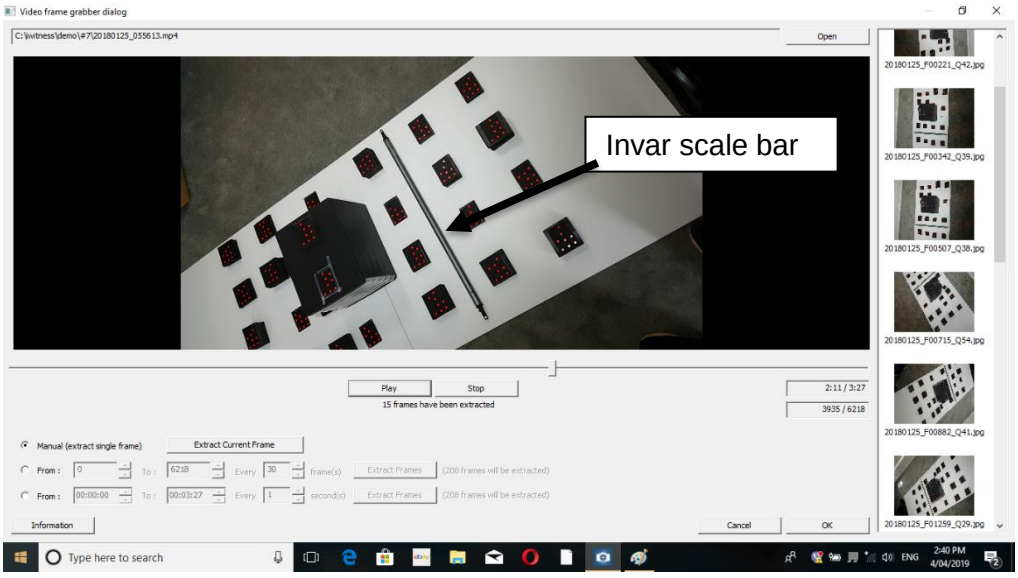

Figure 5.1. Array of target boards and an invar scale bar for smartphone camera calibration in iWitness software

5.2.4 Experimental protocol

In this method, five 2-mm diameter reference points were used on the right barefoot only for further analysis see references (Menz, 2004; Bus & de Lange, 2005). All of the reference points were marked manually. Each subject's subtalar joint was in a neutral position (relaxed state)

and markers mounted on anatomical locations: two markers measuring foot length were mounted on the posterior aspect of the heel and the most distal aspect of the longest toe, and three were mounted on the navicular tuberosity, medial aspect of the first metatarsal head, and the medial side of the calcaneal bone to measure the MLA angle consistent with Tome et al. (2006), Shultz et al. (2011), Balsdon et al. (2016) and Yoon et al. (2017), Figure 5.2. MLA posture is generally calculated as the angle between two 3-dimensional vectors bounded by those markers. Each subject was constantly observed during the five seconds that was required to obtain the digital image to ensure that sitting, 10% WB, 50% WB, 90% WB standing posture.

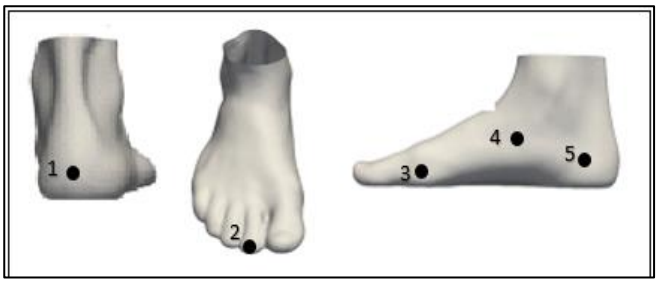

Figure 5.2. Five reference points to measure foot length (1, 2) and MLA angle (3, 4, 5)

Subjects were weighed on a standard scale, and 10% and 90% of each subject's weight were calculated. They then placed their right foot on the scale and their left foot on the ground. The subjects were asked to lower the amount of weight bearing by lifting the foot on the scale straight up and not leaning to either side until the scale showed that 10% of weight bearing had been achieved. Foot measurements were then taken. The process was repeated for 90% of weight bearing. Measurements taken at 10% and 90% of weight bearing may be important in establishing a description of arch mobility (Williams & McClay, 2000). The researcher chose 10% and 90% of weight bearing because they found that these conditions were close to non–weight bearing and full weight bearing respectively, and that subjects could maintain a stable and upright posture in these conditions, see Figure 5.3. Then, the researcher asked each subject to sit on a height adjustable chair, keeping the hip and knee joints at 90^{o} of flexion and the ankle joint in a neutral position, and raise the left leg behind the right leg and place the right foot on ground in a non-weight bearing condition.

Figure 5.3. Subject 10%WB standing

To measure the MLA in a dynamic condition, subjects walked down a 14 m walkway and the researcher placed the three smartphones about halfway along the walkway so the self-selected walking speed was recorded using the smartphones. Four calibrated boards and retro-reflective markers were placed using the self-calibration bundle adjustment digitized points (circles) that were used to calculate the axis-coordinate for three markers (MLA angle) and two markers to compute foot length. Calibration was undertaken to reduce measurement error, and smartphone accuracy testing was carried out before using the devices to record the subjects (Al-Kharaz & Chong, 2019b). Timing clock and LED flash were used at 30 second intervals. Each flash, lasting 0.05 seconds, was used to synchronise the video clips. To evaluate the accuracy of each calibration procedure, the measured calibrated length of the scale bar and ruler were compared to the true length, see Figure 5.3. Stance phase was defined as heel strike (HS), loading response (LR), mid-stance (MS) and terminal stance/heel off (HO) (Mohammed et al., 2016).

The MLA was calculated in a manner similar to the method used by Tome et al. (2006) and Balsdon et al. (2016) using Eq.5.1. The MLA was defined as the angle subtended by two vectors: one (A) from the marker on the medial aspect of the calcaneus to the navicular tuberosity and the other (B) from the head of the first metatarsal to the navicular tuberosity (Leardini et al., 2007; Rabbito et al., 2011).

$$\text{MLA angle} = \cos^{-1}\frac{\vec{A}\cdot\vec{B}}{|A||B|} \qquad \ldots (5.1)$$

5.2.5 Statistical analysis

Mean and standard deviation values were calculated for MLA angles during static (non-WB, 10% WB, 50% WB, 90% WB) and dynamic motion of stance phase of gait (HS, LR, MS and

HO) for all 33 adults. The relationship between the MLA measurements in static and dynamic conditions was examined using 2-tailed Pearson's correlation coefficients at 0.05 and 0.01 levels of significance. The range measurement error using RMSE was less than 0.07 for all image adjustments. The intraclass correlation coefficient (ICC) is a widely used reliability index in test-retest, therefore three test-retests measured the MLA angles in the static condition and during four phases in stance gait for each subject.

5.3 Results

5.3.1 MLA angle in static and dynamic conditions

The mean and standard deviation (SD) were computed for MLA angles obtained for four conditions in the static foot (non-WB, 10% WB, 50% WB, 90% WB) and four phases in the stance phase during gait. Table 5.2, shows that the minimum value of MLA angle in sitting when non-WB was 137.83° and the SD was 7.53, while the maximum value of the MLA angle when dynamic during gait in the mid-stance phase was 150.57° and the SD was 8.66. A larger MLA angle indicates a decrease or flattening of the arch, whereas a smaller, more acute angle indicates an elevation of the MLA.

Table 5.2. Mean static and dynamic barefoot measurement of the MLA angle degrees with standard deviation (SD)

Subject	*Static*				*Dynamic*			
(n=33)	50% WB	10% WB	90% WB	Sitting non-WB	HS	LR	MS	HO
Average	144.79° (9.45)	140.95° (7.67)	141.30° (9.03)	137.83° (7.53)	149.72° (0.1)	149.83° (8.41)	150.57° (8.66)	148.58° (8.76)

5.3.2 MLA angle gender differences

The differences between males and females in static and dynamic conditions were measured. Although there were some differences, no significant differences between males and females were found. Table 5.3 shows that the maximum mean differences of MLA angle in sitting was 3.75 and in terminal step of stance phase during gait was 3.76. Furthermore, the males had a slightly higher MLA angle than females in standing, sitting and in heel off (OH) step during gait.

Table 5.3. Mean static and dynamic barefoot measurement of the MLA angle degrees with standard deviation (SD), and differences between genders

Gender	*Static*				*Dynamic*			
(n=33)	50% WB	10% WB	90% WB	Sitting non-WB	HS	LR	MS	HO
Male (n=18)	145.45°	141.06°	143.64°	139.71°	149.80°	148.8°	149.86°	150.46°
	(10.98)	(5.58)	(6.95)	(6.23)	(10.9)	(7.57)	(6.82)	(7.76)
Female	144.12°	140.85°	138.95°	135.96°	149.60°	150.86°	151.27°	146.70°
(n=15)	(8.08)	(10.65)	(12.00)	(9.32)	(10.8)	(9.41)	(11.49)	(9.92)
Differences	1.33	0.21	4.69	3.75	-0.08	-2.06	-1.41	3.76

5.3.3 Reliability

To explore the change of the MLA angle in the static condition and during walking as it affects reliability and validity, measurements were made on three test-retests in static foot and during dynamic condition. Table 5.4 shows the ICC results. Excellent reliability values in the static condition were 0.98-0.99. During the dynamic condition, the mean value of ICC was 0.86; i.e. less than the static condition. In all, the average value of ICC was (0.92) and the reliability of test-retest in static and dynamic conditions gave an excellent reliability.

Table 5.4. Mean reliability values between test-retest of MLA angle

MLA condition		*Intrarater Coefficient of Correlation*		
		Intraclass correlation	95% Confidence Interval	
			Lower bound	Upper bound
Sitting	Non-WB	0.99	0.87	0.99
Standing	10%WB	0.98	0.63	0.99
	50% WB	0.99	0.73	0.99
	90% WB	0.99	0.73	0.99
Walking	HS	0.78	0.08	0.93
	LR	0.86	0.13	0.96
	MS	0.91	0.44	0.99
	HO	0.89	0.18	0.97
Average		0.92	-	-

5.4 Discussion

The MLA plays an important role in allowing the foot to transfer weight and absorb shocks when walking or running (Staheli et al., 1987), and provides a resilient connection between the forefoot and hindfoot. Therefore, it is necessary to evaluate the arch (Yalçin et al., 2010). To date, there are many methods for evaluating the MLA both statically and dynamically (Cavanagh & Rodgers, 1987; Staheli et al., 1987; Hawes et al., 1992; Volpon, 1994; Chang et al., 2012; Chang et al., 2014), but most techniques are inaccurate or expensive. Close-range photogrammetry is more precise and is inexpensive (Ab Aziz et al., 2010; Herráez et al., 2013). Data were collected for four static and dynamic barefoot conditions in four stance phases during gait. Results of the current study showed that the average value of the MLA angle in four stance phases during gait was slightly more than in the static condition, see Table 5.2. This is consistent with Balsdon et al. (2016) who reported that static barefoot MLA angles were statistically significantly smaller than dynamic angles, meaning the MLA flattened during dynamic gait. A larger MLA angle indicates a decrease or lowering of the MLA (flat arch), whereas a smaller, more acute angle indicates increase in height of the MLA (high arch) (Tome et al., 2006) because an increased height of the MLA leads to the shortening of the distance between the heel bone and the metatarsals and a secondary contracture of the plantar fascia. Such a foot is described as a high-arched foot (Woźniacka et al., 2013). In this study, the MLA angle in dynamic conditions was about (150°) which was higher than the study by Balsdon et al. (2019) because the participants in our study carried more weight. Increasing body weight would increase the pressure on the plantar area, so it is reasonable to postulate a change in foot size would be associated with obesity (Chen et al., 2009).

In the static condition, the observation of the MLA angle was lower at about (137°) when sitting, indicating that the MLA was high in non-WB and the arch also tended to be high. However, in the dynamic condition during walking, the higher mean value in the mid-stance phase was (150.57°) when the foot tends to flatten.

Although no significant gender-based differences were observed in MLA angles under all conditions, the results did show that males had a low-arched foot compared with females when standing and sitting, probably because the foot length and weight of males is greater than females (Nielsen et al., 2009; Ezema et al., 2014). These results contrast with Zhao et al.'s

(2020) outcomes that women tend to have a significantly lower AHI than men.

In the dynamic condition, our finding in (MS) stance phase was consistent with the Fukano and Fukubayashi (2012) study which reported that the MLA angle for females was higher than males during landing, see Figure 5.4. According to the previous study the functional arch deformation is greater in the soft tissues of the foot of females than in those of males (Fukano and Fukubayashi, 2012). Therefore, females have a higher danger of sustaining soft-tissue injuries, such as fasciitis, than males (Scher et al., 2009).

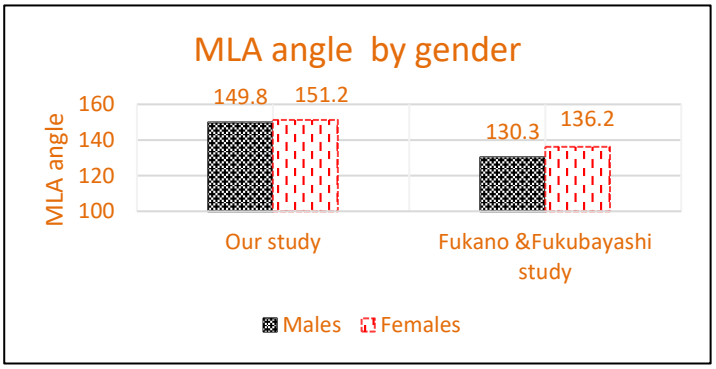

Figure 5.4. The differences of MLA angle between gender in our study during MS stance phase gait and (Fukano and Fukubayashi) study in dynamic condition (landing)

Our results emphasized the results of the Nielsen et al. (2009) study when testing ND during walking and impact of foot length on ND in both genders. Their study found that female and male mean ND was approximately the same (5.2cm and 5.3cm respectively), and that foot length had a significant influence on ND. In the dynamic condition, as shown in Figure 5.5, the MLA angle in males experienced a small decrease after HS and then the arch rose at HO. In contrast, the MLA angle in females started to steadily flatten at HS and drop slightly until HO. There was a higher mean value in the dynamic condition during walking in the mid-stance phase (149.86° and 151.27°) for males and females respectively. Furthermore, when the foot tended to flatten at the LR and MS phases, gait was nearly to the MLA angle measured during standing (WB) in males, similar to the study by Bandholm et al. (2008). In addition, the Ezema et al. (2014) study indicated that male children were twice more likely to be affected by pes planus than female children.

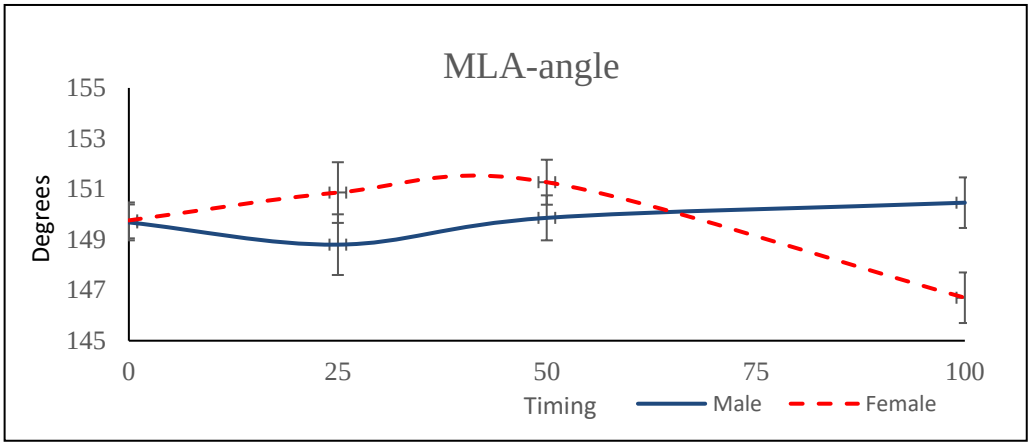

Figure 5.5. The change in MLA angle and standard deviation during the stance phase of gait for males and females

The results of our study are consistent with Bandholm et al. (2008) who showed the high reliability of test-retest ICC values for the MLA during gait of 0.86 in dynamic conditions. Williams and McClay (2000) evaluated the MLA using ND during 10% and 90% WB, and found the ICC was 0.87 and 0.91 respectively. The ICC in the current study was higher (0.98-0.99).

To the best of our knowledge, this is the first study to examine the MLA angle of the foot in static and dynamic conditions for adults using the innovative method of close-range photogrammetry. A few studies recently published have used close-range photogrammetry to measure skeletal foot kinematics in vivo during static and dynamic walking (Al-Baghdadi et al. 2012; Al-Kharaz and Chong 2019b; Al-Kharaz and Chong 2020). These study results might be an extremely valuable reference for clinical screening of the foot arch to decide an accurate treatment protocol. The close-range photogrammetry method allows for improved collaboration between researchers and therapists, and will help further elucidate the differences of the MLA with WB and without WB to avoid the risk of various injuries and pathologic conditions of the foot and lower extremity. In addition, custom foot orthoses are widely prescribed to treat cavus foot pain because they can improve pressure distribution. Kinematic analysis of the foot arch has been used extensively in an attempt to document the effectiveness of foot orthotics which are increasingly prescribed by podiatric physicians, orthopedic surgeons and rehabilitation specialists for patients with chronic cavus foot pain (Burns et al. 2006; Jafarnezhadgero et al. 2017).

5.5 Conclusion

The MLA performs one of the important roles for foot function. The measurement of the MLA angle could indicate foot arch type and behaviour of the foot during static and dynamic conditions using the non-invasive and low cost close-range photogrammetry technique. The self-calibration bundle adjustment was used to measure 3D coordinates of five reference points on the right foot and then compute the MLA angle. The results demonstrated that the arch in sitting tended to be high and the average value of the MLA angle in four stance phases during gait was slightly more than in the static condition. These results validate the importance of the longitudinal arch angle for the foot during physical activity and physical therapy, and may add information to the clinical arena. Another part of foot that is important during physical activity is the ankle which will be discussed in next chapter.

Chapter 6. Investigation of ankle kinematics according to gender during the stance phase of gait

6.1 Introduction

The ankle plays an important role in standing, walking and other activities (Cho et al., 2016; Wei et al., 2016; Fukano et al., 2018). The evaluation of ankle motion ankle is required in footwear design and manufacture. Inappropriate footwear increases discomfort through deformation from poor posture and the risk of foot problems such as bunions, ankle injuries, and chronic foot pain (Lee et al., 2012; Lee & Wang, 2015). It is also essential for identifying forensic and medical problems and acute or chronic injuries in athletes (Wunderlich & Cavanagh, 2001; Fawzy & Kamal, 2010; Blenkinsopp et al., 2012; Davies et al., 2014). Furthermore, the evaluation of ankle motion during walking is essential to develop the production of foot orthoses in the management of foot and ankle disorders (McPoil & Cornwall, 1996). Ankle joint dorsiflexion is an important motion that normally occurs during the midstep phase of the gait cycle. It allows for continued forward progression of the body over the weight bearing foot while both the rearfoot and the forefoot are in contact with the ground (Dananberg et al., 2000). Movement of the dorsiflexion (DF) and plantar flexion (PF) is necessary to allow optimal force generation and balance strategy execution to decrease fall risk (Studenski et al., 1991). Mecagni et al. (2000) reported that inversion (IV) and eversion (EV) ROM was also found to be significantly associated with balance and functional test performance. The limitation of the ankle joint or talocrural (i.e. the joint between the talus and the tibia) ROM influences many aspects of function and balance such as the limitation of plantarflexion and dorsiflexion and reducing postural stability. Several studies reported that limited dorsiflexion impacts many functional movement patterns such as lateral step down, the squat, and even landing from a jump (Bennell & Goldie, 1994; Sung & Kim, 2018). Inability to dorsiflex the ankle to beyond neutral, and gait becomes inefficient, tiring and, at times, painful. Abnormal stresses are placed upon adjacent articulations (Ribbans & Rees, 1999; Macklin et al., 2012). The human body finds ways to compensate and gain the required movement in other joints when ankle joint dorsiflexion is limited. These compensations can lead to conditions such as:

- Arthritis in the midfoot
- Pain in the forefoot (balls of the feet) due to the increase in pressure
- Medial tibial stress syndrome (shin splints)
- Stress fractures in the forefoot
- Sinus tarsi syndrome
- Ulcers on the forefoot (Mueller et al., 2003).

The measurement of ankle motion depends on the ankle joint, and the transverse tarsal and subtalar joints (Chan & Rudins, 1994; Simoneau et al., 2007). Based on a previous study, the stance phase was defined as heel strike (HS), loading response (LR), mid-stance (MS) and terminal stance/heel off (HO) (Mohammed et al., 2016; Takabayashi et al., 2017). The movement of the ankle joint is of great importance as it allows shock absorption on initial contact with the floor, or heel strike, and provides forward propulsion force during the terminal stance phase.

In motion, three cardinal planes (coronal, sagittal and transverse) are important (Chan & Rudins, 1994). Thus, ankle motions within the coronal plane are IV and EV, in the sagittal plane they are DF/upward and PF/downward, and in the transverse plane they are adduction (AD), or internal rotation, of the foot and abduction (AB), or external rotation. Combinations of these motions across both the subtalar and tibiotalar joints create three-dimensional motions called supination and pronation (Chan & Rudins, 1994; Brockett & Chapman, 2016). The ankle is focused primarily on PF and DF. Movement of the DF and PF is necessary to balance performance to decrease the risk of falling (Studenski et al., 1991). Moreover, the ankle IV and EV ROM are also found to be significantly associated with balance and functional test performance (Mecagni et al., 2000).

The ankle centre of rotation was approximated as the midpoint between the tip of the medial malleolus and the tip of the lateral malleolus for dorsiflexion-plantar flexion (DP) and external-internal rotation (EI). The approximation is also valid for inversion-eversion (IE) at ankle neutral position when DP, IE, and EI angles are all zero (Ficanha et al., 2015).

A diversity of apparatus has been used to quantify ankle kinematics while static and during gait, from simple plastic protractors to complex three-dimensional motion systems. The universal goniometer remains the most widely used instrument to measure ankle joint dorsiflexion. It is

simple to use, non-invasive and inexpensive (Rome & Cowieson, 1996; Cho et al., 2016; Johansen et al., 2020). Konor et al. (2012) examined the reliability of three techniques (standard goniometer, digital inclinometer and tape measure) to measure ankle ROM in a weight bearing lunge. All three techniques had good reliability. However, these techniques are difficult to use during walking. Other methods for ankle analysis include a combination of physical examination, observation, and radiographs (Kidder et al., 1996; Fukano et al., 2018; Canton et al., 2020). However, the major drawback of the observation measurement is inaccuracy. Radiographs have several limitations including ionizing radiation exposure and, therefore, potentially carry health risks. They are also relatively expensive and require special facilities (Kidder et al., 1996). A 3D camera system was used to investigate the contribution of the ankle, knee, and hip to the total lower extremity internal rotation and external rotation ROM (Lidge et al., 2020). VICON motion systems and a multi-axis strain gauge force plate imbedded under a custom-built treadmill measured dorsiflexion of the ankle during static standing trials and dynamic trials. Retroreflective markers adhered to the skin at the anatomical landmarks of the lower extremity were used to obtain force and video data (Drewes et al., 2009; Phinyomark et al., 2016). One limitation of VICON motion systems is the need for a laboratory with particular specifications which is relatively expensive. Among optical techniques, close-range photogrammetry is commonly utilised because it is accessible to the majority of professionals, is a non-invasive, high accuracy, low-cost tool, and presents reproducible results with easy registration and archiving (Antoniolli et al., 2018).

Ankle ROM has been shown to vary significantly between individuals due to geographic and cultural differences based on activities of daily living. One influential factor that may change ankle ROM is gender. Brockett and Chapman (2016) compared gender differences and demonstrated that younger females (20 to 39 years old) have a higher ankle ROM compared to males. Murray et al. (1985) indicated that there are minimal differences of ROM between females and males (Sung & Kim, 2018). However, there are very few studies regarding ankle ROM and the difference between adult males and females during gait (Al-Rawi et al., 1985; Hallaceli et al., 2014). This chapter evaluates ankle kinematics during stance phase gait according to the gender of adults.

6.2 Methods

6.2.1 Subjects

Thirty-three adults with healthy feet participated in this study. The details are provided in Tables 4.1 and 5.1.

6.2.2 Foot markers and software

The markers on the body surface are important to shape and motion analysis, as the particular shape of the markers often reflects the underlying structures in the ankle region (Liu et al., 2004b). The ankle joint axis is close to a mediolateral axis through the ankle joint complex. All axes were close to parallel to the bimalleolar axis (Lundberg, 1989). Based on previous studies (Gastwirth, 1996; Tochigi, 2003; Hallaceli et al., 2014; Antoniolli et al., 2018), seven anatomical locations were identified on the right foot and 2-mm diameter self-adhesive stickers were placed on these locations. Table 6.1 explains these markers and Figure 6.1 illustrates the locations of markers.

Table 6.1. Specifics of seven markers and locations

No.	*Definitions of Landmarks*	*Location*
1	The fifth metatarsophalangeal joints, lateral MPJ(LMPJ)	The fifth metatarsal on the lateral side of the foot
2	Lateral malleolus (LM)	Tip of the lateral malleolus
3	Medial malleolus (MM)	Tip of the medial malleolus
4	Lateral of the fibula (LF)	15cm superior the lateral malleolus
5	Top of the second MPJ (SMPJ)	On the dorsal aspect of the head of the second metatarsal
6	Inter-malleolar point (ankle joint centre) (IM)	Anterior midway between medial malleolus and Lateral malleolus
7	Anterior shank (AS)	15cm tibia anterior aspect from the Inter-malleolar point

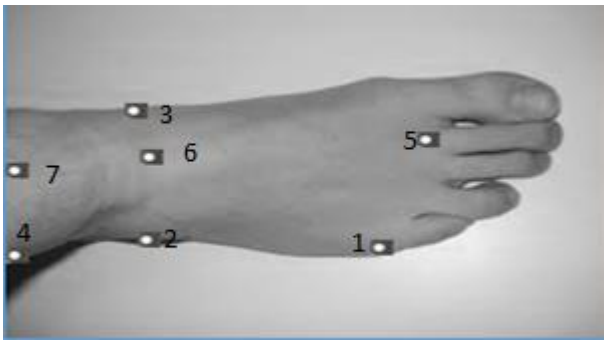

Figure 6.1. Seven markers mounted on the right lower shank

Close-range photogrammetry techniques were used and the subjects' feet were recorded by smartphone cameras during gait. Three-dimensional (3D) coordinates of foot markers were collected from a video recording. To convert the video frames to images for measurement, Virtual Dub software (v 1.6.15) was used. Three-dimensional marker positions were calculated using iWitnessPRO-V4 Photometrix software (2018) and to calibrate the smartphone cameras to avoid errors from lens distortions and to determine foot coordinates using a bundle adjustment technique. MATLAB software calculated the angle created by each of three markers in the coordinate system using the dot product of two vectors. Microsoft Excel software and SPSS version 25 for Windows (IBM Company) were used to analyse data and conduct each statistical analysis.

6.2.3 Experimental procedure

Seven 2 mm diameter reference point markers were used on the bare right foot for further analysis (Menz, 2004; Bus & de Lange, 2005). Subjects placed the subtalar joint in a neutral position (relaxed state) and then markers were mounted on anatomical locations, see Table 6.2. All of the markers were marked manually by the researcher. The subject was standing during the 10 seconds that were required to obtain the digital image to ensure that the subjects' feet were in neutral posture (the ankle joint at neutral flexion). Then, subjects walked down a 14 m walkway. Seven smartphones were placed about half way along the walkway, and a self-selected walking speed was recorded using the smartphones. Self-calibration bundle adjustment was used to digitize the four calibrated boards and retro-reflective markers and calculate the axis-coordinate of each marker. Calibration was undertaken to reduce measurement error calibration, and smartphone accuracy testing was carried out before using the devices on the subjects (Al-Kharaz & Chong, 2019a). A timing clock and the flash of a LED was used at 30 second intervals, with each flash lasting 0.050 seconds to synchronise with the video clips. To evaluate the accuracy of each calibration procedure, the measured calibrated length of the scale bar and ruler were compared to the true length, see Figure 6.2.

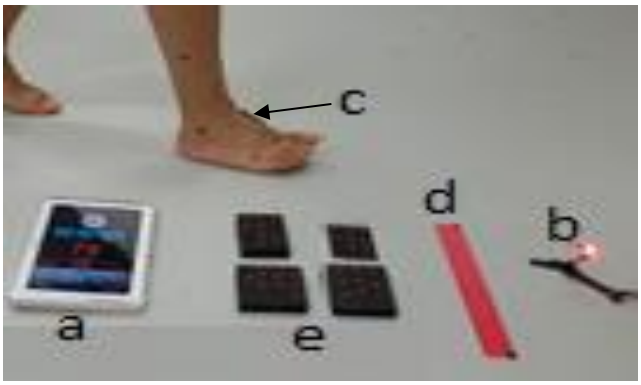

Figure 6.2. (a) Timing clock, (b) Flash of a LED, (c) Scale bar, (d) Ruler and (e) Four calibrated boards for synchronisation and accurate calibration procedure

For measurement the rotational angles, dorsiflexion and plantar flexion angles were defined as the angle created by: (A) the line from LF to LM and (B) the line from LM to LMPJ (Kaufman et al., 1999). Eversion and inversion angles were created by (A) the line from AS to IM and (B) the line from LM to MM during IM in line with Spink et al. (2010). The line (A) from LM to MM and (B) IM to SMPJ created internal-external rotation angles. For this investigation, an X-Y-Z Cardan sequence was applied. This describes sagittal plane motion around an x-axis, coronal plane motion around a y-axis, and transverse plane motion around a z-axis. This is similar to that described by Grood and Suntay (1983). Information from the International Society of Biomechanics (ISB) was used to describe motions of the ankle and subtalar joints. As a result, rotation in the sagittal plane (y-z plane) was defined as dorsiplantarflexion, in the coronal plane (x-z plane) as inversion-eversion, and in the transverse plane (x-y plane) as internal-external rotations, see Figure 6.3.

The change in the position and orientation of the ankle bone angles of each triplane for each of the stance phases (HS, LR, MS, and HO) from the neutral posture was quantified. The rotational angles around the x, y and z axes represent dorsiflexion (+) / plantarflexion (-), inversion (+) / eversion (-) and internal (+) / external (-) rotation, respectively; similar to ISB definitions. The angles were calculated in a manner similar to the method used by Tome et al. (2006) using Eq.6.1.

$$\text{Rotational angle} = \cos^{-1} \frac{\vec{A} \cdot \vec{B}}{|A||B|} \quad \ldots (6.1)$$

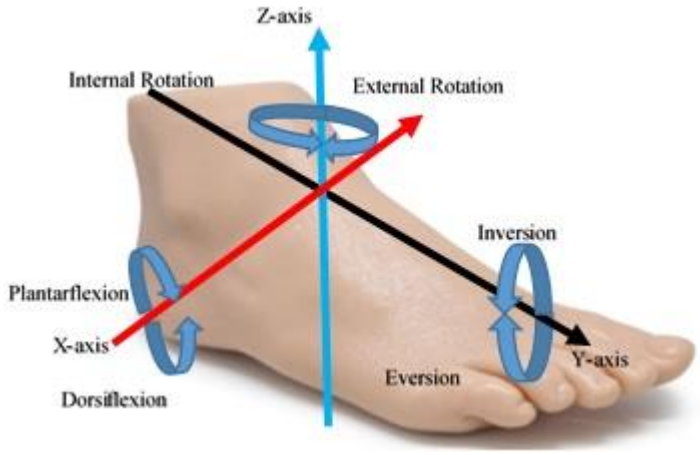

Figure 6.3. Depicts the x-y-z coordinate to describe a screw axis orientation of ankle. The x-axis was oriented PF&DF, the y-axis IN&EV, and the z-axis AD&AB, (Tochigi, 2003)

6.2.4 Statistical analysis

SPSS version 25 for Windows (IBM Company) was used for data processing and analysis. Descriptive analysis used mean and standard deviation for general characteristics. Consistent with previous studies (Chuter, 2010; Kim et al., 2013; Morasiewicz et al., 2017; Miller et al., 2020), the independent Levene's test was used to measure significant ankle ROM differences between genders. The statistical significance level was less than 0.05 in P-value. The intraclass correlation coefficient (ICC) is a widely used reliability index in intra-sessions, so three sessions were used to measure the three cardinal planes' angles in four phases in stance phase during gait for all participants.

6.3 Results

Eighteen males and 15 females participated in this study, see Table 5.1. The mean, standard deviation and mean differences for ROM of the ankle were computed, see Table 6.2. Levene's test for equality of variances and independent sample t-tests were performed to evaluate differences between genders for the ankle kinematic angles, with ($p<0.05$) considered significant. The results demonstrated significant differences between females and males for the transverse plane of ankle ROM ($F=12.21$, $Sig=0.013$ and 95% confidence interval of the differences between -5.312 and 1.587). However, no significant differences of coronal and sagittal planes were found between males and females.

Table 6.2. Mean ±SD of triplane angles during stance phase gait for males and females

Plane	*Males*				*Females*				*Differences*			
	HS	LR	MS	HO	HS	LR	MS	HO	HS	LR	MS	HO
Coronal IV(+)°/ EV(-)°	1.15 ±0.39	-4.12 ±0.99	0.84 ±1.14	2.94 ±0.48	0.85 ±0.33	-5.68 ±1.15	0.34 ±0.20	3.17 ±0.22	0.30	-1.56	0.50	-0.23
Sagittal DF(+)°/ PF(-)°	3.20 ±0.59	9.45 ±3.71	2.73 ±2.66	-7.84 ±2.10	3.67 ±0.10	10.93 0.91	7.55 ±1.46	-12.85 ±0.03	-0.47	-1.48	-4.82	-5.01
Transverse AD(+)°/ AB(-)°	2.51 ±1.41	2.13 ±1.56	2.56 ±0.33	1.72 ±0.46	0.72 ±14.71	3.01 ±15.37	7.00 ±17.67	5.64 ±15.31	1.79	-0.88	-3.92	-3.92

The intraclass correlation coefficient (ICC), lower and upper bounds, and standard error of measurement (SEM) data of triplane angles of the ankle during stance phase for three sessions of both genders are presented in Table 6.3. The average of ICC for the triplane angle during stance phase was 0.89 for males, and for females was 0.83. The overall ICC value of both genders was 0.86 "very good". Furthermore, the SEM for triplane angles of the ankle during stance phase ranged from 2.3 to 9.7 for males, and for females it ranged from 2.3 to 10.6. In total, the SEM of both genders was approximately 5. Note that both the SEM and the ICC are indicative of reliable measures.

Table 6.3. Mean reliability values between intra-sessions errors for ankle of gender groups during gait

Stance phase	*Plane*	*Intra-sessions coefficient of correlation and standard error of measurement*							
		Males				Females			
		Intraclass corr.	95% Confidence interval		SEM	Intraclass corr.	95% Confidence interval		SEM
			Lower bound	Upper bound			Lower bound	Upper bound	
HS	Coronal	0.85	0.68	0.94	6.67	0.89	0.75	0.96	5.01
	Sagittal	0.92	0.83	0.96	2.97	0.98	0.95	0.99	2.30
	Transverse	0.86	0.69	0.94	5.88	0.50	-0.17	0.82	10.63
LR	Coronal	0.95	0.90	0.98	4.26	0.87	0.70	0.95	7.04
	Sagittal	0.94	0.88	0.97	4.87	0.69	0.27	0.88	7.36
	Transverse	0.86	0.70	0.94	6.06	0.63	0.13	0.86	7.93
MS	Coronal	0.96	0.92	0.98	3.90	0.92	0.83	0.97	4.38
	Sagittal	0.98	0.96	0.99	2.37	0.89	0.75	0.96	6.73
	Transverse	0.94	0.88	0.97	3.06	0.79	0.51	0.92	2.81
HO	Coronal	0.92	0.83	0.96	4.13	0.92	0.82	0.97	4.74
	Sagittal	0.94	0.88	0.97	3.69	0.91	0.78	0.96	4.76
	Transverse	0.62	0.18	0.84	7.94	0.95	0.89	0.98	2.96
Average		0.89				0.83			

6.4 Discussion

The aim of this chapter was to evaluate the ankle kinematics during gait according to gender of Middle Eastern adults. Motion of the ankle occurs primarily in the sagittal plane, with plantar- and dorsiflexion occurring predominantly at the tibiotalar joint (Brockett & Chapman, 2016), but also includes eversion, inversion, and internal and external rotation. In the literature, the overall ROM in the sagittal plane moves from 10° to 20° of DF and 40° to 55° of PF. The ROM in the coronal plane is about 23° IN and 12° EV, while in the transverse plane the ROM is between 5-6° (Valderrabano et al., 2003). In our results, the ROM of DF was 4° to 13° and 5° to 13° for PF. In the coronal plane the ankle ROM was approximately 4° to 6° and in the transverse plane the ROM was between 3° and 23°.

In general, the ankle joint begins in a few degrees of dorsiflexion at heel strike and then rapidly leads to plantar flexes under the control of an eccentric (lengthening) contraction of the ankle dorsiflexors (primarily anterior tibialis) until the foot is flat on the ground. At this stage, the foot is in mid-stance to maintain body balance during the entire gait cycle (Wei et al., 2016). At the position of foot flat, the ankle begins the process of dorsiflexion. The foot becomes stationary and the tibia becomes the moving segment. The heel then begins to lift at the beginning of double support, causing a rapid ankle plantar flexion at the termination of the stance phase (De Ridder et al., 2013; Frontera et al., 2019). In our results, for both genders, the ankle joint was slightly dorsiflexed on HS. After heel contact, the ankle rapidly dorsiflexed to a maximum of 13°, just prior to MS. The ankle then plantar flexed progressively, reaching a maximum PF of 13° until HO. A small range of IN in the coronal plane on HS then gradually moved to EV until MS, then increased slightly to IN on HO. In the transverse plane, all stance phases were AD in both genders.

In females, the transverse plane of ankle ROM was significantly larger in the stance phase of gait (Sig=0.013) compared with males. However, there were no significant differences between genders in relation to ankle joint ROM in the sagittal and coronal planes. Since females tend to have more ligamentous laxity than males (Schwarz et al., 2011), females are thought to have better flexibility than males in the ankle joint, causing females to have a larger ankle ROM than males. Many previous studies report that females have larger ankle ROM than males (Kerrigan et al., 1998; Kato et al., 2005; Røislien et al., 2009; Ko et al., 2011; Fukano et al., 2018; Sung

& Kim, 2018). The outcomes of our study are consistent with these studies.

Furthermore, to reduce the risk of balance-related falls and to prevent balance-related ankle injury, ankle ROM differences between females and males should be considered. Murray et al. (1985) established that there are minimal ROM differences between females and males. The ROM during stance was greatest for DP in both gender and least for EI in males (Sung & Kim, 2018). Our findings are consistent with the study conducted by Murray et al. (1985). Overall, females have greater ankle ROM planes during the stance phase except the beginning of walking (HS) values, when males had values converging with females, see Figure 6.4.

Reliability determination is essential for validity. The acceptable intraclass reliability was determined through analysis from three testing sessions focusing on the reliability of ankle kinematics. Reliability mean value between intra-sessions for the female group was 0.83 and for the male group it was 0.89. The composite measure of ankle kinematics results demonstrates good reliability (ICC=0.86) compared with Konor et al. (2012) which had very good reliability (ICC>0.85) when measuring with a goniometer.

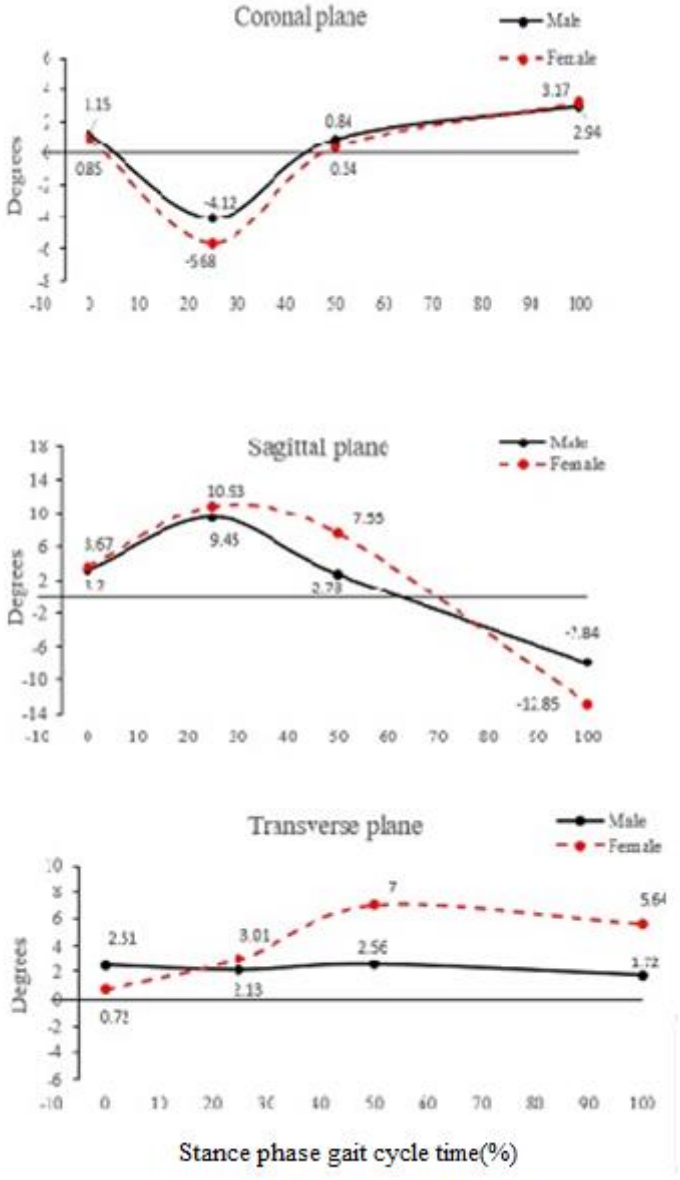

Figure 6.4. Ankle kinematics during stance phase of gait for males and females

6.5 Summary and conclusion

The ankle plays an important role in human locomotion because the ankle's ROM is necessary to balance the body and decrease the risk of falling during human walking for both genders. However, little information exists on sex-based variations in ankle joint kinematics during the stance phase of gait.

Thirty three participants (18 males and 15 females) were recruited in the study and they walked at a self-selected speed. Seven retro-reflective targets were mounted on the skin of each participant's right foot and seven smartphone cameras were used to capture videos. A self-calibration method using a photogrammetric bundle adjustment technique determined the ankle coordinates.

The results demonstrated that the females had a significantly greater range of ankle motion than the males in the transverse plane throughout the stance phase, and the maximum mean angle of adduction in the heel strike phase for males was higher than for females. The maximum mean angle of inversion/eversion rotation of the ankle for females and males was closer. No significant differences in the range of ankle motion in the coronal and sagittal planes were observed between the males and females. The overall value of the ICC was 0.86, which is considered "very good".

In conclusion, this study demonstrates the gender difference of ankle ROM. Specifically, our results show that females have more joint laxity and flexible ankle ROM than males and males have a higher ROM of AD in the HS phase. Therefore, it is necessary to plan and assess the training program for ankle ROM in males. Further research is needed to ascertain the most effective way to improve ankle joint flexibility in males. This would be beneficial for fall prevention, especially for older adults. These results may contribute to the effectiveness of understanding gender differences in ankle function and may be useful for understanding and treating ankle joint pathologies with a gender-specific method. The outcomes emphasize that the close-range photogrammetry technique can easily measure joint angles during gait. Ankle kinematics during uneven surfaces also requires further investigation, therefore the next chapter assesses the ankle during unsteady gait.

Chapter 7. Assessment of ankle kinematics during normal and unsteady walking

7.1 Introduction

Gait analysis for research into lower extremities has often focused on regular ground walking at a self-selected speed to perform various daily activities. However, most falls occur outdoors and lower extremity injuries are caused by environmental factors such as uneven surfaces, narrow paths, and sloping surfaces (Gates et al., 2012; Gates et al., 2013; Hamacher et al., 2019; Kim et al., 2019). Furthermore, walking on a poorly lit path or with closed eyes leads to disturbed balance in gait (Tulchin et al., 2010b). Recently, uneven surfaces have become a topic of growing interest, especially in the disparate areas of orthopaedics and rehabilitation (Eckardt & Kibele, 2017). The ability to walk independently on an uneven surface is identified as one of the criteria to distinguish the highest functional improvements in a clinical evaluation indicating excellent clinical reliability for patients (Kim et al., 2019; Romkes et al., 2020). During walking, the ankle joint is of great importance as it allows shock absorption on initial contact with the floor (heel strike) and provides forward propulsion force during the terminal stance phase. A well-balanced body is important because previous research has shown that the foot joints are susceptible to injury (Silverman et al., 2012; Novak & Brouwer, 2013), and during unsteady gait an acute ankle sprain may occur and develop into a residual condition called chronic ankle instability (David et al., 2013). Therefore, studying ankle kinematics is important for the prevention of fall during walking on different surfaces.

Stable walking on an even surface enables healthy subjects to have increased ROM during gait, particularly as this involves hip and knee flexion and ankle dorsiflexion. The increased ROM improves minimum foot clearance (Bruijn et al., 2009; Gates et al., 2012; Blair et al., 2018), and increases walking speed and step length during uneven surface walking (Kim et al., 2019). Sometimes, when walking over potentially slippery surfaces, people take shorter steps and exhibit a flatter shoe–floor angle at heel strike (Gates et al., 2012). Other adaptations to adjusted walking on uneven surfaces include increased step time and step width variability, change in stance phase duration, and increased foot height (Romkes et al., 2020). In slope walking, there is an increase in knee flexion and ankle dorsiflexion, while in upslope walking, the foot induces kinematic postural changes that are needed for toe clearance at heel strike (Breloff et al., 2019). Different instruments have been used to measure ankle kinematics during walking on both even

and uneven surfaces (Lay et al., 2006; Dixon & Pearsall, 2010; Tulchin et al., 2010a; Gates et al., 2012; Shultz & Goldfarb, 2018; Breloff et al., 2019), but most of them have used the VICON system. Dixon and Pearsall (2010) recruited ten young adult males. The participants were required to walk barefoot along an inclinable walkway using a six camera VICON system. They reported a decreased inversion of the up-slope ankle and increased inversion of the down-slope ankle. Tulchin et al. (2010a) studied the effects of surface slope on foot kinematics in twenty-four healthy adults using a twelve camera VICON motion capture system operating at 120 Hz (VICON, Denver, CO) and found differences in sagittal plane ROM. A study by Breloff et al. (2019) compared lower extremity kinematics of the upslope and downslope legs with level walking using the VICON 612 system at 120 Hz. Although the VICON system is one of the key players in optoelectronic motion capture systems based on markers (Merriaux et al., 2017), and it is a very accurate and reliable optical motion capture system (Bai et al., 2017), there are some major disadvantages including the system's high price, the need for technical support (Levanon, 2013), and its lack of availability in many clinical settings (Pfister et al., 2014).

Photogrammetry has the potential to be used as an alternative low-cost and accurate motion analysis technique. Recently, researchers have used photogrammetry to investigate the dynamic characteristics of structures (Lee and Rhee, 2013; Gwashavanhu et al., 2016). One advantage of photogrammetry is that it is a non-invasive tool for posture evaluation (Antoniolli et al., 2018). Video images have several potential advantages over other techniques in terms of time consumption, cost, and potential image distortion of the development process, such that video-based optoelectronic systems are (nowadays) the most popular in movement analysis (Chiari et al., 2005). In the last few years, video cameras have been used for capturing and modelling the three dimensional surface of the whole human body and for more specific dynamic segments of the human body such as the foot (Al-Baghdadi et al., 2011; Ferber & Benson, 2011; Hong et al., 2011; Al-Kharaz & Chong, 2019a), foot arch (Al-Kharaz & Chong, 2020), and the leg (Alshadli et al., 2011). Kinematic data captured by a video camera system is one of the most powerful tools to analyse human motion (Kim et al., 2009). Because of this advantage, it was used in the current study to achieve high accuracy at low cost. Therefore, the purpose of this chapter is to discuss ankle kinematics assessment during normal and unsteady gait using close-range photogrammetry and through trials on adults.

7.2 Methods

7.2.1 Participants

Thirty three adults from Middle Eastern countries underwent gait analysis with informed consent, see Tables 4.1 and 5.1.

7.2.2 Data collection procedure

To increase the risk of falls, various experiments were designed to imitate an unsteady gait by changing the walking environment, including walking with eyes closed, walking on a single beam, and dragging ankle weights. These three walking conditions were compared with normal gait. Four walking conditions were performed by each subject as shown in Figure 7.1, and the subjects performed three trials for each condition:

1. Normal gait: subjects walked normally and barefoot at a self-selected speed while the smartphone cameras recorded
2. Eyes closed: subjects walked barefoot in a straight line on 14m walkway with their eyes close at a self-selected speed while the smartphone cameras recorded
3. Single beam: subjects walked barefoot in a straight line on a wood beam while the smartphone cameras recorded. The beam length was 140cm and width 4cm and the height 2.4cm. Because of the beam's elevated path, the subjects attempted to maintain their centre of gravity during gait
4. Dragging ankle weights: subjects had 2 kg of weights tied at their ankles (creating the experience of heaviness) and walking barefoot.

To measure ankle ROM during the four gait conditions, participants were fitted with seven reflective markers placed over the bony landmarks of the foot and ankle (see Figure 6.1) in accordance with Table 7.1. The 3-D positions of the highly reflective markers were measured using seven Smartphone Galaxy 6.0 devices positioned around the foot being recorded. The software iWitnessPRO-V4 Photometrix (2018) was used to calibrate the smartphone cameras to avoid errors from lens distortions and to determine ankle coordinates using a bundle adjustment technique. Microsoft Excel software and SPSS version 25 for Windows (IBM Company) were used to analyse data and conduct each statistical analysis. Analyses of Variance (ANOVA) with ($p<0.05$) statistical comparison were used to evaluate the ankle kinematic angle

differences between the normal and three unsteady conditions for the four phases of gait. MATLAB software calculated the angles created by these seven markers in the coordinate system of sagittal, coronal and transverse planes of the ankle in a manner similar to the method used by Tome et al. (2006), using Eq.7.1.

To measure the rotational angles, dorsiflexion and plantar flexion angles were defined as the angle created by the (A) line from LF to LM and (B) the line from LM to LMPJ (Kaufman et al., 1999). Eversion and inversion angles were created by (A) the line from AS to IM and (B) the line from LM to MM during IM in line with Spink et al. (2010). The line (A) from LM to MM and (B) IM to SMPJ created internal-external rotation angles.

$$\text{Angle} = \cos^{-1} \frac{\vec{A} \cdot \vec{B}}{|A||B|} \qquad \ldots (7.1)$$

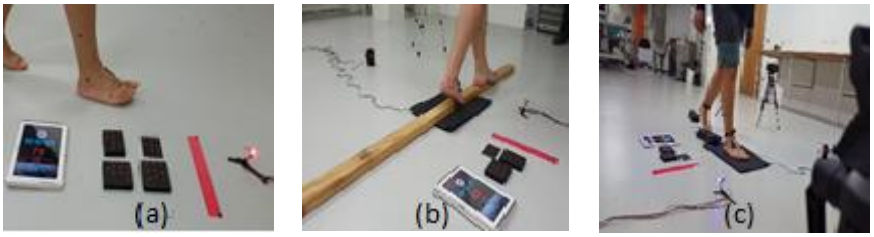

Figure 7.1. Three unsteady walking conditions ((a) Eyes closed, (b) On single beam and (c) Dragging of ankle weights) with timing clock, flash of a LED, scale bar, ruler and four calibrated boards for the accuracy calibration procedure

Table 7.1. Specifics of seven markers and locations.

No.	*Definitions of Landmarks*	*Location*
1	The fifth metatarsophalangeal joints, lateral MPJ (LMPJ)	The fifth metatarsal on the lateral side of the foot. (Gajdosik et al., 1987; Gastwirth, 1996; Hallaceli et al., 2014)
2	Lateral malleolus (LM)	Tip of the lateral malleolus. (Gajdosik et al. 1987; Gastwirth, 1996; Hallaceli et al., 2014)
3	Medial malleolus (MM)	Tip of the medial malleolus. (Gajdosik et al., 1987; Gastwirth, 1996; Hallaceli et al., 2014)
4	Lateral of the fibula (LF)	15cm Superior the lateral malleolus (Gajdosik et al., 1987; Hallaceli et al., 2014; Antoniolli et al., 2018)
5	Top of the second MPJ (SMPJ)	On the dorsal aspect of the head of the second metatarsal. (Tochigi et al., 2003; Antoniolli et al,. 2018)
6	Inter-malleolar point (ankle joint centre) (IM)	Anterior midway between medial malleolus and lateral Malleolus (Tochigi et al., 2003; Antoniolli et al., 2018)
7	Anterior shank (AS)	15cm tibia anterior aspect from the inter-malleolar point.(Tochigi et al., 2003; Antoniolli et al., 2018)

The change in the position and orientation of the ankle bone angles of each triplane for each of the stance phases from the neutral posture was quantified. The rotational angles around the x, y and z axes represented dorsiflexion (+) / plantarflexion (-), inversion (+) / eversion (-) and internal (+) / external (-) rotation, respectively; similar to the International Society of Biomechanics (ISB) definitions (Tochigi, 2003), see Figure 6.3. The rotation in the sagittal plane (y-z plane) was defined as dorsiflexion-plantarflexion (DF-PF), in the coronal plane (x-z plane) as inversion-eversion (IN-EV), and in the transverse plane (x-y plane) as internal-external rotations (IR-ER).

7.3 Results

The results of the thirty three participants, whose ankle kinematics during normal gait and three-unsteady gait trials (eyes closed, on single beam and dragging ankle weights) in four phases of stance phase (heel strike, loading response, mid-stance and terminal stance) are recorded in Table 7.2. The difference between normal and three unsteady gait trials was evaluated. The maximum mean differences between eyes closed and walking on a single beam was (1.548°) while the minimum mean differences between walking dragging of ankle weight and on single beam was (0.004°). The results demonstrated no significant differences in ankle kinematics between the normal and three-unsteady gaits, see Table 7.3. Three trials were conducted and reliability coefficients were used to assess agreement between them. The intraclass correlation coefficient, which describes the degree of agreement of the repeated measures of three testing sessions, focused on the reliability of ankle kinematics during normal and unsteady gait. Reliability mean value between intra-sessions for the normal gait was 0.86 and the average for unsteady gait was 0.78. Thus, the composite measure of ankle kinematics results demonstrated very good reliability (ICC=0.82).

Table 7.2. Mean of triplane angles during stance phase of gait in normal, eyes closed, single beam and dragging ankle weights

Stance phases	*Planes*	*Normal gait (°)*	*Eyes closed (°)*	*Single beam (°)*	*Dragging of ankle weights (°)*
Heel strike	Coronal	1.00	3.38	1.29	2.18
	Sagittal	3.43	11.72	7.90	5.22
	Transverse	0.90	8.48	2.99	2.56
Loading response	Coronal	-4.90	-0.47	-0.44	-0.24
	Sagittal	10.19	8.43	7.66	8.13
	Transverse	0.44	4.71	3.11	2.00
Mid-stance	Coronal	0.59	2.59	2.67	2.49
	Sagittal	5.14	3.40	3.19	3.95
	Transverse	4.78	0.65	0.82	2.97
Terminal stance	Coronal	3.05	5.06	3.90	4.53
	Sagittal	-10.34	-6.58	-3.80	-3.57
	Transverse	3.68	1.09	0.21	0.19

Table 7.3. One-way ANOVA Post Hoc Bonferroni to evaluate the ankle kinematic angles differences between normal and three unsteady of four stance phases of gait

Multiple Comparisons

Dependent Variable:

Bonferroni

Conditions		Mean Difference	Std. Error	Sig.	95% Confidence Interval	
					Lower Bound	Upper Bound
1- Normal	2	-0.676	1.205	1.0	-4.004	2.650
	3	0.871	1.203	1.0	-2.455	4.199
	4	0.867	1.202	1.0	-2.460	4.195
2- Closed eyes	1	0.676	1.207	1.0	-2.650	4.004
	3	1.548	1.206	1.0	-1.779	4.875
	4	1.544	1.204	1.0	-1.783	4.871
3- On Beam	1	-0.871	1.206	1.0	-4.199	2.455
	2	-1.548	1.203	1.0	-4.875	1.779
	4	-0.004	1.201	1.0	-3.331	3.323
4- Weight	1	-0.867	1.205	1.0	-4.195	2.460
	2	-1.544	1.207	1.0	-4.871	1.783
	3	0.004	1.204	1.0	-3.323	3.331

7.4 Discussion

The purpose of this chapter was to assess the ankle kinematics during normal and three unsteady types of gait. Several previous studies reported on ankle joint kinetics during up- and down-slope walking or on rocking supports (Kaya et al., 2003; Lay et al., 2006; Franz et al., 2012; Silverman et al., 2012; Gates et al., 2013; Novak & Brouwer, 2013), but these studies did not

discuss ankle kinematics. Some studies articulated the kinematics of the ankle on a sloping surface (Lay et al., 2006; Damavandi et al., 2010), and other studies compared foot kinematics on treadmill and ground-surface walking (Alton et al., 1998; Riley et al., 2007). However, this study is the first to evaluate ankle kinematics during normal and unsteady gait using close-range photogrammetry and trialing on adults.

The triplane angles of the ankle were varied in the sagittal plane during heel strike phase, the foot was nearly flat and there was almost no ankle plantarflexion during normal and unsteady gait. Peak dorsiflexion angle was (11.72°) during eyes closed. The subjects maintained dorsiflexion of their ankles until terminal stance changed to plantarflexion in all gaits. However, this study reports no significant differences in ankle dorsiflexion or plantarflexion between normal and unsteady gait which is consistent with previous studies that compared differences between treadmill and overground conditions (Alton et al., 1998; Riley et al., 2007).

In the coronal plane, the ankle has less kinematics than the sagittal plane and it always tends to inversion during all gaits except for the loading response phase which tends to eversion to give greater stability. As can be seen in Table 7.2, the normal gait in the loading response phase has a higher ankle kinematics value because the subjects in unsteady gait are walking slowly according to Dingwell and Marin (2006). Studies conducted by England and Granata (2007) show that slow walking is more stable than fast walking. The ankle kinematics values in the mid-stance phase in all unsteady gaits were very close because the subjects's bodies were more stable in this phase. In the transverse plane, all ankle kinematics have positive values, indicating that all subjects in this phase have internal rotation (adduction) in order to help the body push forward.

As can be seen in Table 7.3, the maximum of mean difference values between normal and all unsteady gait reached (0.871°) showing that the triplanes of ankle angles during unsteady gait were consistent with normal gait, while the ankle angle is considerably less consistent when walking on a single beam, dragging weight, and eyes closed, where the mean differences were (1.548°) between eyes closed and on single beam gait, and (1.544°) between eyes closed and drag weight gait.

In spite of the lack of significant differences between normal and unsteady walking, Table 7.2 shows that in the heel strike the eyes closed gait has higher ankle kinematics values than other

gait types; perhaps because closed eyes lead to an increase in sway (disturbed balance) (Yelnik et al., 2015) and the ankle joint attempts to plays a dominant role in balancing (Gates et al., 2013).

Overall, gait patterns showed an increased dorsiflexion angle at initial contact followed by a continuous plantarflexion movement until terminal stance, similar to that reported by Nigg et al. (2010). Because the foot was nearly flat at heel strike, there was almost no ankle plantarflexion during initial contact when walking on an irregular surface. Subjects dorsiflexed their ankles quickly during mid-stance when walking over an irregular surface, but still maintained similar dorsiflexion prior to terminal stance compared to normal ground (Gates et al., 2012). Decreasing inversion/eversion motion at heel strike until mid-stance then slightly increasing at terminal stance is consistent with other studies (Silverman et al., 2012; Novak & Brouwer, 2013). All participants had internal ankle rotation in the stance phase for normal and unsteady gait due to the internal rotation that occurs during dorsiflexion (Brockett & Chapman, 2016) and the ankle in dorsiflexion was more stable in the majority of the conditions tested, see Figure 7.2.

Table 7.3 shows the mean differences between normal and unsteady walking. The maximum mean differences between eyes closed and walking on beam (±1.548°). This means that the orientation and behaviour of subjects' ankles varied when walking under these conditions. In contrast, the minimum mean differences between walking on beam and dragging weight was (±0.004°), indicating that the subjects' walking behaviour was the same in these conditions.

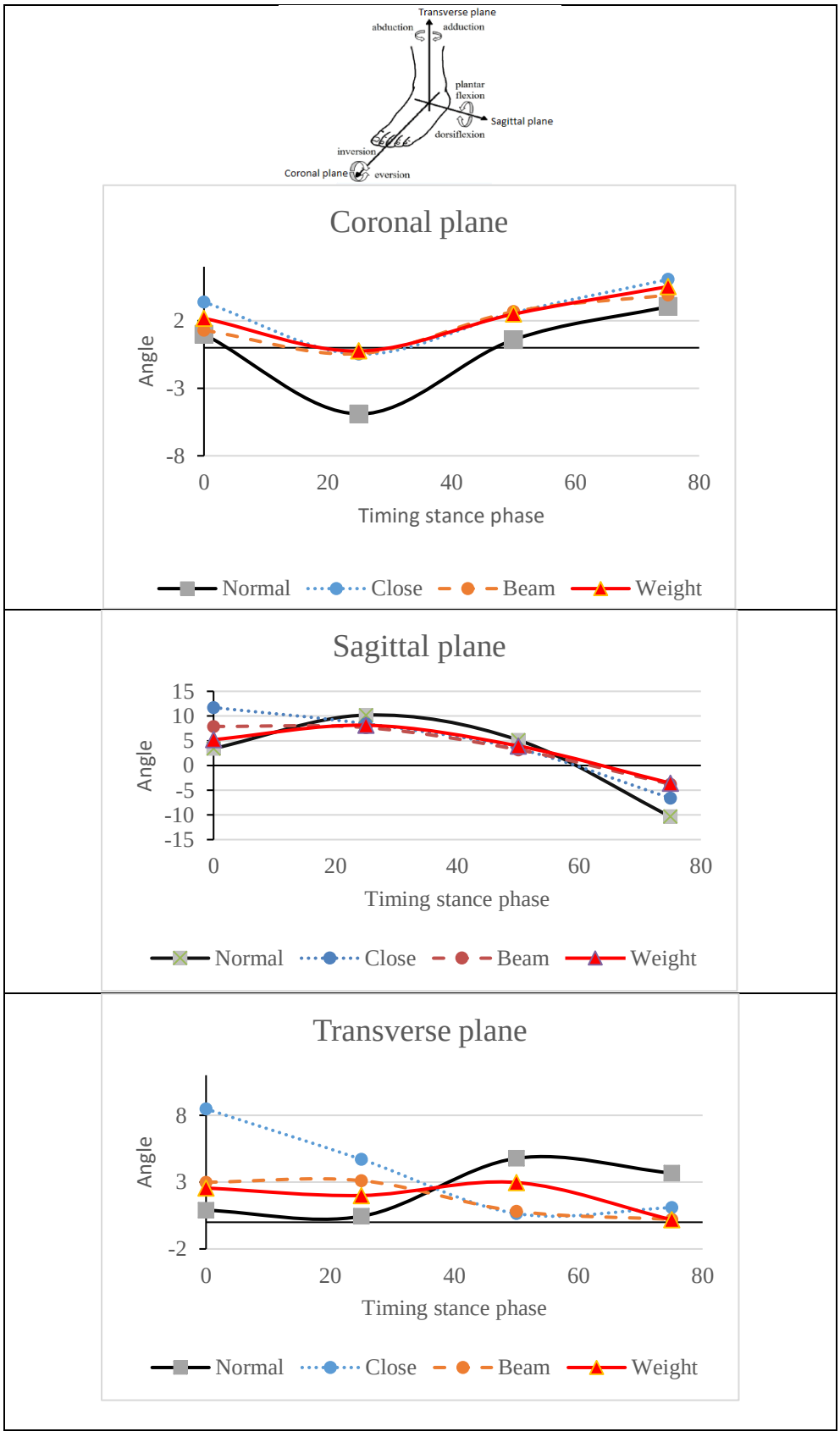

Figure 7.2. Angles of three planes of ankle kinematics during stance phase of gait in normal, closed eyes, single beam, and dragging weight

7.5 Summary and Conclusion

The ankle joint is of great importance during gait as it allows shock absorption and provides forward propulsion force during the terminal stance phase in both normal and unsteady gait. The aim of this chapter was to evaluate ankle kinematics during instance phase in normal and unsteady gait. Thirty-three adults from Middle Eastern countries were recruited. Seven reflective markers were placed over the bony landmarks of foot and ankle of each participant, and measurement were taken using seven smartphone cameras. Ankle coordinates were determined using a photogrammetric bundle adjustment technique during normal gait and three unsteady gait trials ((1) eyes closed, (2) on single beam, and (3) dragging ankle weights) in four phases of stance (heel strike, loading response, mid-stance and terminal stance). The findings were that the eyes closed gait has higher ankle kinematics values than other gait conditions in heel strike phase (3.38°, 11.72°, and 8.48°) in the coronal, sagittal, and transverse planes, respectively.

However, no significant differences in ankle kinematics were found between the normal and the three unsteady gaits, and the results demonstrated very good reliability (ICC=0.82). The information obtained from this study enhances understanding of the kinematics of the human ankle in the stance phase during normal and unsteady walking. A better understanding of the biomechanical ankle variables involved could help prevent potential falls. Furthermore, this knowledge could help with prosthetic design, as well as the design and manufacture of shoes.

The results show that close-range photogrammetry can measure ankle and other joints accurately and reliably whilst undertake various activities and are in a variety of conditions.

Chapter 8. Conclusion and future directions

8.1 Conclusion

Advancing the knowledge of human foot function and ankle kinematics in daily activities' impact on foot performance and is a crucial field of human health research. This knowledge is particularly important for the study and treatment of pathological injuries, deformed feet and ankle sprain, and to help design appropriate therapeutic footwear that fits the individual foot's shape features. In this thesis, a number of investigations were implemented to capture 3D video images of the foot shape and ankle kinematics during walking to assist in understanding the morphology and structural behaviour of the foot and ankle kinematics during gait.

This study introduces close-range photogrammetric techniques using HD smartphone cameras which are becoming popular for capturing accurate 3D models of the human body. They have also been shown to be useful for the study of the human foot morphology and ankle behaviour during normal and unsteady gait. The study discusses various methods of measuring foot shape, behaviour of the MLA, and kinematics of ankle. Five objectives were established to accomplish the research aim. These objectives were: 1) Determine the quality of smartphone cameras and close range photogrammetry system for simultaneous accurate 3D imaging system of the human foot shape; 2) Investigation of the 3D human foot shape characteristics between females and males; 3) Evaluation and determination of the Medial Longitudinal Arch (MLA) in static and dynamic conditions; 4) Validation and investigation of 3D ankle kinematics during gait according to genders; and 5) Assessment and determination of the ankle kinematics in normal and unsteady gait. Below are the conclusions of the study based on each research objective.

Objective 1

An investigation of 3D foot morphology was achieved during this study. Many techniques have been used to measure foot shape and analyse foot dimensions include foot print, calliper, and radiographic. Most of these techniques are either high cost or poor quality. However, this study used high accuracy and cheap tools to capture foot dimensions using smartphone cameras and a close-range photogrammetry technique. Close-range photogrammetry has enabled non-contact, high accuracy and low cost measurement of foot dimensions. The research study concluded that the RMS of smartphone camera calibration ranging between 0.2 and 0.7 pixels, and that means high quality stability of the lens for all smartphone cameras used to capture foot

images. In this study 14 foot dimensions and 11 foot parameters were computed and repeated that for the same adults for three sessions. The average reliability using ICC and SEM indicated a high level of agreement of the repeatable measures. The results indicate that close-range photogrammetry is a reliable and simple technique to measure foot morphology.

Objective 2

Very few studies have investigated the 3D foot shape characteristics of adult females and males of Middle Eastern populations. The outcome of the research shows that all the mean values of foot dimensions and parameters in males were higher than females except the FI and the AHI_TFL; females have higher mean values. There were significant differences between FL, TFL, AL, FB, HB, BIB, MB, HMF, NH, AJH, BG, HG, AHR, NNH_TFL, NNH_I, CSI, CSIR and SAI characteristics of the feet of each gender. The high value of CSIR for both genders indicates that the participants in our results have flat feet. Compared to other countries, the adults of Middle Eastern countries have smaller differences in foot shape than other ethnicities that should be incorporated into designing shoes to meet the requirements for the shoe fit and comfort of Middle Eastern adults.

Objective 3

Foot type is classified as either pes cavus (high-arched), pes planus (flat foot/low-arched) or normally arched depending on the structure of the MLA. Most of apparatus and methods used to evaluate and classify the foot are based on ND in the static condition. However, in this study, tests showed that the video-based photogrammetric system developed is suitable for the mapping of the plantar surface during sitting, standing and walking, and that HD smartphone video cameras can be used to produce accurate mapping precision of ±0.3 mm and high quality 3D textured models. Our results show that the MLA in sitting (non-WB) was (137.83°) and in 50% standing was (144.79°). MLA values in 10% WB and 90% WB standing were (140.95°) and (141.30°), respectively. During dynamic conditions in the stance phase, MLA values were (149.72°), (149.83°), (150.57°) and (148.58°). These results show that the arch in sitting tended to be high and the average value of the MLA angle in four stance phases during gait was slightly more than in the static condition. These results validate the importance of the longitudinal arch angle for the foot during physical activity and physical therapy, and may add information to the clinical arena. The close-range photogrammetry technique developed could be used to evaluate

the extent of tissue/structural, compression/stretching and loading variation at different locations of the plantar surface when walking on level and inclining surfaces.

Objective 4

This objective was achieved using 3D photogrammetric measurement to validate and investigate ankle joint kinematics during the stance phase of gait according to gender. The tests show that females had a significantly greater range of ankle motion than the males in the transverse plane throughout the stance phase, and the maximum mean angle of adduction in the heel strike phase for males was higher than for females. The maximum mean angle of inversion/eversion rotation of the ankle for females and males was closer. No significant differences in range of ankle motion in the coronal and sagittal planes were observed between males and females. The overall value of the ICC was 0.86, which is considered “very good”.

In conclusion, this study demonstrates the gender difference of ankle ROM. Specifically, our results show that females have more joint laxity and flexible ankle ROM than males, and males have a higher ROM of AD in the HS phase. Therefore, it is necessary to assess and plan training programs for ankle ROM in males. Further research is needed to ascertain the most effective way to improve ankle joint flexibility in males. This would be beneficial for the prevention of falls, especially for older adults. These results may contribute to the effectiveness of understanding gender differences in ankle function and may be useful to understand and treat ankle joint pathologies in a gender-specific way. The test results show that the video-based photogrammetric technique developed provides accurate values for major phases of gait were used in the testing: HS, LR, MS and TO.

Objective 5

To achieve the last objective, close-range photogrammetry was used to assess and determine the ankle kinematics during normal and unsteady walking. During unsteady walking, four walking conditions were performed by each subject and the subjects performed three trials for each condition (walking eyes closed, walking on a single beam and walking while dragging ankle weights). The findings were that the eyes closed gait has higher ankle kinematics values than other gait conditions in the heel strike phase. However, no significant differences in ankle kinematics were found between the normal and the 3-unsteady gaits, and the results

demonstrated very good reliability (ICC=0.82). The information obtained from this study enhances understanding of the kinematics of the human ankle in the stance phase during normal and unsteady walking. A better understanding of the biomechanical ankle variables involved could help prevent falls. Furthermore, this knowledge could help to improve surgical techniques and prosthetic design, as well as the design and manufacture of shoes.

In conclusion, this research was successful because it has provided convincing answers to the research questions, and it has accomplished all the research objectives.

Table 8.1 Overview of main points of objectives

Objectives	Conclusions
Objective 1	-The RMS of smartphone camera calibration ranging between 0.2 and 0.7 pixels, and that means high quality stability of the lens for all smartphone cameras used to capture foot images. -The results indicate that close-range photogrammetry is a reliable and simple technique to measure foot morphology.
Objective 2	-All the mean values of foot dimensions and parameters in males were higher than females except the FI and the AHI_TFL. -There were significant differences between FL, TFL, AL, FB, HB, BIB, MB, HMF, NH, AJH, BG, HG, AHR, NNH_TFL, NNH_I, CSI, CSIR and SAI characteristics of the feet of each gender.
Objectives 3	-MLA in sitting (non-WB) was (137.83°) and in 50% standing was (144.79°). MLA values in 10% WB and 90% WB standing were (140.95°) and (141.30°), respectively. -During dynamic conditions in the stance phase, MLA values were (149.72°), (149.83°), (150.57°) and (148.58°). -Results show that the arch in sitting tended to be high and the average value of the MLA angle in four stance phases during gait was slightly more than in the static condition.
Objective 4	-Females had a significantly greater range of ankle motion than the males in the transverse plane throughout the stance phase. - The overall value of the ICC was 0.86, which is considered “very good”. -It is necessary to assess and plan training programs for ankle ROM in males.

	- Close-range photogrammetry technique can easily measure joint angles during normal and unsteady gait.
Objective 5	No significant differences in ankle kinematics were found between the normal and the 3-unsteady gaits. -Results demonstrated very good reliability (ICC=0.82).

8.2 Future directions

Overall, the results achieved by this study demonstrate the effectiveness of close-range photogrammetric techniques for high accuracy metric analysis of foot morphology and ankle kinematics during gait. Furthermore, the study may open doors to new and further investigations into the foot and to capture accurate dynamic foot data and carry out tests to determine the suitability of data for preventing the occurrence of falls during unsteady gait. As an extension of this research, investigations could provide vital information about the characteristics of foot morphology and could involve another foot classification method known as the Foot Posture Index (FPI) which has gained popularity due to its high validity and reliability. The development of effective methods for monitoring a large sample of the population from Middle Eastern countries or other geographical locations could give still more reliability.

The study investigates ankle kinematics therefore could involve the kinematics of a complete 3D model of the whole foot including forefoot and hindfoot during the stance phase of gait. Furthermore, research could include plantar surface pressure data of the dynamic foot during gait. Subsequently, research could be carried out to determine the correlation between the centre of pressure (COP) and the plantar rotation angle during gait for each segment of the foot.

Further works could also include developing a comprehensive human ankle evaluation in ascent or descent conditions during gait, which increase the probability of ankle sprain. However, images alone provide only partial information about the foot and ankle, and the foot pressure data could provide the kinetics information about the force and pressure of the dynamic foot during gait. In addition, the close-range photogrammetry technique and imaging sensors can be used to capture details of footwear with the ground surface during gait. This could be useful for designing and manufacturing foot orthotics and footwear. Other suitable applications could include detailed studies on foot deformities.

References

Ab Aziz, SA, Majid, ZB & Setan, HB 2010, 'Application of close range photogrammetry in crime scene investigation (CSI) mapping using Iwitness and crime zone software', *Geoinformation Science Journal*, vol. 10, no. 1, pp. 1-16.

Abboud, R 2002, '(i) Relevant foot biomechanics', *Current Orthopaedics*, vol. 16, no. 3, pp. 165-79.

Abledu, JK, Abledu, GK, Offei, EB & Antwi, EM 2015, 'Determination of sex from footprint dimensions in a Ghanaian population', *PLoS One*, vol. 10, no. 10, p. e0139891.

Agnihotri, AK, Purwar, B, Googoolye, K, Agnihotri, S & Jeebun, N 2007, 'Estimation of stature by foot length', *Journal of forensic and legal medicine*, vol. 14, no. 5, pp. 279-83.

Ahmadi, FF & Layegh, NF 2014, 'Integration of close range photogrammetry and expert system capabilities in order to design and implement optical image based measurement systems for intelligent diagnosing disease', *Measurement*, vol. 51, no. 5, pp. 9-17.

Al-Baghdadi, JA, Chong, AK, McDougall, K & Alshadli, D 2012, 'An investigation of the 3-dimensional surface capture techniques of the human foot', *Proceedings of the International Workshop on Geoinformation Advances 2012*, Universiti Teknologi Malaysia, pp. 26-47.

Al-Baghdadi, JA, Chong, AK, McDougall, K, Alshadli, D, Milburn, P & Newsham-West, R 2011, 'A dense surface modelling technique for foot surface imaging', *Proceedings of the Surveying and Spatial Sciences Biennial Conference (SSSC 2011)*, Scion, pp. 295-302.

Al-Kharaz, A & Chong, AK 2018, 'High accuracy smartphone video calibration for human foot surface mapping', *2018 IEEE 3rd International Conference on Image, Vision and Computing (ICIVC)*, IEEE, pp. 542-5.

Al-Kharaz, A & Chong, AK 2019a, '3D Video Images for Comparing Indian and Iraqi Women's Foot Width Surface Shape Associated with Stance Phase of Gait', *Proceedings of the 2019 2nd International Conference on Information Science and Systems*, pp. 22-6.

Al-Kharaz, A & Chong, AK 2019b, 'Analysis of Gender Related Foot Morphology in Iraqi Adults Using Videogrammetry During Gait', *2019 IEEE 9th Symposium on Computer Applications & Industrial Electronics (ISCAIE)*, IEEE, pp. 108-13.

Al-Kharaz, A & Chong, AK 2020, 'Impact of anthropometric characteristics on the medial longitudinal arch in static and dynamic loading using photogrammetry images', *Series on Biomechanics*, vol. 34, no. 2, pp.56-61.

Al-Rawi, ZS, Al-Aszawi, AJ & Al-Chalabi, T 1985, 'Joint mobility among university students in Iraq', *Rheumatology*, vol. 24, no. 4, pp. 326-31.

Alshadli, D, Chong, AK, McDougall, K, Ahmed, J & Ali, A-B 2011, 'Skin texture-enhancement for automated 3D point cloud generation in charcot-marie-tooth disease application', *IEEE*

2011 10th International Conference on Electronic Measurement & Instruments, IEEE, pp. 6-10.

Alton, F, Baldey, L, Caplan, S & Morrissey, M 1998, 'A kinematic comparison of overground and treadmill walking', *Clinical Biomechanics*, vol. 13, no. 6, pp. 434-40.

Amstutz, E, Teshima, T, Kimura, M, Mochimaru, M & Saito, H 2008, 'PCA-based 3D shape reconstruction of human foot using multiple viewpoint cameras', *International Journal of Automation and Computing*, vol. 5, no. 3, pp. 217-25.

Antoniolli, A, Ducati, LMA, Schmit, EFD & Candotti, CT 2017, 'Feet positioning in the semi-static postural evaluation through photogrammetry: a systematic review', *Motricidade*, vol. 13, no. 4, pp. 62-73.

Antoniolli, A, Candotti, CT, Gelain, GM, Schmit, EFD, Ducatti, LMA, Melo, MdO & Loss, JF 2018, 'Influence of feet position on static postural assessment by means of photogrammetry: a comparative study', *European Journal of Physiotherapy*, vol. 20, no. 3, pp. 166-71.

Antunes, P, Dias, G, Coelho, A, Rebelo, F & Pereira, T 2008, 'Non-linear finite element modelling of anatomically detailed 3D foot model', *Report paper*, pp. 1-11.

Ashizawa, K, Kumakura, C, Kusumoto, A & Narasaki, S 1997, 'Relative foot size and shape to general body size in Javanese, Filipinas and Japanese with special reference to habitual footwear types', *Annals of human biology*, vol. 24, no. 2, pp. 117-29.

Atamturk, D 2010, 'Estimation of sex from the dimensions of foot, footprints, and shoe', *Anthropologischer Anzeiger*, vol. 68, no. 1, pp. 21-9.

Azevedo, AM, Oliveira, R, Vaz, JR & Cortes, N 2020, 'Oxford foot model kinematics in landings: A comparison between professional dancers and non-dancers', *Journal of Science and Medicine in Sport*, vol. 23, no. 4, pp. 347-52.

Bai, Y, Hu, H, Li, Y, Zhao, C, Luo, L and Wang, R, 2017, September. 'Research Methods for Human Activity Space Based on Vicon Motion Capture System'. In *2017 5th International Conference on Enterprise Systems (ES)*, IEEE, pp. 202-206.

Balsdon, M, Dombroski, C, Bushey, K & Jenkyn, TR 2019, 'Hard, soft and off-the-shelf foot orthoses and their effect on the angle of the medial longitudinal arch: A biplane fluoroscopy study', *Prosthetics and orthotics international*, vol. 43, no. 3, pp. 331-8.

Balsdon, ME, Dombroski, CE, Bushey, KM & Jenkyn, TR 2021, 'Impression Methods for Custom Foot Orthoses—Comparing Semi–Weight-Bearing Foam and Non–Weight-Bearing Plaster Using a Kinematic Measurement of the Medial Longitudinal Arch', *JPO: Journal of Prosthetics and Orthotics*, vol 33, no. 1, pp. 26-33.

Balsdon, ME, Bushey, KM, Dombroski, CE, LeBel, M-E & Jenkyn, TR 2016, 'Medial longitudinal arch angle presents significant differences between foot types: a biplane fluoroscopy study', *Journal of biomechanical engineering*, vol. 138, no. 10, pp. 101007-1-6.

Bandholm, T, Boysen, L, Haugaard, S, Zebis, MK & Bencke, J 2008, 'Foot medial longitudinal-arch deformation during quiet standing and gait in subjects with medial tibial stress syndrome', *The Journal of Foot and Ankle Surgery*, vol. 47, no. 2, pp. 89-95.

Barazzetti, L, Scaioni, M & Remondino, F 2010, 'Orientation and 3D modelling from markerless terrestrial images: combining accuracy with automation', *The Photogrammetric Record*, vol. 25, no. 132, pp. 356-81.

Barisch-Fritz, B, Plank, C & Grau, S 2016, 'Evaluation of the rule-of-thumb: calculation of the toe allowance for developing feet', *Footwear Science*, vol. 8, no. 3, pp. 119-27.

Barisch-Fritz, B, Schmeltzpfenning, T, Plank, C & Grau, S 2014, 'Foot deformation during walking: differences between static and dynamic 3D foot morphology in developing feet', *Ergonomics*, vol. 57, no. 6, pp. 921-33.

Behling, A-V, Manz, S, von Tscharner, V & Nigg, BM 2020, 'Pronation or foot movement—What is important', *Journal of Science and Medicine in Sport*, vol. 23, no. 4, pp. 366-71.

Behling, A-V & Nigg, BM 2020, 'Relationships between the foot posture Index and static as well as dynamic rear foot and arch variables', *Journal of biomechanics*, vol. 98, 109448, pp.1-7.

Bennell, KL & Goldie, PA 1994, 'The differential effects of external ankle support on postural control', *Journal of Orthopaedic & Sports Physical Therapy*, vol. 20, no. 6, pp. 287-95.

Bibby, S, Kerster, R, McN, R, Alexander, R & Bennett, M 1987, 'The spring in the arc of the human foot', *Nature*, vol. 325, no. 8, p. 147-49.

Bidmos, MA & Asala, SA 2003, 'Discriminant function sexing of the calcaneus of the South African whites', *Journal of forensic sciences*, vol. 48, no. 6, pp. 1213-8.

Bieman, LH & Harding, KG 1997, '3D imaging using a unique refractive optic design to combine moiré and stereo', *Three-Dimensional Imaging and Laser-based Systems for Metrology and Inspection III*, International Society for Optics and Photonics, pp. 2-10.

Bindurani, MK, Kavyashree, AN, Asha, KR & Lakshmiprabha, S 2017, 'Determination of sex from foot dimensions', *International Journal of Anatomy and Research* vol. 5, no. 4.3, pp. 4702-4706.

Black, JT & Pappa, RS 2003, 'Videogrammetry using projected circular targets: proof-of-concept test', Hampton, Virginia, US.

Blair, S, Lake, M.J, Ding, R and Sterzing, T 2018, 'Magnitude and variability of gait characteristics when walking on an irregular surface at different speeds', *Human movement science*, vol. 59, no. 3, pp.112-120.

Blenkinsopp, R, Harland, A, Price, D, Lucas, T & Roberts, J 2012, 'A method to measure dynamic dorsal foot surface shape and deformation during linear running using digital image correlation', *Procedia engineering*, vol. 34, no. 8, pp. 266-71.

Bonnefoy-Mazure, A & Armand, S 2015,'Normal gait', *Orthopedic management of children with cerebral palsy*, (chapter 16). Amsterdam: Elsevier, pp. 200-211.

Borlin, N 2014, 'Fundamentals of Photogrammetry', Department of Computing Science Umea University, Sweden.

BPT, ACUP, Arulsingh, W, KR, R & Raj, JO 2015, 'Does BMI variation change the height of foot arch in healthy adults: a cross sectional study', *The Foot and Ankle Online Journal*, vol. 8, no. 4, pp. 1-4.

Branthwaite, H, Chockalingam, N & Greenhalgh, A 2013, 'The effect of shoe toe box shape and volume on forefoot interdigital and plantar pressures in healthy females', *Journal of foot and ankle research*, vol. 6, no. 1, pp. 28-37.

Breloff, S.P, Wade, C and Waddell, D.E 2019,'Lower extremity kinematics of cross-slope roof walking', *Applied ergonomics*, vol. *75*, no. 2, pp. 134-142.

Brockett, CL & Chapman, GJ 2016, 'Biomechanics of the ankle', *Orthopaedics and trauma*, vol. 30, no. 3, pp. 232-8.

Brody, D.M 1982, 'Techniques in the evaluation and treatment of the injured runner', *The orthopedic clinics of north America*, vol. 13, no. 3, pp.541-558.

Brooks, RE & Heflinger, LO 1969, 'Moiré gauging using optical interference patterns', *Applied Optics*, vol. 8, no. 5, pp. 935-9.

Brown, D 1971,'Close-range camera calibration', *Photogrammetric Engineering*, vol. 37**,** no. 8, pp. 855-66.

Brown, D 1976, 'The Bundle Adjustment-Progress and Prospects. Invited Paper of Commision III', *ISP Congress*, Helsinki, 1976, p.33.

Bruijn, SM, van Dieën, JH, Meijer, OG & Beek, PJ 2009, 'Is slow walking more stable?', *Journal of biomechanics*, vol. 42, no. 10, pp. 1506-12.

Budhabhatti, SP, Erdemir, A, Petre, M, Sferra, J, Donley, B & Cavanagh, PR 2007, 'Finite element modeling of the first ray of the foot: a tool for the design of interventions', *Journal of Biomechanical Engineering*, vol. 129, no. 5, pp. 750-756.

Buldt, AK & Menz, HB 2018, 'Incorrectly fitted footwear, foot pain and foot disorders: a systematic search and narrative review of the literature', *Journal of foot and ankle research*, vol. 11, no. 1, p. 43.

Burns, J, Crosbie, J, Ouvrier, R and Hunt, A 2006, 'Effective orthotic therapy for the painful cavus foot: a randomized controlled trial', *Journal of the American Podiatric Medical Association*, vol. 96, no. 3, pp.205-211.

Bus, SA & de Lange, A 2005, 'A comparison of the 1-step, 2-step, and 3-step protocols for obtaining barefoot plantar pressure data in the diabetic neuropathic foot', *Clinical Biomechanics*, vol. 20, no. 9, pp. 892-9.

Bushey, KM 2012, 'Investigation of in-vivo hindfoot and orthotic interactions using bi-planar x-ray fluoroscopy', MSc thesis in Engineering Science, the University of Western Ontario,Canada .

Butler, RJ, Davis, IS & Hamill, J 2006, 'Interaction of arch type and footwear on running mechanics', *The American Journal of Sports Medicine*, vol. 34, no. 12, pp. 1998-2005.

Canton, S, Anderst, W & Hogan, MV 2020, 'In Vivo Ankle Kinematics Revealed Through Biplane Radiography: Current Concepts, Recent Literature, and Future Directions', *Current Reviews in Musculoskeletal Medicine*, vol. 13, no. 1, pp. 1-9.

Cashmere, T, Smith, R & Hunt, A 1999, 'Medial longitudinal arch of the foot: stationary versus walking measures', *Foot & ankle international*, vol. 20, no. 2, pp. 112-8.

Castaneda, V, Mateus, D & Navab, N 2011, 'Stereo time-of-flight', *2011 International Conference on Computer Vision*, IEEE, pp. 1684-91.

Catherwood, T, McCaughan, E, Greer, E, Spence, R, McIntosh, S & Winder, R 2011, 'Validation of a passive stereophotogrammetry system for imaging of the breast: a geometric analysis', *Medical engineering & physics*, vol. 33, no. 8, pp. 900-905.

Cavanagh, PR & Rodgers, MM 1987, 'The arch index: a useful measure from footprints', *Journal of biomechanics*, vol. 20, no. 5, pp. 547-51.

Chaiwanichsiri, D, Tantisiriwat, N & Janchai, S 2008, 'Proper shoe sizes for Thai elderly', *The Foot*, vol. 18, no. 4, pp. 186-91.

Chan, CW & Rudins, A 1994, 'Foot biomechanics during walking and running', *Mayo Clinic Proceedings*, Elsevier, vol. 69, No. 5, pp. 448-61.

Chang, H-W, Chieh, H-F, Lin, C-J, Su, F-C & Tsai, M-J 2014, 'The relationships between foot arch volumes and dynamic plantar pressure during midstance of walking in preschool children', *PLoS One*, vol. 9, no. 4, p. e94535.

Chang, H-W, Lin, C-J, Kuo, L-C, Tsai, M-J, Chieh, H-F & Su, F-C 2012, 'Three-dimensional measurement of foot arch in preschool children', *Biomedical engineering online*, vol. 11, no. 1, p. 76.

Chang, J-H, Wang, S-H, Kuo, C-L, Shen, HC, Hong, Y-W & Lin, L-C 2010, 'Prevalence of flexible flatfoot in Taiwanese school-aged children in relation to obesity, gender, and age', *European journal of pediatrics*, vol. 169, no. 4, pp. 447-52.

Chen, F, Brown, GM & Song, M 2000, 'Overview of 3-D shape measurement using optical methods', *OptEn*, vol. 39, no. 1, pp. 10-22.

Chen, J-P, Chung, M-J & Wang, M-J 2009, 'Flatfoot prevalence and foot dimensions of 5–to 13-year-old children in Taiwan', *Foot & ankle international*, vol. 30, no. 4, pp. 326-32.

Cheung, JT-M & Zhang, M 2005, 'A 3-dimensional finite element model of the human foot and ankle for insole design', *Archives of physical medicine and rehabilitation*, vol. 86, no. 2, pp. 353-8.

Cheung, JT-M & Nigg, BM 2008, 'Clinical applications of computational simulation of foot and ankle', *Sport-Orthopädie-Sport-Traumatologie-Sports Orthopaedics and Traumatology*, vol. 23, no. 4, pp. 264-71.

Chiari, L, Della Croce, U, Leardini, A and Cappozzo, A 2005, 'Human movement analysis using stereophotogrammetry: Part 2: Instrumental errors', *Gait & posture*, vol. *21, no.* 2, pp.197-211.

Cho, KH, Jeon, Y & Lee, H 2016, 'Range of motion of the ankle according to pushing force, gender and knee position', *Annals of rehabilitation medicine*, vol. 40, no. 2, p. 271.

Cho, S, Park, J & Kwon, O 2004, 'Gender differences in three dimensional gait analysis data from 98 healthy Korean adults', *Clinical Biomechanics*, vol. 19, no. 2, pp. 145-52.

Chong, AK 2011, 'Low-cost compact cameras: A medical application in CMT disease monitoring', *The Photogrammetric Record*, vol. 26, no. 134, pp. 263-73.

Chong, AK 2012, 'Exploiting HD Camcorders for Close-Up Human Movement Applications', *The Photogrammetric Record*, vol. 27, no. 138, pp. 227-37.

Chong, AK, Al-Baghdadi, JAA & Milburn, PB 2015, 'The effect of fixing kinesiology tape onto the plantar surface during the loading phase of gait', *Proceedings of the 17th International Conference on Biomechanics and Biomedical Engineering (ICBBE 2015)*, World Academy of Science, Engineering and Technology, pp. 177-181.

Chong, AK, Milburn, P, Newsham-West, R & Voert, M 2009, 'High-accuracy photogrammetric technique for human spine measurement', *The Photogrammetric Record*, vol. 24, no. 127, pp. 264-79.

Chong, AK, Milburn, P, West, RN, ter Voert, M & Croftc, H 2008, 'Recent practical applications of close-range photogrammetry for complex motion study', *Int Arch Photogramm Rem Sens Spatial Inform Sci*, vol. 37, no. Part B5, pp. 921-6.

Chong, AK, Alshadli, D, AL-Baghdadi, JAA, Milburn, P & Newsham-West, R 2013, 'A video-based system for plantar surface acquisition during gait', *Proceedings of the 31st International Conference on Biomechanics in Sports (ISBS 2013)*, National Taiwan Normal University, pp. 1-4.

Chromy, A & Zalud, L 2014, 'Robotic 3D scanner as an alternative to standard modalities of medical imaging', *SpringerPlus*, vol. 3, no. 1, p. 13.

Chuter, V, Payne, C & Miller, K 2003, 'Variability of neutral-position casting of the foot', *Journal of the American Podiatric Medical Association*, vol. 93, no. 1, pp. 1-5.

Chuter, VH 2010, 'Relationships between foot type and dynamic rearfoot frontal plane motion', *Journal of foot and ankle research*, vol. 3, no. 1, pp. 1-6.

Ciccarelli, A, Mantini, S, Scrimaglio, R, Sorrenti, S & Colaiacomo, B 2011, 'Geometric morphometric approach in the study of the footprint variation in children between 6 and 12 years of age', *Journal of Anatomy and Embryology*, vol. 116, pp. 43-43.

Cornwall, MW & McPoil, TG 2011, 'Relationship between static foot posture and foot mobility', *Journal of foot and ankle research*, vol. 4, no. 1, p. 4.

Cortizo, E, Yeras, AM, Lepore, J & Garavaglia, M 2003, 'Application of the structured illumination method to study the topography of the sole of the foot during a walk', *Optics and lasers in engineering*, vol. 40, no. 1-2, pp. 117-32.

Cooper, M & Robson, S 2001, 'Theory of close range photogrammetry', In: Atkinson, KB , ed. Close-Range Photogrammetry and Machine Vision. Latheronwheel, Scotland: Whittles Publishing; 2001, pp. 9–50.

Cote K.P, Brunet M.E, Gansneder B.M, Shultz S.J 2005, 'Effects of pronated and supinated foot postures on static and dynamic postural stability', *Journal of Athletic Training*, vol. 40, no. 1, pp. 41-46.

Costea, M, Sarghie, B, Mihai, A and Rezus, E 2017, 'Classification of the elderly foot types based on plantar footprints', *Procedia engineering*, vol. 181, no. 12, pp.36-43.

Coudert, T, Vacher, P, Smits, C & Van der Zande, M 2006, 'A method to obtain 3D foot shape deformation during the gait cycle', *9th International Symposium on the 3D analysis of Human Movement*, pp.1-4.

Cowan, D.N, Robinson, J.R, Jones, B.H, Polly Jr, D.W and Berrey Jr, B.H 1994, 'Consistency of visual assessments of arch height among clinicians', *Foot & ankle international*, vol. 15, no. 4, pp.213-217.

Cross, JA, McHenry, BD, Molthen, R, Exten, E, Schmidt, TG & Harris, GF 2017, 'Biplane fluoroscopy for hindfoot motion analysis during gait: A model-based evaluation', *Medical engineering & physics*, vol. 43, no. 5, pp. 118-23.

Cui, Y, Schuon, S, Chan, D, Thrun, S & Theobalt, C 2010, '3D shape scanning with a time-of-flight camera', *2010 IEEE Computer Society Conference on Computer Vision and Pattern Recognition*, IEEE, pp. 1173-80.

D'Apuzzo, N 2003, 'Human body motion capture from multi-image video sequences', *Videometrics VII*, International Society for Optics and Photonics, vol. 5013,no. 6, pp. 54-61.

Dahle, LK, Mueller, M, Delitto, A & Diamond, JE 1991, 'Visual assessment of foot type and relationship of foot type to lower extremity injury', *Journal of Orthopaedic & Sports Physical Therapy*, vol. 14, no. 2, pp. 70-4.

Dai, X-Q, Li, Y, Zhang, M & Cheung, JT-M 2006, 'Effect of sock on biomechanical responses of foot during walking', *Clinical Biomechanics*, vol. 21, no. 3, pp. 314-21.

Damavandi, M, Dixon, PC & Pearsall, DJ 2010, 'Kinematic adaptations of the hindfoot, forefoot, and hallux during cross-slope walking', *Gait & posture*, vol. 32, no. 3, pp. 411-5.

Dananberg, HJ, Shearstone, J & Guillano, M 2000, 'Manipulation method for the treatment of ankle equinus', *Journal of the American Podiatric Medical Association*, vol. 90, no. 8, pp. 385-9.

David, P, Halimi, M, Mora, I, Doutrellot, P-L & Petitjean, M 2013, 'Isokinetic testing of evertor and invertor muscles in patients with chronic ankle instability', *Journal of applied biomechanics*, vol. 29, no. 6, pp. 696-704.

Davies, C, Hackman, L & Black, S 2014, 'The foot in forensic human identification–A review', *The Foot*, vol. 24, no. 1, pp. 31-6.

de la Vega, I, Graebe, J, Härtner, L, Dudschig, C & Kaup, B 2015, 'Starting off on the right foot: strong right-footers respond faster with the right foot to positive words and with the left foot to negative words', *Frontiers in Psychology*, vol. 6, no. 1, p. 292-306.

De Menezes, M, Rosati, R, Ferrario, VF & Sforza, C 2010, 'Accuracy and reproducibility of a 3-dimensional stereophotogrammetric imaging system', *Journal of Oral and Maxillofacial Surgery*, vol. 68, no. 9, pp. 2129-35.

De Ridder, R, Willems, T, Vanrenterghem, J, Robinson, M, Pataky, T & Roosen, P 2013, 'Gait kinematics of subjects with ankle instability using a multisegmented foot model', *Med Sci Sports Exerc*, vol. 45, no. 11, pp. 2129-36.

Del Vecchio, S, De Araújo, PA, Rubio, JCC, Pinotti, M & Sesselmann, M 2012, '3D measurement of human plantar foot by projection moiré technique', *International Journal of Mechatronics and Manufacturing Systems*, vol. 5, no. 1, pp. 3-16.

Derawi, MO, Nickel, C, Bours, P & Busch, C 2010, 'Unobtrusive user-authentication on mobile phones using biometric gait recognition', *2010 Sixth International Conference on Intelligent Information Hiding and Multimedia Signal Processing*, IEEE, pp. 306-11.

Dingwell, JB & Marin, LC 2006, 'Kinematic variability and local dynamic stability of upper body motions when walking at different speeds', *Journal of biomechanics*, vol. 39, no. 3, pp. 444-52.

Dixon, PC & Pearsall, DJ 2010, 'Gait dynamics on a cross-slope walking surface', *Journal of applied biomechanics*, vol. 26, no. 1, pp. 17-25.

Dobson, JA, Riddiford-Harland, DL, Bell, AF & Steele, JR 2018, 'The three-dimensional shapes of underground coal miners' feet do not match the internal dimensions of their work boots', *Ergonomics*, vol. 61, no. 4, pp. 588-602.

Dombroski, CE, Balsdon, M & Adam, F 2014, 'A low cost 3D scanning and printing tool for clinical use in the casting and manufacture of custom foot Orthoses', *Proceedings of the 5th International Conference on 3D Body Scanning Technologies, Lugano, Switzerland*, pp. 21-2.

Domjanić, J 2015, 'Geometric morphometrics in the analysis of bilateral feet symmetry', *Tekstil: časopis za tekstilnu tehnologiju i konfekciju*, vol. 64, no. 3-4, pp. 103-8.

Drewes, LK, McKeon, PO, Kerrigan, DC & Hertel, J 2009, 'Dorsiflexion deficit during jogging with chronic ankle instability', *Journal of Science and Medicine in Sport*, vol. 12, no. 6, pp. 685-7.

Ebrahim, MA-B 2004, 'Using mobile phone digital cameras in digital close range photogrammetry', *Assiut University, Ebrahim@ acc. aun. eun. eg*.

Echeita, JA, Hijmans, JM, Smits, S, Van der Woude, LH & Postema, K 2016, 'Age-related differences in women's foot shape', *Maturitas*, vol. 94, no. 12, pp. 64-69.

Eckardt, N and Kibele, A 2017,'Automatic identification of gait events during walking on uneven surfaces', *Gait &posture*, vol. 52,no. 2, pp. 83-86.

England, SA & Granata, KP 2007, 'The influence of gait speed on local dynamic stability of walking', *Gait & posture*, vol. 25, no. 2, pp. 172-8.

Evin, A, Souter, T, Hulme-Beaman, A, Ameen, C, Allen, R, Viacava, P, Larson, G, Cucchi, T & Dobney, K 2016, 'The use of close-range photogrammetry in zooarchaeology: Creating accurate 3D models of wolf crania to study dog domestication', *Journal of Archaeological Science: Reports*, vol. 9, no. 5, pp. 87-93.

Ezema, C.I, Abaraogu, U.O and Okafor, G.O 2014, 'Flat foot and associated factors among primary school children: A cross-sectional study', *Hong Kong Physiotherapy Journal*, vol. 32, no. 1, pp.13-20.

Fawzy, HE-D 2019, 'Study the accuracy of digital close range photogrammetry technique software as a measuring tool', *Alexandria Engineering Journal*, vol. 58, no. 1, pp. 171-9.

Fawzy, IA & Kamal, NN 2010, 'Stature and body weight estimation from various footprint measurements among Egyptian population', *Journal of forensic sciences*, vol. 55, no. 4, pp. 884-8.

Ferber, R & Benson, B 2011, 'Changes in multi-segment foot biomechanics with a heat-mouldable semi-custom foot orthotic device', *Journal of foot and ankle research*, vol. 4, no. 1, p. 18.

Ferran, N.A & Maffulli, N 2006, 'Epidemiology of sprains of the lateral ankle ligament complex', *Foot and ankle clinics*, vol. 11, no. 3, pp.659-662.

Ferran, NA, Oliva, F & Maffulli, N 2009, 'Ankle instability', *Sports medicine and arthroscopy review*, vol. 17, no. 2, pp. 139-45.

Ficanha, EM, Rastgaar, M & Kaufman, KR 2015, 'Ankle mechanics during sidestep cutting implicates need for 2-degrees of freedom powered ankle-foot prostheses', *Journal of Rehabilitation Research & Development*, vol. 52, no. 1, pp. 97-112.

Franco, AH 1987, 'Pes cavus and pes planus: analyses and treatment', *Physical Therapy*, vol. 67, no. 5, pp. 688-94.

Franz, JR, Lyddon, NE & Kram, R 2012, 'Mechanical work performed by the individual legs during uphill and downhill walking', *Journal of biomechanics*, vol. 45, no. 2, pp. 257-62.

Fraser, CS 1992, 'Photogrammetric measurement to one part in a million', *PgERS*, vol. 58, no. 3, pp. 305-10.

Fraser, C 2015, 'Advances in close-range photogrammetry', In *Photogrammetric week*, vol. 15, no. 3, pp. 257-268.

Fraser, C 1996, 'Network Design, KB Atkinson', *Close range photogrammetry and machine vision*, pp. 256-281.

Fraser, C & Al-Ajlouni, S 2006, 'Zoom-dependent camera calibration in digital close-range photogrammetry', *Photogrammetric Engineering & Remote Sensing*, vol. 72, no. 9, pp. 1017-26.

Fraser, C & Edmundson, K 1996, 'The metric impact of reduction optics in digital cameras', *The Photogrammetric Record*, vol. 15, no. 87, pp. 437-446.

Frontera, WR, DeLisa, JA, Gans, BM & Robinson, LR 2019, *DeLisa's physical medicine and rehabilitation: principles and practice*, Lippincott Williams & Wilkins.

Fryer, J 1989, 'Camera calibration in non-topographic photogrammetry', *Non-topographic photogrammetry*.

Fryer, J 2001, 'Introduction in close range photogrammetry and machine vision', *Whittles Publishing, Caithness, UK*, vol. *371*, pp. 1-7.

Fryer, J & Brown, D 1986,'Lens distortion for close-range photogrammetry', *Photogrammetric engineering and remote sensing*, vol. 52, no. 1, pp. 51-58.

Fukano, M & Fukubayashi, T 2012, 'Gender-based differences in the functional deformation of the foot longitudinal arch', *The Foot*, vol. 22, no. 1, pp. 6-9.

Fukano, M, Fukubayashi, T & Banks, SA 2018, 'Sex differences in three-dimensional talocrural and subtalar joint kinematics during stance phase in healthy young adults', *Human movement science*, vol. 61, no. 5, pp. 117-25.

Furlanetto, TS, Candotti, CT, Comerlato, T & Loss, JF 2012, 'Validating a postural evaluation method developed using a Digital Image-based Postural Assessment (DIPA) software', *Computer methods and programs in biomedicine*, vol. 108, no. 1, pp. 203-12.

Gabriel, RC, Abrantes, J, Granata, K, Bulas-Cruz, J, Melo-Pinto, P & Filipe, V 2008, 'Dynamic joint stiffness of the ankle during walking: gender-related differences', *Physical Therapy in sport*, vol. 9, no. 1, pp. 16-24.

Gajdosik, RL & Bohannon, RW 1987, 'Clinical measurement of range of motion: review of goniometry emphasizing reliability and validity', *Physical Therapy*, vol. 67, no. 12, pp. 1867-72.

Gastwirth, B 1996, 'Biomechanical examination of the foot and lower extremity', *Clinical biomechanics of the lower extremities*, p. 131.

Gates, DH, Dingwell, JB, Scott, SJ, Sinitski, EH & Wilken, JM 2012, 'Gait characteristics of individuals with transtibial amputations walking on a destabilizing rock surface', *Gait & posture*, vol. 36, no. 1, pp. 33-9.

Gates, DH, Scott, SJ, Wilken, JM & Dingwell, JB 2013, 'Frontal plane dynamic margins of stability in individuals with and without transtibial amputation walking on a loose rock surface', *Gait & posture*, vol. 38, no. 4, pp. 570-5.

Giladi, M, Milgrom, C, Stein, M, Kashtan, H, Margulies, J, Chisin, R, Steinberg, R & Aharonson, Z 1985, 'The low arch, a protective factor in stress fractures. A prospective study of 295 military recruits', *Orthop Rev*, vol. 14, no. 11, pp. 709-12.

Goda, I, L'Hostis, G & Guerlain, P 2019, 'In-situ non-contact 3D optical deformation measurement of large capacity composite tank based on close-range photogrammetry', *Optics and lasers in engineering*, vol. 119, no. 8, pp. 37-55.

Gomes, PF, Sesselmann, M, Faria, CD, Araújo, PA & Teixeira-Salmela, LF 2010, 'Measurement of scapular kinematics with the moiré fringe projection technique', *Journal of biomechanics*, vol. 43, no. 6, pp. 1215-9.

Gonda, E & Katayama, K 2006, 'Big feet in Polynesia: a somatometric study of the Tongans', *Anthropological Science*, vol. 114, no. 2, pp. 127-131.

Granshaw, S 1980, 'Bundle adjustment methods in engineering photogrammetry', *The Photogrammetric Record*, vol. 10, no. 56, pp. 181-207.

Grau, S & Barisch-Fritz, B 2017, 'Improvement of fit of security shoes–evaluation of dynamic foot structure', *Footwear Science*, vol. 9, no. sup1, pp. S36-S7.

Grood, ES & Suntay, WJ 1983, 'A joint coordinate system for the clinical description of three-dimensional motions: application to the knee', *Journal of biomechanical Engineering*, vol. 105, no. 2, pp. 136-144.

Grossman, G 2003, 'Measuring dancer's active and passive turnout', *Journal of Dance Medicine & Science*, vol. 7, no. 2, pp. 49-55.

Guldemond, NA, Leffers, P, Sanders, AP, Emmen, H, Schaper, NC & Walenkamp, GH 2006, 'Casting methods and plantar pressure: effects of custom-made foot orthoses on dynamic plantar pressure distribution', *Journal of the American Podiatric Medical Association*, vol. 96, no. 1, pp. 9-18.

Gwashavanhu, B, Oberholster, AJ & Heyns, PS 2016, 'Rotating blade vibration analysis using photogrammetry and tracking laser Doppler vibrometry', *Mechanical Systems and Signal Processing*, vol. 76, no. 7, pp. 174-86.

Hajaghazadeh, M, Minaei, RE, Allahyari, T & Khalkhali, H 2018, 'Anthropometric Dimensions of Foot in Northwestern Iran and Comparison with Other Populations', *Health Scope*, vol. 7, no. 3,pp. 1-8.

Haleem, A & Javaid, M 2019, '3D scanning applications in medical field: a literature-based review', *Clinical Epidemiology and Global Health*, vol. 7, no. 2, pp. 199-210.

Hallaceli, H, Uruc, V, Uysal, HH, Özden, R, Hallaçeli, Ç, Soyuer, F, İnce Parpucu, T, Yengil, E & Cavlak, U 2014, 'Normal hip, knee and ankle range of motion in the Turkish population', *Acta Orthop Traumatol Turc*, vol. 48, no. 1, pp. 37-42.

Hamacher, D, Liebl, D, Hödl, C, Heßler, V, Kniewasser, C, Thönnessen, T and Zech, A 2019, 'Gait stability and its influencing factors in older adults', *Frontiers in physiology*, vol. *9*, no.1955, pp. 1-11.

Hamid, NA & Ahmad, A 2014, 'Calibration of high resolution digital camera based on different photogrammetric methods', *IOP Conference Series: Earth and Environmental Science*, IOP Publishing, vol. 18, no. 1, p. 012030.

Hartley, R & Kang, SB 2007, 'Parameter-free radial distortion correction with center of distortion estimation', *IEEE Transactions on Pattern Analysis and Machine Intelligence*, vol. 29, no. 8, pp. 1309-21.

Hawes, MR & Sovak, D 1994, 'Quantitative morphology of the human foot in a North American population', *Ergonomics*, vol. 37, no. 7, pp. 1213-26.

Hawes, MR, Nachbauer, W, Sovak, D & Nigg, BM 1992, 'Footprint parameters as a measure of arch height', *Foot & ankle*, vol. 13, no. 1, pp. 22-6.

Hawes, MR, Sovak, D, Miyashita, M, Kang, S-j, Yoshihuku, Y & Tanaka, S 1994, 'Ethnic differences in forefoot shape and the determination of shoe comfort', *Ergonomics*, vol. 37, no. 1, pp. 187-96.

Hedrick, EA, Malcolm, P, Wilken, JM & Takahashi, KZ 2019, 'The effects of ankle stiffness on mechanics and energetics of walking with added loads: a prosthetic emulator study', *Journal of neuroengineering and rehabilitation*, vol. 16, no. 1, pp. 1-15.

Herman, GT 2009, *Fundamentals of computerized tomography: image reconstruction from projections*, Springer Science & Business Media.

Herráez, J, Martínez-Llario, J, Coll, E, Rodríguez, J & Martin, M 2013, 'Design and calibration of a 3D modeling system by videogrammetry', *Measurement Science and Technology*, vol. 24, no. 3, p. 035001.

Hill, K, Schwarz, J, Flicker, L & Carroll, S 1999, 'Falls among healthy, community-dwelling, older women: a prospective study of frequency, circumstances, consequences and prediction accuracy', *Australian and New Zealand journal of public health*, vol. 23, no. 1, pp. 41-8.

Hill, M, Naemi, R, Branthwaite, H and Chockalingam, N 2017, 'The relationship between arch height and foot length: Implications for size grading', *Applied ergonomics*, vol. 59, no. 2, pp.243-250.

Hisham, S, Mamat, CR & Ibrahim, MA 2012, 'Multivariate statistical analysis for race variation from foot anthropometry in the Malaysian population', *Australian Journal of Forensic Sciences*, vol. 44, no. 3, pp. 285-93.

Holowka, N, Wallace, I and Lieberman, D 2018, 'Foot strength and stiffness are related to footwear use in a comparison of minimally-vs. conventionally-shod populations', *Scientific reports*, vol. 8, *no.* 1, pp.1-12.

Hong, Y, Wang, L, Xu, DQ & Li, JX 2011, 'Gender differences in foot shape: a study of Chinese young adults', *Sports biomechanics*, vol. 10, no. 2, pp. 85-97.

Hui, B, Wen, G, Zhao, Z & Li, D 2012, 'Line-scan camera calibration in close-range photogrammetry', *Optical Engineering*, vol. 51, no. 5, p. 053602.

Ito, K, Hosoda, K, Shimizu, M, Ikemoto, S, Kume, S, Nagura, T, Imanishi, N, Aiso, S, Jinzaki, M & Ogihara, N 2015, 'Direct assessment of 3D foot bone kinematics using biplanar X-ray fluoroscopy and an automatic model registration method', *Journal of foot and ankle research*, vol. 8, no. 1, pp. 1-10.

iWitnessPRO User Manual, 2018.www.photometrix.com.au.

Jafarnezhadgero, A.A., Shad, M.M. and Majlesi, M 2017, 'Effect of foot orthoses on the medial longitudinal arch in children with flexible flatfoot deformity: A three-dimensional moment analysis', *Gait & posture*, vol. 55, no. 5, pp. 75-80.

Janisse, DJ 1992, 'The art and science of fitting shoes', *Foot & ankle*, vol. 13, no. 5, pp. 257-262.

Jensen, RR, Paulsen, RR & Larsen, R 2009, 'Analysis of gait using a treadmill and a time-of-flight camera', *Workshop on Dynamic 3D Imaging*, Springer, pp. 154-66.

Jiang, R & Jauregui, DV 2010, 'Development of a digital close-range photogrammetric bridge deflection measurement system', *Measurement*, vol. 43, no. 10, pp. 1431-8.

Johansen, M, Haslund-Thomsen, H, Kristensen, J & Skou, ST 2020, 'Photo-Based Range-of-Motion Measurement: Reliability and Concurrent Validity in Children With Cerebral Palsy', *Pediatric Physical Therapy*, vol. 32, no. 2, pp. 151-60.

Johnson, JT, Hughes, S & van Dam, J 2009, 'A stereo-videogrammetry system for monitoring wind turbine blade surfaces during structural testing', *ASME Early Career Technical Journal*, vol. 8, no. 1, pp. 1-10.

Jung, S, Lee, S, Boo, J & Park, J 2001, 'A classification of foot types for designing footwear of the Korean elderly', *Proceedings of the 5th Symposium on Footwear Biomechanics, Zurich, Switzerland*, pp. 48-49.

Kanai, Y, Mutsuzaki, H and Komuro, T 2019, 'Intra-rater reliability of arch height ratio measurement using the navicular tuberosity on the surface of the body in children with Down syndrome', *Journal of physical therapy science*, vol. 31, no. 5, pp.449-452.

Kaneda, K, Harato, K, Oki, S, Ota, T, Yamada, Y, Yamada, M, Matsumoto, M, Nakamura, M, Nagura, T and Jinzaki, M 2019, 'Three-dimensional kinematic change of hindfoot during full weightbearing in standing: an analysis using upright computed tomography and 3D-3D surface registration', Journal of orthopaedic surgery and research, vol 14, no. 1, pp.1-8.

Kato, E, Oda, T, Chino, K, Kurihara, T, Nagayoshi, T, Fukunaga, T & Kawakami, Y 2005, 'Musculotendinous factors influencing difference in ankle joint flexibility between women and men', *International Journal of Sport and Health Science*, vol. 3, no. Special_Issue_2005, pp. 218-25.

Kau, CH, Olim, S & Nguyen, JT 2011, 'The future of orthodontic diagnostic records', *Seminars in orthodontics*, Elsevier, vol. 17, no. 1, pp. 39-45.

Kaufman, KR, Brodine, SK, Shaffer, RA, Johnson, CW & Cullison, TR 1999, 'The effect of foot structure and range of motion on musculoskeletal overuse injuries', *The American Journal of Sports Medicine*, vol. 27, no. 5, pp. 585-93.

Kaya, M, Leonard, T & Herzog, W 2003, 'Coordination of medial gastrocnemius and soleus forces during cat locomotion', *Journal of Experimental Biology*, vol. 206, no. 20, pp. 3645-55.

Ker, R, Bennett, M, Bibby, S, Kester, R & Alexander, RM 1987, 'The spring in the arch of the human foot', *Nature*, vol. 325, no. 6100, pp. 147-9.

Kerkhoffs, G, van Rijn, R, Struijs, P, Nusman, C & Maas, M 2020, 'The Adult Ankle and Foot', *Measurements in Musculoskeletal Radiology*, Springer, Berlin, Heidelberg, pp. 631-80.

Kerrigan, DC, Todd, MK & Croce, UD 1998, 'Gender differences in joint biomechanics during walking normative study in young adults', *American Journal of Physical Medicine & Rehabilitation*, vol. 77, no. 1, pp. 1-7.

Kidder, SM, Abuzzahab, FS, Harris, GF & Johnson, JE 1996, 'A system for the analysis of foot and ankle kinematics during gait', *IEEE transactions on rehabilitation engineering*, vol. 4, no. 1, pp. 25-32.

Kim, D-J, Pradhan, G & Prabhakaran, B 2009, 'Analyzing coordination of upper and lower extremities in human gait', *Proceedings of the Fourth International Conference on Body Area Networks*, pp. 1-7.

Kim, H, Cho, S and Lee, H 2019, 'Effects of passive Bi-axial ankle stretching while walking on uneven terrains in older adults with chronic stroke', *Journal of biomechanics*, vol. 89, no. 8, pp.57-64.

Kim, K-M, Ingersoll, CD & Hertel, J 2015, 'Facilitation of Hoffmann reflexes of ankle muscles in prone but not standing positions by focal ankle-joint cooling', *Journal of sport rehabilitation*, vol. 24, no. 2, pp. 130-9.

Kim, Y, Lim, J-M & Yoon, B 2013, 'Changes in ankle range of motion and muscle strength in habitual wearers of high-heeled shoes', *Foot & ankle international*, vol. 34, no. 3, pp. 414-9.

Kimura, M, Mochimaru, M & Kanade, T 2008, 'Measurement of 3D foot shape deformation in motion', *Proceedings of the 5th ACM/IEEE International Workshop on Projector camera systems*, pp. 1-8.

Kimura, M, Mochimaru, M & Kanade, T 2011, '3D measurement of feature cross-sections of foot while walking', *Machine Vision and Applications*, vol. 22, no. 2, pp. 377-88.

Kimura, M, Mochimaru, M, Kouchi, M & Kanade, T 2005, '3D cross-sectional shape measurement of the foot while walking', *Proceedings of the 7th Symposium on Footwear Biomechanics, International Society of Biomechanics*, pp. 34-5.

Ko, S-u, Tolea, MI, Hausdorff, JM & Ferrucci, L 2011, 'Sex-specific differences in gait patterns of healthy older adults: results from the Baltimore Longitudinal Study of Aging', *Journal of biomechanics*, vol. 44, no. 10, pp. 1974-9.

Koehler-McNicholas, S, Nickel, E, Medvec, J, Barrons, K, Mion, S and Hansen, A 2017, 'The influence of a hydraulic prosthetic ankle on residual limb loading during sloped walking', *PloS one*, vol. 12, no. 3, pp.1-18.

Kong, PW, Lim, CY, Ding, R & Sterzing, T 2015, 'Subjective evaluation of running footwear depends on country and assessment method: A bi-national study', *Ergonomics*, vol. 58, no. 9, pp. 1589-604.

Konor, MM, Morton, S, Eckerson, JM & Grindstaff, TL 2012, 'Reliability of three measures of ankle dorsiflexion range of motion', *International journal of sports physical therapy*, vol. 7, no. 3, p. 279.

Kortaberria, G, Olarra, A, Tellaeche, A & Minguez, R 2017, 'Close range photogrammetry for direct multiple feature positioning measurement without targets', *Journal of sensors*, vol. 2017, Article ID 1605943, pp. 1-10.

Kouchi, M 1998, 'Foot dimensions and foot shape: differences due to growth, generation and ethnic origin', *Anthropological Science*, vol. 106, no. Supplement, pp. 161-188.

Kouchi, M 2003, 'Inter-generation differences in foot morphology: aging or secular change?', *Journal of human ergology*, vol. 32, no. 1, pp. 23-48.

Krause, DA, Cloud, BA, Forster, LA, Schrank, JA & Hollman, JH 2011, 'Measurement of ankle dorsiflexion: a comparison of active and passive techniques in multiple positions', *Journal of sport rehabilitation*, vol. 20, no. 3, pp. 333-44.

Krauss, I, Grau, S, Mauch, M, Maiwald, C & Horstmann, T 2008a, 'Sex-related differences in foot shape', *Ergonomics*, vol. 51, no. 11, pp. 1693-709.

Krauss, I, Stacoff, A, Axmann, D, Ziegler, C, Grau, S & Horstmann, T 2008b, 'Comparison of gait data using two different protocols for ankle joint kinematics', *Journal of foot and ankle research*, vol. 1, no. 1, pp. 1-2.

Krauss, I, Valiant, G, Horstmann, T & Grau, S 2010, 'Comparison of female foot morphology and last design in athletic footwear—are men's lasts appropriate for women?', *Research in Sports Medicine*, vol. 18, no. 2, pp. 140-156.

Krishan, K, Kanchan, T, Passi, N and DiMaggio, J.A 2012, 'Heel–ball (HB) index: sexual dimorphism of a new index from foot dimensions', *Journal of forensic sciences*, vol. 57, no. 1, pp.172-175.

Ladeira, P, Bastos, E, Vanini, J and Alonso, N 2001, 'Use of stereophotogrammetry for evaluating craniofacial deformities: a systematic review', *Revista Brasileira de Cirurgia Plástica*, vol. *28*, no. 1, pp.147-155.

Lay, AN, Hass, CJ & Gregor, RJ 2006, 'The effects of sloped surfaces on locomotion: a kinematic and kinetic analysis', *Journal of biomechanics*, vol. 39, no. 9, pp. 1621-8.

Leardini, A, O'Connor, J, Catani, F & Giannini, S 1999, 'Kinematics of the human ankle complex in passive flexion; a single degree of freedom system', *Journal of biomechanics*, vol. 32, no. 2, pp. 111-8.

Leardini, A, Benedetti, MG, Berti, L, Bettinelli, D, Nativo, R & Giannini, S 2007, 'Rear-foot, mid-foot and fore-foot motion during the stance phase of gait', *Gait & posture*, vol. 25, no. 3, pp. 453-62.

Ledoux, WR, Rohr, ES, Ching, RP & Sangeorzan, BJ 2006, 'Effect of foot shape on the three-dimensional position of foot bones', *Journal of orthopaedic research*, vol. 24, no. 12, pp. 2176-86.

Lee, H & Rhee, H 2013, '3-D measurement of structural vibration using digital close-range photogrammetry', *Sensors and Actuators A: Physical*, vol. 196, no. 1, pp.63-69.

Lee, SY & Hertel, J 2008, 'Static Foot Alignment and Passive Range of Motion Influence Maximum Rearfoot Eversion During Running: 768May 29 1: 45 PM-2: 00 PM', *Medicine & Science in Sports & Exercise*, vol. 40, no. 5, p. S59.

Lee, Y-C & Wang, M-J 2015, 'Taiwanese adult foot shape classification using 3D scanning data', *Ergonomics*, vol. 58, no. 3, pp. 513-23.

Lee, Y-C, Chao, W-Y & Wang, M-J 2012, 'Foot shape classification using 3D scanning data', *2012 Southeast Asian Network of Ergonomics Societies Conference (SEANES)*, IEEE, pp. 1-6.

Lee, Y-C, Lin, G & Wang, M-JJ 2014, 'Comparing 3D foot scanning with conventional measurement methods', *Journal of foot and ankle research*, vol. 7, no. 1, p. 44.

Lee, Y-C, Kouchi, M, Mochimaru, M & Wang, M-J 2015, 'Comparing 3D foot shape models between Taiwanese and Japanese females', *Journal of human ergology*, vol. 44, no. 1, pp. 11-20.

Leifer, J, Weems, B, Kienle, SC & Sims, AM 2011, 'Three-dimensional acceleration measurement using videogrammetry tracking data', *Experimental Mechanics*, vol. 51, no. 2, pp. 199-217.

Levanon, Y. 2013,'The advantages and disadvantages of using high technology in hand rehabilitation', *Journal of Hand Therapy*, vol. *26, no.* 2, pp.179-183.

Li, J-D, Lu, T-W, Lin, C-C, Kuo, M-Y, Hsu, H-C & Shen, W-C 2017, 'Soft tissue artefacts of skin markers on the lower limb during cycling: effects of joint angles and pedal resistance', *Journal of biomechanics*, vol. 62, no. 13, pp. 27-38.

Li, L 2014, 'Time-of-flight camera–an introduction', *Technical white paper*, no. SLOA190B.

Lidge, DP, Amasay, T & Arbel, V 2020, 'Contribution of the Ankle, Knee, and Hip to Total Lower Extremity Internal/External Rotation', *International Journal of Exercise Science: Conference Proceedings*, vol 2, no. 12, p. 129.

Lindner, M, Schiller, I, Kolb, A & Koch, R 2010, 'Time-of-flight sensor calibration for accurate range sensing', *Computer Vision and Image Understanding*, vol. 114, no. 12, pp. 1318-28.

Liu, T, Burner, A, Jones, T & Barrows, D 2012, 'Photogrammetric techniques for aerospace applications', *Progress in Aerospace Sciences*, vol. 54,no. 6, pp.1-58.

Liu, S, Cui, Y, Sanchez, S & Stricker, D 2011, 'Foot scanning and deformation estimation using time-of-flight cameras', *Footwear Science*, vol. 3, no. sup1, pp. S98-S9.

Liu, X, Kim, W & Drerup, B 2004a,'3D characterization and localization of anatomical landmarks of the foot', In *Proceedings of the 2004 ACM SIGGRAPH international conference on Virtual Reality continuum and its applications in industry* (pp. 253-256). ACM.

Liu, X, Kim, W & Drerup, B 2004b, '3D characterization and localization of anatomical landmarks of the foot by FastSCAN', *Real-time imaging*, vol. 10, no. 4, pp.217-228.

López-López, D, Expósito-Casabella, Y, Losa-Iglesias, M, Bengoa-Vallejo, RBd, Saleta-Canosa, JL & Alonso-Tajes, F 2016, 'Impact of shoe size in a sample of elderly individuals', *Revista da Associação Médica Brasileira*, vol. 62, no. 8, pp. 789-94.

Luhmann, T 2010, 'Close range photogrammetry for industrial applications'. *ISPRS Journal of Photogrammetry and Remote Sensing*, vol. *65, no.*6, pp. 558-569.

Luhmann, T, & Robson, S 2006, Close Range Photogrammetry: Principles, Techniques and Applications, Whittles Publishing, Dunbeath. Available from: ProQuest Ebook Central.

Luhmann, T, Robson, S, Kyle, S & Boehm, J 2014, *Close-range photogrammetry and 3D imaging*, Walter de Gruyter.

Lundberg, A 1989, 'Kinematics of the ankle and foot: in vivo roentgen stereophotogrammetry', *Acta Orthopaedica Scandinavica*, vol. 60, no. sup233, pp. 1-26.

Lundberg, A, Goldie, I, Kalin, B & Selvik, G 1989, 'Kinematics of the ankle/foot complex: plantarflexion and dorsiflexion', *Foot & ankle*, vol. 9, no. 4, pp. 194-200.

Luo, G, Houston, VL, Mussman, M, Garbarini, M, Beattie, AC & Thongpop, C 2009, 'Comparison of male and female foot shape', *Journal of the American Podiatric Medical Association*, vol. 99, no. 5, pp. 383-390.

Luximon, A & Luximon, Y 2011, 'Preliminary study on dynamic foot model', *International Conference on Digital Human Modeling*, Springer, pp. 321-7.

Macklin, K, Healy, A & Chockalingam, N 2012, 'The effect of calf muscle stretching exercises on ankle joint dorsiflexion and dynamic foot pressures, force and related temporal parameters', *The Foot*, vol. 22, no. 1, pp. 10-7.

Madden, MC & Karlan, MS 1979, 'Moiré photography as a means of topographical mapping of the human face', *Annals of biomedical engineering*, vol. 7, no. 2, pp. 95-102.

Majid, Z, Chong, AK, Ahmad, A, Setan, H & Samsudin, AR 2005, 'Photogrammetry and 3D laser scanning as spatial data capture techniques for a national craniofacial database', *The Photogrammetric Record*, vol. 20, no. 109, pp. 48-68.

Manna, I, Pradhan, D, Ghosh, S, Kar, SK & Dhara, P 2001, 'A comparative study of foot dimension between adult male and female and evaluation of foot hazards due to using of footwear', *Journal of physiological anthropology and applied human science*, vol. 20, no. 4, pp. 241-6.

Mauch, M, Grau, S, Krauss, I, Maiwald, C & Horstmann, T 2008, 'Foot morphology of normal, underweight and overweight children', *International journal of obesity*, vol. 32, no. 7, pp. 1068-75.

McCollough, CH & Zink, FE 1999, 'Performance evaluation of a multi-slice CT system', *Medical physics*, vol. 26, no. 11, pp. 2223-30.

McHenry, R, Arnold, G, Wang, W & Abboud, R 2015, 'Footwear in rock climbing: Current practice', *The Foot*, vol. 25, no. 3, pp. 152-8.

McPoil, TG & Cornwall, MW 1996, 'Relationship between three static angles of the rearfoot and the pattern of rearfoot motion during walking', *Journal of Orthopaedic & Sports Physical Therapy*, vol. 23, no. 6, pp. 370-5.

McPoil, TG, Vicenzino, B, Cornwall, MW, Collins, N & Warren, M 2009, 'Reliability and normative values for the foot mobility magnitude: a composite measure of vertical and medial-lateral mobility of the midfoot', *Journal of foot and ankle research*, vol. 2, no. 1, pp. 6-18.

Mecagni, C, Smith, JP, Roberts, KE & O'Sullivan, SB 2000, 'Balance and ankle range of motion in community-dwelling women aged 64 to 87 years: a correlational study', *Physical Therapy*, vol. 80, no. 10, pp. 1004-11.

Menz, HB 2004, 'Two feet, or one person? Problems associated with statistical analysis of paired data in foot and ankle medicine', *The Foot*, vol. 14, no. 1, pp. 2-5.

Menz, HB 2005, 'Analysis of paired data in physical therapy research: time to stop double-dipping?', *JOSPT, Inc.*, vol. 35, no. 8, pp. 477-478.

Menz, HB, Auhl, M, Ristevski, S, Frescos, N & Munteanu, SE 2014, 'Evaluation of the accuracy of shoe fitting in older people using three-dimensional foot scanning', *Journal of foot and ankle research*, vol. 7, no. 1, p. 3.

Merriaux, P, Dupuis, Y, Boutteau, R, Vasseur, P and Savatier, X 2017,'A study of vicon system positioning performance', *Sensors*, vol. 17, no. 7, pp. 2-18.

Mickle, KJ, Steele, JR & Munro, BJ 2008, 'Is the foot structure of preschool children moderated by gender?', *Journal of Pediatric Orthopaedics*, vol. 28, no. 5, pp. 593-6.

Mikhail, E. M,Bethel, J. S & Mcglone, J. C 2001. *Introduction to Modern Photogrammetry*, John Wiley & Sons Inc.

Miller, H, Fawcett, L & Rushton, A 2020, 'Does gender and ankle injury history affect weightbearing dorsiflexion in elite artistic gymnasts?', *Physical Therapy in sport*, vol. 42, no. 2, pp. 46-52.

Mishra, M, Bruniaux, P, Crepin, D & Hamad, B 2017, 'Studying foot anthropometric measures using 3D scanning method', *Proceedings of the* Clotech 2017, Lodz, Poland, pp. 8-36.

Mohammed, S, Same, A, Oukhellou, L, Kong, K, Huo, W & Amirat, Y 2016, 'Recognition of gait cycle phases using wearable sensors', *Robotics and Autonomous Systems*, vol. 75,no. 1, pp. 50-9.

Moneim, WMA, Hady, RHA, Maaboud, RMA, Fathy, HM & Hamed, AM 2008, 'Identification of sex depending on radiological examination of foot and patella', *The American journal of forensic medicine and pathology*, vol. 29, no. 2, pp. 136-40.

Moorthy, TN & Mond, T 2018, 'Individualizing characteristics of footprints in Malaysian Chinese for person identification in forensic perspective', *South India Medico-Legal Association*, vol. 10, no. 2, pp. 59-69.

Morasiewicz, P, Dejnek, M, Urbański, W, Dragan, SŁ, Kulej, M & Dragan, SF 2017, 'Radiological evaluation of ankle arthrodesis with Ilizarov fixation compared to internal fixation', *Injury*, vol. 48, no. 7, pp. 1678-83.

Moring, I, Ailisto, H, Koivunen, V & Myllylä, R 1989, 'Active 3-D vision system for automatic model-based shape inspection', *Optics and lasers in engineering*, vol. 10, no. 3-4, pp. 149-60.

Morrison, SC, Durward, BR, Watt, GF & Donaldson, MD 2007, 'Anthropometric Foot Structure of Peripubescent Children with Excessive versus Normal Body MassA Cross-sectional Study', *Journal of the American Podiatric Medical Association*, vol. 97, no. 5, pp. 366-70.

Moudgil, R, Kaur, R, Menezes, RG, Kanchan, T & Garg, RK 2008, 'Foot index: is it a tool for sex determination?', *Journal of forensic and legal medicine*, vol. 15, no. 4, pp. 223-226.

Mousavi, SH, Hijmans, JM, Moeini, F, Rajabi, R, Ferber, R, van der Worp, H & Zwerver, J 2020, 'Validity and reliability of a smartphone motion analysis app for lower limb kinematics during treadmill running', *Physical Therapy in sport*, vol. 43, no. 3, pp. 27-35.

Mrozkowiak, M 2010, 'Measurements using projection moire of the length and width of feet in standing females and males aged 4 to 18 years', *Annales Academiae Medicae Stetinensis*, vol. 56, no. 1, pp. 70-3.

Mueller, MJ, Sinacore, DR, Hastings, MK, Strube, MJ & Johnson, JE 2003, 'Effect of Achilles Tendon Lengthening on Neuropathic Plantar Ulcers*: A Randomized Clinical Trial', *JBJS*, vol. 85, no. 8, pp. 1436-45.

Muir, B, Rietdyk, S & Haddad, J 2014, 'Gait initiation: the first four steps in adults aged 20–25 years, 65–79 years, and 80–91 years', *Gait & posture*, vol. 39, no. 1, pp. 490-4.

Murley, GS, Menz, HB & Landorf, KB 2009, 'A protocol for classifying normal-and flat-arched foot posture for research studies using clinical and radiographic measurements', *Journal of foot and ankle research*, vol. 2, no. 1, pp. 22-35.

Musumeci, G 2016, 'Welcome to the new open access Journal of Functional Morphology and Kinesiology', *J. Funct. Morphol. Kinesiol*, vol. 1, no. 1, pp. 1-5.

Myronenko, A & Song, X 2010, 'Point set registration: Coherent point drift', *IEEE Transactions on Pattern Analysis and Machine Intelligence*, vol. 32, no. 12, pp. 2262-75.

Nicholson, K, Church, C, Takata, C, Niiler, T, Chen, BP-J, Lennon, N, Sees, JP, Henley, J & Miller, F 2018, 'Comparison of three-dimensional multi-segmental foot models used in clinical gait laboratories', *Gait & posture*, vol. 63, no. 5, pp. 236-41.

Nielsen, RG, Rathleff, MS, Simonsen, OH & Langberg, H 2009, 'Determination of normal values for navicular drop during walking: a new model correcting for foot length and gender', *Journal of foot and ankle research*, vol. 2, no. 1, p. 12.

Nigg, B, Fisher, V & Ronsky, J 1994, 'Gait characteristics as a function of age and gender', *Gait & posture*, vol. 2, no. 4, pp. 213-20.

Nigg, BM, Federolf, P & Landry, SC 2010, 'Gender differences in lower extremity gait biomechanics during walking using an unstable shoe', *Clinical Biomechanics*, vol. 25, no. 10, pp. 1047-52.

Nilsson, MK, Friis, R, Michaelsen, MS, Jakobsen, PA & Nielsen, RO 2012, 'Classification of the height and flexibility of the medial longitudinal arch of the foot', *Journal of foot and ankle research*, vol. 5, no. 1, p. 3.

Nishiyama, S, Minakata, N, Kikuchi, T & Yano, T 2015, 'Improved digital photogrammetry technique for crack monitoring', *Advanced Engineering Informatics*, vol. 29, no. 4, pp. 851-8.

Nixon, BP, Armstrong, DG, Wendell, C, Vazquez, JR, Rabinovich, Z, Kimbriel, HR, Rosales, MA & Boulton, AJ 2006, 'Do US veterans wear appropriately sized shoes? The Veterans Affairs shoe size selection study', *Journal of the American Podiatric Medical Association*, vol. 96, no. 4, pp. 290-2.

Novak, AC & Brouwer, B 2013, 'Kinematic and kinetic evaluation of the stance phase of stair ambulation in persons with stroke and healthy adults: a pilot study', *Journal of applied biomechanics*, vol. 29, no. 4, pp. 443-52.

Novak, B, Možina, J & Jezeršek, M 2014. 3D laser measurements of bare and shod feet during walking. *Gait & posture*, vol. 40, no. 1, pp. 87-93.

Novelline, RA & Squire, LF 2004, *Squire's fundamentals of radiology*, La Editorial, UPR.

O'Connor, K, Bragdon, G & Baumhauer, JF 2006, 'Sexual dimorphism of the foot and ankle', *Orthopedic Clinics*, vol. 37, no. 4, pp. 569-74.

Oggier, T, Büttgen, B, Lustenberger, F, Becker, G, Rüegg, B & Hodac, A 2005, 'SwissRanger SR3000 and first experiences based on miniaturized 3D-TOF cameras', *Proc. of the First Range Imaging Research Day at ETH Zurich*.

Ogon, M, Aleksiev, AR, Pope, MH, Wimmer, C & Saltzman, CL 1999, 'Does arch height affect impact loading at the lower back level in running?', *Foot & ankle international*, vol. 20, no. 4, pp. 263-6.

Okita, N, Meyers, SA, Challis, JH & Sharkey, NA 2009, 'An objective evaluation of a segmented foot model', *Gait & posture*, vol. 30, no. 1, pp. 27-34.

Onodera, AN, Sacco, ICN, Morioka, EH, Souza, PS, de Sá, MR & Amadio, AC 2008, 'What is the best method for child longitudinal plantar arch assessment and when does arch maturation occur?', *The Foot*, vol. 18, no. 3, pp. 142-149.

Otsuka, R, Yatsuya, H, Miura, Y, Murata, C, Tamakoshi, K, Oshiro, K, Nishio, N, Ishikawa, M, Zhang, HM & Shiozawa, M 2003, 'Association of flatfoot with pain, fatigue and obesity in Japanese over sixties', *[Nihon koshu eisei zasshi] Japanese journal of public health*, vol. 50, no. 10, pp. 988-98.

Papuga, MO & Burke, JR 2011, 'The reliability of the associate platinum digital foot scanner in measuring previously peveloped footprint characteristics: a technical note', *Journal of manipulative and physiological therapeutics*, vol. 34, no. 2, pp. 114-118.

Panero, E, Gastaldi, L & Rapp, W 2017, 'Two-segments foot model for biomechanical motion analysis', *International Conference on Robotics in Alpe-Adria Danube Region*, Springer, pp. 988-95.

Pfister, A, West, A.M, Bronner, S and Noah, J.A 2014, 'Comparative abilities of Microsoft Kinect and Vicon 3D motion capture for gait analysis', *Journal of medical engineering & technology*, vol. 38, no. 5, pp.274-280.

Phinyomark, A, Osis, ST, Hettinga, BA, Kobsar, D & Ferber, R 2016, 'Gender differences in gait kinematics for patients with knee osteoarthritis', *BMC musculoskeletal disorders*, vol. 17, no. 1, pp. 1-12.

Picón-Reátegui, E, Buskirk, E, Doi, K, Kuroshima, A & Hiroshige, T 1979, 'Anthropometric characteristics and body composition of Ainu and other Japanese: comparison with other racial groups', *American Journal of Physical Anthropology*, vol. 50, no. 3, pp. 393-400.

Pirker, W & Katzenschlager, R 2017, 'Gait disorders in adults and the elderly', *Wiener Klinische Wochenschrift*, vol. 129, no. 3-4, pp. 81-95.

Pohl, MB & Farr, L 2010, 'A comparison of foot arch measurement reliability using both digital photography and calliper methods', *Journal of foot and ankle research*, vol. 3, no. 1, p. 14.

Price, C & Nester, C 2016, 'Foot dimensions and morphology in healthy weight, overweight and obese males', *Clinical Biomechanics*, vol. 37, no. 7, pp. 125-130.

Rabbito, M, Pohl, MB, Humble, N & Ferber, R 2011, 'Biomechanical and clinical factors related to stage I posterior tibial tendon dysfunction', *Journal of Orthopaedic & Sports Physical Therapy*, vol. 41, no. 10, pp. 776-84.

Raghavendra, R, Raja, KB, Pflug, A, Yang, B & Busch, C 2013, '3d face reconstruction and multimodal person identification from video captured using smartphone camera', *2013 IEEE International Conference on Technologies for Homeland Security (HST)*, IEEE, pp. 552-7.

Rao, S, Saltzman, C & Yack, HJ 2006, 'Ankle ROM and stiffness measured at rest and during gait in individuals with and without diabetic sensory neuropathy', *Gait & posture*, vol. 24, no. 3, pp. 295-301.

Razavi, R, Hill, DL, Keevil, SF, Miquel, ME, Muthurangu, V, Hegde, S, Rhode, K, Barnett, M, van Vaals, J & Hawkes, DJ 2003, 'Cardiac catheterisation guided by MRI in children and adults with congenital heart disease', *The Lancet*, vol. 362, no. 9399, pp. 1877-82.

Razeghi, M & Batt, M 2002, 'Foot type classification: A critical review of current methods', *Gait and Posture, vol.* 15, no. 3, pp. 282-291.

Remondino, F & Fraser, C 2006, 'Digital camera calibration methods: considerations and comparisons', *International Archives of Photogrammetry, Remote Sensing and Spatial Information Sciences*, vol. 36, no. 5, pp. 266-72.

Ribbans, W & Rees, J 1999, 'Management of equinus contractures of the ankle in haemophilia', *Haemophilia*, vol. 5, pp. 46-52.

Ridola, C & Palma, A 2001, 'Functional anatomy and imaging of the foot', *Italian journal of anatomy and embryology= Archivio italiano di anatomia ed embriologia*, vol. 106, no. 2, pp. 85-98.

Riegger, CL 1988, 'Anatomy of the ankle and foot', *Physical Therapy*, vol. 68, no. 12, pp. 1802-14.

Riley, PO, Paolini, G, Della Croce, U, Paylo, KW & Kerrigan, DC 2007, 'A kinematic and kinetic comparison of overground and treadmill walking in healthy subjects', *Gait & posture*, vol. 26, no. 1, pp. 17-24.

Roaas, A & Andersson, GB 1982, 'Normal range of motion of the hip, knee and ankle joints in male subjects, 30–40 years of age', *Acta Orthopaedica Scandinavica*, vol. 53, no. 2, pp. 205-8.

Robinovitch, SN, Feldman, F, Yang, Y, Schonnop, R, Leung, PM, Sarraf, T, Sims-Gould, J & Loughin, M 2013, 'Video capture of the circumstances of falls in elderly people residing in long-term care: an observational study', *The Lancet*, vol. 381, no. 9860, pp. 47-54.

Robinson, J, Frederick, E & Cooper, L 1984, 'Running participation and foot dimensions', *Medicine & Science in Sports & Exercise*, vol. 16, no. 2, pp. 200-209.

Rogati, G, Leardini, A, Ortolani, M & Caravaggi, P 2019, 'Validation of a novel Kinect-based device for 3D scanning of the foot plantar surface in weight-bearing', *Journal of foot and ankle research*, vol. 12, no. 1, pp. 46-54.

Røislien, J, Skare, Ø, Gustavsen, M, Broch, NL, Rennie, L & Opheim, A 2009, 'Simultaneous estimation of effects of gender, age and walking speed on kinematic gait data', *Gait & posture*, vol. 30, no. 4, pp. 441-5.

Rome, K & Cowieson, F 1996, 'A reliability study of the universal goniometer, fluid goniometer, and electrogoniometer for the measurement of ankle dorsiflexion', *Foot & ankle international*, vol. 17, no. 1, pp. 28-32.

Romkes, J, Freslier, M, Rutz, E and Bracht-Schweizer, K 2020, 'Walking on uneven ground: How do patients with unilateral cerebral palsy adapt?', *Clinical biomechanics*, vol. 74, no. 4, pp.8-13.

Root, ML 1977, 'Normal and abnormal function of the foot', *Clinical Biomechanics*, vol. 2.

Ross, J 2018, 'Scanning Technology and Orthotic Casting: What You Should Know', *Podiatry today*, vol. 31, np. 6, pp. 42-47.

Rossi, WA 1983, 'The high incidence of mismated feet in the population', *Foot & ankle*, vol. 4, no. 2, pp. 105-12.

Saadatseresht, M, Samadzadegan, F & Azizi, A 2005, 'Automatic camera placement in vision metrology based on a fuzzy inference system', *Photogrammetric Engineering & Remote Sensing*, vol. 71, no. 12, pp. 1375-85.

Sacco, IC, Onodera, AN, Bosch, K & Rosenbaum, D 2015, 'Comparisons of foot anthropometry and plantar arch indices between German and Brazilian children', *BMC pediatrics*, vol. 15, no. 1, p. 4.

Sachithanandam, V and Joseph, B 1995, 'The influence of footwear on the prevalence of flat foot. A survey of 1846 skeletally mature persons', *The Journal of bone and joint surgery. British volume*, vol. 77, no. 2, pp. 254-257.

Samson, W, Van Hamme, A, Sanchez, S, Chèze, L, Van Sint Jan, S & Feipel, V 2012, 'Dynamic footprint analysis by time-of-flight camera', *Computer methods in biomechanics and biomedical engineering*, vol. 15, no. sup1, pp. 180-2.

Samson, W, Van Hamme, A, Sanchez, S, Chèze, L, Jan, SVS & Feipel, V 2014, 'Foot roll-over evaluation based on 3D dynamic foot scan', *Gait & posture*, vol. 39, no. 1, pp. 577-82.

Sansoni, G, Trebeschi, M & Docchio, F 2009, 'State-of-the-art and applications of 3D imaging sensors in industry, cultural heritage, medicine, and criminal investigation', *Sensors*, vol. 9, no. 1, pp. 568-601.

Schaiwanichsiri, D, Tantisiriwat, N and Janchai, S 2008, 'Proper shoe sizes for Thai elderly', *The Foot*, vol. 18, no. 4, pp. 186-191.

Schenk, T 2005, *Introduction to photogrammetry*, The Ohio State University, Columbus.

Scher, C.D.L, Belmont Jr, L.C.P.J, Bear, M.R, Mountcastle, S.B, Orr, J.D and Owens, M.B.D 2009, 'The incidence of plantar fasciitis in the United States military', *JBJS*, vol. 91, no. 12, pp.2867-2872.

Schmeltzpfenning, T, Plank, C, Fritz, B, Aswendt, P & Grau, S 2011, '3D dynamic behaviour of foot structure may provide additional information for last design', *Footwear Science*, vol. 3, no. sup1, pp. S147-S8.

Schwarz, NA, Kovaleski, JE, Heitman, RJ, Gurchiek, LR & Gubler-Hanna, C 2011, 'Arthrometric measurement of ankle-complex motion: normative values', *Journal of athletic training*, vol. 46, no. 2, pp. 126-32.

Schwarzkopf, R, Perretta, DJ, Russell, TA & Sheskier, SC 2011, 'Foot and shoe size mismatch in three different New York City populations', *The Journal of Foot and Ankle Surgery*, vol. 50, no. 4, pp. 391-4.

Scott, G, Menz, HB & Newcombe, L 2007, 'Age-related differences in foot structure and function', *Gait & posture*, vol. 26, no. 1, pp. 68-75.
Sen, J, Kanchan, T & Ghosh, S 2011, 'Sex estimation from foot dimensions in an indigenous Indian Population', *Journal of forensic sciences*, vol. 56, no. s1, pp. S148-S153.

Shariff, SM, Merican, AF & Shariff, AA 2019, 'Development of new shoe-sizing system for Malaysian women using 3D foot scanning technology', *Measurement*, vol. 140, no. 10, pp. 182-4.

Shariff, SM, Merican, AF & Shariff, AA 2020, 'Foot morphological between ethnic groups', in *Anthropometry, Apparel Sizing and Design*, Elsevier, pp. 317-30.

Sherman, S, 2010, *Emergency orthopaedics*, McGraw-Hill, Chapter 23.

Shiang, T-Y, Lee, S-H, Lee, S-J & Chu, WC 1998, 'Evaluating different footprints parameters as a predictor of arch height', *IEEE engineering in medicine and biology magazine*, vol. 17, no. 6, pp. 62-6.

Shu, Y, Mei, Q, Fernandez, J, Li, Z, Feng, N & Gu, Y 2015, 'Foot morphological difference between habitually shod and unshod runners', *PLoS One*, vol. 10, no. 7, p. e0131385.

Shultz, A.H and Goldfarb, M 2018, 'A unified controller for walking on even and uneven terrain with a powered ankle prosthesis', *IEEE Transactions on Neural Systems and Rehabilitation Engineering*, vol. *26, no.* 4, pp.788-797.

Shultz, R, Kedgley, E & Jenkyn, T, 2011, 'Quantifying skin motion artifact error of the hindfoot and forefoot marker clusters with the optical tracking of a multi-segment foot model using single-plane fluoroscopy', *Gait & posture*, vol. 34, no.1, pp.44-48.

Silverman, AK, Wilken, JM, Sinitski, EH & Neptune, RR 2012, 'Whole-body angular momentum in incline and decline walking', *Journal of biomechanics*, vol. 45, no. 6, pp. 965-71.

Simoneau, E, Martin, A & Van Hoecke, J 2007, 'Effects of joint angle and age on ankle dorsi- and plantar-flexor strength', *Journal of Electromyography and Kinesiology*, vol. 17, no. 3, pp. 307-16.

Sinclair, J, Greenhalgh, A, Edmundson, CJ, Brooks, D & Hobbs, SJ 2012, 'Gender differences in the kinetics and kinematics of distance running: implications for footwear design', *International Journal of Sports Science and Engineering*, vol. 6, no. 2, pp. 118-28.

Sinclair, JK, Chockalingam, N & Vincent, H 2014, 'Gender differences in multi-segment foot kinematics and plantar fascia strain during running', *Foot and Ankle Online Journal*, vol. 7, no. 4, pp. 1-8.

Spink, MJ, Fotoohabadi, MR & Menz, HB 2010, 'Foot and ankle strength assessment using hand-held dynamometry: reliability and age-related differences', *Gerontology*, vol. 56, no. 6, pp. 525-32.

Spyrou, L & Aravas, N 2012, 'Muscle-driven finite element simulation of human foot movements', *Computer methods in biomechanics and biomedical engineering*, vol. 15, no. 9, pp. 925-34.

Stagni, R, Leardini, A, Ensini, A & Cappello, A 2005, 'Ankle morphometry evaluated using a new semi-automated technique based on X-ray pictures', *Clinical Biomechanics*, vol. 20, no. 3, pp. 307-11.

Staheli, LT, Chew, DE & Corbett, M 1987, 'The longitudinal arch. A survey of eight hundred and eighty-two feet in normal children and adults', *The Journal of bone and joint surgery. American volume*, vol. 69, no. 3, pp. 426-8.

Štajer, T, Burger, H & Vidmar, G 2011, 'Influence of casting method on effectiveness of foot orthoses using plantar pressure distribution: a preliminary study', *Prosthetics and orthotics international*, vol. 35, no. 4, pp. 411-7.

Stanković, K, Booth, BG, Danckaers, F, Burg, F, Vermaelen, P, Duerinck, S, Sijbers, J & Huysmans, T 2018, 'Three-dimensional quantitative analysis of healthy foot shape: a proof of concept study', *Journal of foot and ankle research*, vol. 11, no. 1, pp. 8-21.

Stewart, SF 1970, 'Human Gait and the Human Foot: An Ethnological Study of Flatfoot: Part I', *Clinical Orthopaedics and Related Research (1976-2007)*, vol. 70, pp. 111-23.

Stolwijk, N, Koenraadt, K, Louwerens, J, Grim, D, Duysens, J & Keijsers, N 2014, 'Foot lengthening and shortening during gait: a parameter to investigate foot function?', *Gait & posture*, vol. 39, no. 2, pp. 773-7.

Studenski, S, Duncan, PW & Chandler, J 1991, 'Postural responses and effector factors in persons with unexplained falls: results and methodologic issues', *Journal of the American Geriatrics Society*, vol. 39, no. 3, pp. 229-34.

Sturmer, M, Penne, J & Hornegger, J 2008, 'Standardization of intensity-values acquired by time-of-flight-cameras', *2008 IEEE Computer Society Conference on Computer Vision and Pattern Recognition Workshops*, IEEE, pp. 1-6.

Sung, E-S & Kim, J-H 2018, 'Relationship between ankle range of motion and Biodex Balance System in females and males', *Journal of exercise rehabilitation*, vol. 14, no. 1, p. 133.

Surer, E & Kose, A 2011, 'Methods and technologies for gait analysis', in *Computer Analysis of Human Behavior*, Springer, pp. 105-23.

Takabayashi, T, Edama, M, Nakamura, E, Yokoyama, E, Kanaya, C & Kubo, M 2017, 'Coordination among the rearfoot, midfoot, and forefoot during walking', *Journal of foot and ankle research*, vol. 10, no. 1, pp. 1-9.

Takasaki, H 1970, 'Moiré topography', *Applied Optics*, vol. 9, no. 6, pp. 1467-72.

Takasaki, H 1982, 'Moiré topography from its birth to practical application', *Optics and lasers in engineering*, vol. 3, no. 1, pp. 3-14.

Telfer, S & Woodburn, J 2010, 'The use of 3D surface scanning for the measurement and assessment of the human foot', *Journal of foot and ankle research*, vol. 3, no. 1, pp. 1-9.

Telfer, S, Kindig, MW, Sangeorzan, BJ & Ledoux, WR 2017, 'Metatarsal shape and foot type: a geometric morphometric analysis', *Journal of biomechanical engineering*, vol. 139, no. 3, pp. 1-8.

Thabet, AK, Trucco, E, Salvi, J, Wang, W & Abboud, RJ 2014, 'Dynamic 3D shape of the plantar surface of the foot using coded structured light: a technical report', *Journal of foot and ankle research*, vol. 7, no. 1, p. 5.

Thoms, V & Rome, K 1997, 'Effect of subject position on the reliability of measurement of active ankle joint dorsiflexion', *The Foot*, vol. 7, no. 3, pp. 153-8.

Tobias, KE, George, MD, Vitalis, E & Baxter-Grillo, D 2014, 'Sexual Dimorphism of Correlations of feet anthropometric parameters and Height (stature) among Undergraduate students of a University, Western Nigeria', *IOSR Journal of Dental and Medical Sciences*, vol. 13, no. 4, pp. 46-53.

Tochigi, Y 2003, 'Effect of Arch Supports on Ankle—Subtalar Complex Instability: A Biomechanical Experimental Study', *Foot & ankle international*, vol. 24, no. 8, pp. 634-9.

Tománková, K, Přidalová, M & Gába, A 2015, 'The impact of obesity on foot morphology in women aged 48 years or older', *Acta Gymnica*, vol. 45, no. 2, pp. 69-75.

Tomassoni, D, Traini, E & Amenta, F 2014, 'Gender and age related differences in foot morphology', *Maturitas*, vol. 79, no. 4, pp. 421-7.

Tome, J, Nawoczenski, DA, Flemister, A & Houck, J 2006, 'Comparison of foot kinematics between subjects with posterior tibialis tendon dysfunction and healthy controls', *Journal of Orthopaedic & Sports Physical Therapy*, vol. 36, no. 9, pp. 635-44.

Treleaven, P & Wells, J 2007, '3D body scanning and healthcare applications', *Computer*, vol. 40, no. 7, pp. 28-34.

Triggs, B, McLauchlan, PF, Hartley, RI & Fitzgibbon, AW 1999, 'Bundle adjustment—a modern synthesis', *International workshop on vision algorithms*, Springer, pp. 298-372.

Tulchin, K, Orendurff, M & Karol, L 2010a, 'A comparison of multi-segment foot kinematics during level overground and treadmill walking', *Gait & posture*, vol. 31, no. 1, pp. 104-8.

Tulchin, K, Orendurff, M & Karol, L 2010b, 'The effects of surface slope on multi-segment foot kinematics in healthy adults', *Gait & posture*, vol. 32, no. 4, pp. 446-50.

Udin, WS & Ahmad, A 2011, 'Calibration of high resolution digital camera using self-calibration bundle adjustment method', *2011 IEEE 7th International Colloquium on Signal Processing and its Applications*, IEEE, pp. 137-41.

Urbanova, P, Hejna, P & Jurda, M 2015, 'Testing photogrammetry-based techniques for three-dimensional surface documentation in forensic pathology', *Forensic science international*, vol. 250, no. 1, pp. 77-86.

Valderrabano, V, Hintermann, B, Nigg, B, Stefanyshyn, D and Stergiou, P 2003,'Kinematic changes after fusion and total replacement of the ankle part 1: range of motion', *Foot & ankle international*, vol. 24, no. 12, pp. 881-887.

Valença, J, Júlio, E & Araújo, H 2012, 'Applications of photogrammetry to structural assessment', *Experimental Techniques*, vol. 36, no. 5, pp. 71-81.

Van Loon, B, Maal, T, Plooij, J, Ingels, K, Borstlap, W, Kuijpers-Jagtman, A, Spauwen, P & Berge, S 2010, '3D stereophotogrammetric assessment of pre-and postoperative volumetric changes in the cleft lip and palate nose', *International journal of oral and maxillofacial surgery*, vol. 39, no. 6, pp. 534-540.

Vass, G & Perlaki, T 2003, 'Applying and removing lens distortion in post production', *Proceedings of the 2nd Hungarian Conference on Computer Graphics and Geometry*, pp. 9-16.

Vecchio, S, Araújo, P, Rubio, J, Pinotti, M & Sesselmann, M 2012, '3D measurement of human plantar foot by projection moiré technique', *International Journal of Mechatronics and Manufacturing Systems*, vol. 5, no. 1, pp. 3-16.

Villarroya, MA, Esquivel, JM, Tomás, C, Moreno, LA, Buenafé, A & Bueno, G 2009, 'Assessment of the medial longitudinal arch in children and adolescents with obesity: footprints and radiographic study', *European journal of pediatrics*, vol. 168, no. 5, pp. 559-67.

Volpon, JB 1994, 'Footprint analysis during the growth period', *Journal of pediatric orthopedics*, vol. 14, no. 1, pp. 83-5.

Voracek, M, Fisher, ML, Rupp, B, Lucas, D & Fessler, DM 2007, 'Sex differences in relative foot length and perceived attractiveness of female feet: relationships among anthropometry, physique, and preference ratings', *Perceptual and Motor Skills*, vol. 104, no. 3_suppl, pp. 1123-38.

Wang, J, Shi, F, Zhang, J & Liu, Y 2008, 'A new calibration model of camera lens distortion', *Pattern recognition*, vol. 41, no. 2, pp. 607-15.

Wang, L, Pedersen, PC, Strong, DM, Tulu, B, Agu, E & Ignotz, R 2014, 'Smartphone-based wound assessment system for patients with diabetes', *IEEE Transactions on Biomedical Engineering*, vol. 62, no. 2, pp. 477-88.

Ward, CV, Kimbel, WH & Johanson, DC 2011, 'Complete fourth metatarsal and arches in the foot of Australopithecus afarensis', *Science*, vol. 331, no. 6018, pp. 750-3.

Wei, J, Chen, H, Chen, P, Lu, Z, Wei, C, Hou, A, Sun, T, Liu, Q, Li, W & Lu, Z 2016, 'Development of parallel mechanism with six degrees of freedom for ankle rehabilitation', *2016 International Conference on Advanced Robotics and Mechatronics (ICARM)*, IEEE, pp. 353-8.

Wester-Ebbinghaus, W 1988, 'Analytics in non-topographic Photogrammetry', *ISPRS Cong., Com. v., Kyoto*, pp.380-390.

Whitehead, K & Hugenholtz, CH 2014, 'Remote sensing of the environment with small unmanned aircraft systems (UASs), part 1: A review of progress and challenges', *Journal of Unmanned Vehicle Systems*, vol. 2, no. 3, pp. 69-85.

Williams, DS & McClay, IS 2000, 'Measurements used to characterize the foot and the medial longitudinal arch: reliability and validity', *Physical Therapy*, vol. 80, no. 9, pp. 864-71.

Witana, CP, Xiong, S, Zhao, J & Goonetilleke, RS 2006, 'Foot measurements from three-dimensional scans: A comparison and evaluation of different methods', *International Journal of Industrial Ergonomics*, vol. 36, no. 9, pp. 789-807.

Wolf, P and Dewitt, B 2000. *Elements of photogrammetry: with applications in GIS* (Vol. 3). New York: McGraw-Hill.

Wong, JY, Oh, AK, Ohta, E, Hunt, AT, Rogers, GF, Mulliken, JB & Deutsch, CK 2008, 'Validity and reliability of craniofacial anthropometric measurement of 3D digital photogrammetric images', *The Cleft Palate-Craniofacial Journal*, vol. 45, no. 3, pp. 232-9.

Wong, Y, Kim, W & Ying, N 2005, 'Passive motion characteristics of the talocrural and the subtalar joint by dual Euler angles', *Journal of biomechanics*, vol. 38, no. 12, pp. 2480-5.

Woźniacka, R, Bac, A, Matusik, S, Szczygieł, E & Ciszek, E 2013, 'Body weight and the medial longitudinal foot arch: high-arched foot, a hidden problem?', *European journal of pediatrics*, vol. 172, no. 5, pp. 683-91.

Wu, L 2007, 'Nonlinear finite element analysis for musculoskeletal biomechanics of medial and lateral plantar longitudinal arch of virtual chinese human after plantar ligamentous structure failures', *Clinical Biomechanics*, vol. 22, no. 2, pp. 221-9.

Wunderlich, RE & Cavanagh, PR 2001, 'Gender differences in adult foot shape: implications for shoe design', *Medicine and science in sports and exercise*, vol. 33, no. 4, pp. 605-11.

Xiong, S, Goonetilleke, RS, Witana, CP, Weerasinghe, TW & Au, EYL 2010, 'Foot arch characterization: a review, a new metric, and a comparison', *Journal of the American Podiatric Medical Association*, vol. 100, no. 1, pp. 14-24.

Xu, M, Hong, Y, Li, J.X and Wang, L 2018, 'Foot morphology in Chinese school children varies by sex and age', *Medical science monitor: international medical journal of experimental and clinical research*, vol. *24*, no. 1, pp.4536-4546.

Yadav, S, Parash, M, Shimmi, S, Chaudhary, B and Khan, G 2015, 'Digital Photography: An alternative for estimation of different dimensions of foot', *Pharmaceutical and Biological Evaluations Journal*, vol. 2, no. 3, PP. 60-63.

Yalçin, N, Esen, E, Kanatli, U & Yetkin, H 2010, 'Evaluation of the medial longitudinal arch: a comparison between the dynamic plantar pressure measurement system and radiographic analysis', *Acta Orthop Traumatol Turc*, vol. 44, no. 3, pp. 241-5.

Yelnik, A, Ponche, ST, Andriantsifanetra, C, Provost, C, Calvalido, A & Rougier, P 2015, 'Walking with eyes closed is easier than walking with eyes open without visual cues: The Romberg task versus the goggle task', *Annals of physical and rehabilitation medicine*, vol. 58, no. 6, pp. 332-5.

Yeras, AM, Peña, RG & Junco, R 2003, 'Moiré topography: alternative technique in health care', *Optics and lasers in engineering*, vol. 40, no. 1-2, pp. 105-16.

Yoon, H-b, Kim, J-h, Park, J-h & Jeon, H-s 2017, 'Comparison of the Foot Muscle EMG and Medial Longitudinal Arch Angle During Short Foot Exercises at Different Ankle Position', Physical Therapy Korea, vol. 24, no. 4, pp. 46-53.

Yoshida, Y,Saito, S.,Aoki, Y,Kouchi, M & Mochimaru, M. Shape completion and modeling of 3D foot shape while walking. International Symposium on Optomechatronic Technologies (ISOT) 29-31 Oct 2012 Paris, France.

Youdas, JW, Bogard, CL & Suman, VJ 1993, 'Reliability of goniometric measurements and visual estimates of ankle joint active range of motion obtained in a clinical setting', *Archives of physical medicine and rehabilitation*, vol. 74, no. 10, pp. 1113-8.

Zeidan, H, Suzuki, Y, Kajiwara, Y, Nakai, K, Shimoura, K, Yoshimi, S, Tatsumi, M, Nishida, Y, Bito, T & Aoyama, T 2019, 'Comparison of the changes in the structure of the transverse arch of the normal and hallux valgus feet under different loading positions', *Applied System Innovation*, vol. 2, no. 1, pp. 1-10.

Zhang, C & Yao, W 2008, 'The Comparisons of 3D Analysis Between Photogrammetry and Computer Vision', *The International Archives of the Photogrammetry, Remote Sensing and Spatial Information Sciences*, vol. 37, pp. 33-6.

Zhao, J, Xiong, S, Bu, Y & Goonetilleke, RS 2008, 'Computerized girth determination for custom footwear manufacture', *Computers & Industrial Engineering*, vol. 54, no. 3, pp. 359-73.

Zhao, X, Tsujimoto, T, Kim, B, Katayama, Y & Tanaka, K 2017, 'Characteristics of foot morphology and their relationship to gender, age, body mass index and bilateral asymmetry in Japanese adults', *Journal of back and musculoskeletal rehabilitation*, vol. 30, no. 3, pp. 527-35.

Zhao, X, Gu, Y, Yu, J., Ma, Y and Zhou, Z 2020, 'The Influence of Gender, Age, and Body Mass Index on Arch Height and Arch Stiffness', *The Journal of Foot and Ankle Surgery*, vol. 59, no. 2, pp.298-302.

Zuil-Escobar, JC, Martínez-Cepa, CB, Martín-Urrialde, JA & Gómez-Conesa, A 2018, 'Medial longitudinal arch: Accuracy, reliability, and correlation between navicular drop test and footprint parameters', *Journal of manipulative and physiological therapeutics*, vol. 41, no. 8, pp. 672-9.

Appendix A

Anthropometric data of participants (18 males and 15 Females)

No	*Age*	*Height*	*Weight*	*BMI*
1	32	184	119.3	35.23
2	44	167	94.6	33.92
3	35	174	85.9	28.37
4	28	182	88.5	26.71
5	40	182	88.5	26.71
6	40	166	82.2	29.83
7	34	180	69.8	21.54
8	30	175	85.4	27.88
9	44	169	93.7	32.8
10	39	176	90	29.05
11	40	172	80.2	27.1
12	42	162	70.6	26.9
13	29	179	104.6	32.64
14	42	178	94.6	29.85
15	32	173	107.3	35.85
16	30	178	78.9	24.9
17	47	185	107	31.26
18	39	181	77.1	23.53
19	25	167	52.8	18.93
20	38	157	73.9	29.98
21	36	158	60.2	24.11
22	33	163	66.3	24.95
23	28	166	55.9	20.28
24	37	164	62.2	23.12
25	38	156	71	29.17
26	36	165	55.2	20.27
27	42	160	48.7	19.02
28	46	156	74.2	30.48
29	43	160	77.9	30.42
30	46	154	67	28.25
31	32	165	72	26.44
32	34	162	68	25.91
33	37	157	68	27.58

Appendix B

Bundle adjustment Principles

Bundle adjustment also known as bundle triangulation bundle block adjustment, multi-image triangulation, and multi-image orientation is a method for the simultaneous numerical fit of an unlimited number of spatially distributed images (bundles of rays), see Figure B.1. It uses tie points in the object surface that can be reconstructed in three dimensions. Bundle adjustment is a very general technique which combines elements of geodetic and photogrammetric triangulation, space resection and camera calibration. Since the early 1980s, bundle adjustment has been accepted in all areas photogrammetry. Input data for bundle adjustments are typically photogrammetric image coordinates generated by digital cameras and the outputs of the bundle adjustment process are corrections of image coordinates, interior and exterior orientations, statistics error analysis, and the principal results of 3D coordinates of object points (Luhmann et al., 2014).

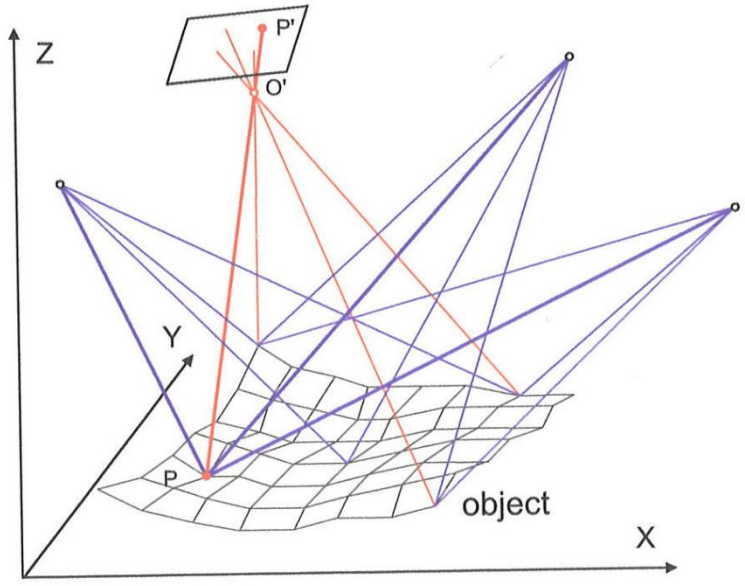

Figure B.1: Multi-image triangulation (Luhmann et al., 2014)

The mathematical model of the bundle adjustment is based on collinearity equations (Wolf & DeWitt, 2000; Luhmann et al., 2014). The coordinates of an object point P can be derived from the position vector to the perspective center X_0 and the vector from the perspective center to the

object point X*, see Figure 3.2.

$$X = X_0 + X^* \quad \ldots(b.1)$$

Vector X* is given in the object coordinate system. The image vector $\mathbf{x}'$ may be transformed into object space by rotation matrix R and a scaling factor *m*. Then, since it is in the same direction as x*:

$$X^* = m.R.\mathbf{x}' \quad \ldots(b.2)$$

Where

$$R=\begin{bmatrix} r11 & r12 & r13 \\ r21 & r22 & r23 \\ r31 & r32 & r33 \end{bmatrix} \quad \text{and}$$

r11= cos ϕ cos κ,

r12 = sin ω sin ϕ cos κ + cos ω sin κ,

r13 = -cos ω sin ϕ cos κ + sin ω sin κ,

r21 =- cos ϕ sin κ,

r22= - sin ω sin ϕ sin κ + cos ω cos κ, …(b.4)

r23 = cos ω sin ϕ sin κ + sin ω cos κ,

r31 = sin ϕ,

r32 = - sin ω cos ϕ,

r33 = cos ω cos ϕ.

Where ω, κ, ϕ (tilt about horizontal axis), κ (roll around optical axis) and ϕ (azimuth). Hence, the projection of an image point into a corresponding object point is given by:

$$X= X_0 + m.R.\mathbf{x}'$$

$$\begin{bmatrix} X \\ Y \\ Z \end{bmatrix}=\begin{bmatrix} X_0 \\ Y_0 \\ Z_0 \end{bmatrix} + m \,.\, \begin{bmatrix} r11 & r12 & r13 \\ r21 & r22 & r23 \\ r31 & r32 & r33 \end{bmatrix}.\begin{bmatrix} x' \\ y' \\ z' \end{bmatrix} \quad \ldots(b.5)$$

By inverting eq. (b.5), adding the principal point H′ (x_0', y_0') and introducing correction terms $\Delta x'(\Delta x, \Delta y)$(image distortion parameters), the image coordinates are given by:

$$\mathbf{x}'-x_0' - \Delta x' = \frac{1}{m} \,.\, R^{-1}.\,(X-X_0)$$

$$\begin{bmatrix} x'-{x_0}'-\Delta x \\ y'-{y_0}'-\Delta y \\ z' \end{bmatrix} = \frac{1}{m} \cdot \begin{bmatrix} r11 & r21 & r31 \\ r12 & r22 & r32 \\ r13 & r23 & r33 \end{bmatrix} \cdot \begin{bmatrix} X-X_0 \\ Y-Y_0 \\ Z-Z_0 \end{bmatrix}$$

By dividing the first and second equations by the third equation, the unknown scaling factor m is eliminated and the collinearity equations follow:

$$x' = x'_0 + z' \frac{r11(X-X_0) + r21(Y-Y_0) + r31(Z-Z_0)}{r13(X-X_0) + r23(Y-Y_0) + r33(Z-Z_0)} + \Delta x'$$
$$y' = y'_0 + z' \frac{r12(X-X_0) + r22(Y-Y_0) + r32(Z-Z_0)}{r13(X-X_0) + r23(Y-Y_0) + r33(Z-Z_0)} + \Delta y'$$

…(b.6)

Equation (b.6) describe the transformation of object coordinates (X, Y, Z) into corresponding image coordinates (x', y') as functions of the interior orientation parameters (x'_0, y'_0, c, $\Delta x', \Delta y'$) and exterior orientation parameters ($X_0, Y_0, Z_0, \omega, \kappa, \phi$) of one image (Luhmann et al., 2014).

Appendix C

Letter of confirm

Date: 9/05/2019

The places of the markers on foot segments that are motion during walking have been seen in detail. It is confirmed that the positions of the markers on foot segments have been chosen properly and accurately.

Kind Regards,

Sam

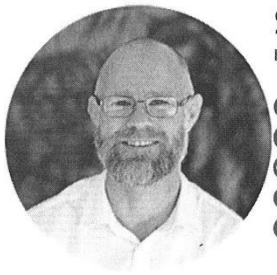

SAM JOHNSTON
PODIATRIST

07 4638 3022 | 07 4667 1633
sam@thepodiatrist.net.au
www.thepodiatrist.net.au
14 Ipswich Street Toowoomba QLD 4350
Shop 2/44-46 Wood Street Warwick QLD 4370

the podiatrist

Appendix D

Ethical Clearance Forms

Human ethics clearance has to be obtained for all research involving human participation according to the laws of the Office of Research and Higher Degrees at the University of Southern Queensland (USQ). Therefore, in this study two ethical clearance forms were given to each participant, whether male or female, to ensure that they understood the purpose and nature of the study, and to obtain their approval to participate in the study. These forms are:

- Participant Information Sheet
- Consent Form.

A sample of these two forms is presented below:

University of Southern Queensland

The University of Southern Queensland

Participant Information Sheet

TO: ***Participants***

Full Project Title: 3D photogrammetric images to evaluate foot morphology and ankle kinematics during gait of Middle Eastern adults

Principle Researcher: Dr Albert Chong
Student Researcher: Ali Abdulmunim Ibrahim Al-Kharaz

Associate Researcher(s):

This research project is part of a PhD where the aim is to develop an approach that provides low-cost, high-quality 3D surface models that can be used to study the dynamics of the foot. Please read this Plain Language Statement carefully. Its purpose is to explain to you as openly and clearly as possible all the procedures involved so that you can make a fully informed decision as to whether you are going to participate. Feel free to ask questions about any information in the document. You may also wish to discuss the project with a relative or friend or your local health worker. Feel free to do this.

Once you understand what the project is about and if you agree to take part in it, it is asked that you sign the attached Consent Form. By signing the Consent Form, you indicate that you understand the information and that you give your consent to participate in the research project.

1. Purpose of Research

Accurately collecting and analysing pressure and kinematic data of the foot during gait trials often requires the use of advanced and expensive equipment. As such, this type of equipment is not readily available in all clinics where gait assessments would be useful in helping to assess common movement abnormalities (such as cerebral palsy). With the recent advancement in video technology in smartphones, there perhaps is now an option for clinics that don't have large amounts of funding, or staff with advanced expertise in using biomechanical equipment, to undertake accurate gait assessments. Thus, the first purpose of the research is to develop an accurate photogrammetric approach that provides low-cost, high-quality and non-invasive 3D surface models of the human foot. If successful, this will allow us to study the dynamics of the foot, foot dorsal and plantar performance and the foot plantar pressure/force during gait using smartphone video. In addition, previous research has yet to measure the precise alterations of the plantar aspect of the foot contours in relation to distribution and location of ground reaction forces during the stance phase of the gait cycle and thus the investigation of this will be the second purpose of the research.

The outcomes of the research will result in an in-depth understanding of: 1) the stress of plantar structures of the foot via determining the weight distribution on the foot during gait; 2) the biomechanical aspects of dorsal and plantar structures during gait via analyzing foot movement; and 3) a low-risk, low-cost method of analysing dynamic performance of the foot using smartphone video.

2. Procedures

- Prior to agreeing to participate in the experiment, participants will need to meet the requirements for being included in this experiment:
    - No current or recent history of neuromuscular disease or injury that may impact on the person's ability to walk
    - No requirement to use an assistive device to walk
    - Aged between 18-50 years
- Participants who agree to be a part of this study will be required to visit the (S113) at the University of Southern Queensland, Toowoomba Campus for one session of about 15 min in duration.

- Once the informed consent document has been signed, participants will be asked to remove their shoes in preparation for the trials.
- Participants will then be asked to walk with a natural speed along a 4-m long walking platform. Embedded in the walking platform is a pressure mat that sits flush with the level of the walking platform. Participants will be required to perform three trials walking along the platform and over the pressure mat. While the participant is walking along the walking platform, pairs of smartphone cameras arranged around the walking platform will record the feet and legs of the participant.

3. Expected Benefits

Participants will not directly benefit from the study. However, the wider community that the participant is a member of will benefit from the development of a low-cost, low-risk and accurate method of analysing the foot during gait. This will assist doctors and other clinics to achieve an appropriate individualised treatment strategy for the patients who suffer from foot problems.

4. Risks

As the participants will be walking as they normally do during day-to-day activities, there are no added risks of participating in this study.

5. Confidentiality

Video footage requires a large storage capacity. Because of limited computing resources, these video clips will be discarded as soon as the models are derived and analysed. Any information obtained in connection with this project that can identify you will remain confidential. It will only be disclosed with your permission, subjected to legal requirements.

The results of this project are planned to be published in a scientific journal or conference presentation. In any publication, information will be provided in such a way that you cannot be identified including the removal of any names, images or video that could identify an individual. ***The results from the research will not target an individual and thus group data will be presented. Personal data that will be collected will be restricted to information pertinent for the accurate running of the research and ensures that suitable participants are only included.***

6. Voluntary Participation

Participation is entirely voluntary. If you do not wish to take part you are not obliged to**.** If you decide to take part and later change your mind, you are free to withdraw from the project at any stage. Any information already obtained from you will be destroyed.

Your decision whether to take part or not to take part, or to take part and then withdraw, will not affect your ***relationship with*** the University of Southern Queensland.

Before you make your decision, a member of the research team will be available to answer any questions you have about the research project. You can ask for any information you want. Please only sign the Consent Form once you have had a chance to ask your questions and have received satisfactory answers.

If you decide to withdraw from this project, please notify a member of the research team. This notice will allow the research team to inform you if there are any special requirements linked to withdrawing.

7. Queries or Concerns

Should you have any queries regarding the progress or conduct of this research, you can contact the principal researcher:

Ali Abdulmunim AL-Kharaz
Faculty of Engineering and Surveying
Toowoomba

ph: +61 403680102
Email: Ali.Al-Kharaz@usq.edu.au

If you have any ethical concerns with how the research is being conducted or any queries about your rights as a participant please feel free to contact the University of Southern Queensland Ethics Officer on the following details.

Ethics and Research Integrity Officer
Office of Research and Higher Degrees
University of Southern Queensland
West Street, Toowoomba 4350
Ph: +61 7 4631 2690
Email: ***ethics@usq.edu.au***

University of Southern Queensland

The University of Southern Queensland

Consent Form

TO: ***Participants***

Full Project Title: 3D photogrammetric images to evaluate foot morphology and ankle kinematics during gait of Middle Eastern adults

HREC Number : H18REA168

Principle Researcher: Ali Abdulmunim Ibrahim Al-Kharaz; Email: Ali.Al-Kharaz@usq.edu.au

Principle Researcher: Dr Albert Chong; Email: albertkon-fook.chong@usq.edu.au

I agree for that by signing below:

- I have read the Participant Information Sheet and the nature and purpose of the research project has been explained to me. I understand and agree to take part.
- I understand the purpose of the research project and my involvement in it.
- I have had any questions answered to my satisfaction.
- I understand that I may withdraw from the research project at any stage and that this will not affect my status now or in the future.
- I confirm that I am between the ages 18 to 50 years.
- I understand that while information gained during the study may be published, I will not be identified and my personal results will remain confidential.
- I understand that any data collected may be used in future research activities
- I understand that only my foot will be videotaped during the study.

Name of participant…….....

Signed……**Date**…….

Please return this sheet to a research team member prior to participating.